Kinetic Study of Plastic Waste Pyrolysis Reactions

Camila Geirinhas Cameira

Thesis to obtain the Master of Science Degree in

Chemical Engineering

Supervisors: Prof. Dr. Kevin Van Geem
Prof. Dr. Maria Amélia Lemos

Examination Committee

Chairperson: Prof. Dr. Sebastião Alves
Supervisor: Prof. Dr. Maria Amélia Lemos
Member of the committee: Prof. Dr. Carlos Henriques

July 2021

Acknowledgements

I want to start by thanking the institution that was my second home during the first five years of my extended six years in becoming an engineer, Instituto Superior Técnico, and to Ghent University for receiving me for the last stage of the journey. To my supervisors, Prof. Maria Amélia Lemos, and Prof. Kevin Van Geem, I am very grateful for all the guidance provided during the development of the work. After showing their support from day one, I want to deeply thank Prof. Francisco Lemos, Sepehr Madanikashani, Onur Dogu, and Koenraad Beirnaert.

It was not always a happy journey, but definitely one worth going for. I could not feel more blessed by the supporting system that I have been discovering I have. It feels close to home even though it is spread in so many people and places.

To Vasco Saltão, for motivating me in critical moments in the past year, Nadine Antunes for the endless working nights and companionship, Margarida Durão for the unconditional friendship and for helping in navigating all the big changes life is throwing at us, Luke Mason-Hobbs for being right here next to me even if physically far away and for always pushing me to be better, and Mariana Lamas for the endless support and for being my solid rock, always making sure I had fun and enjoyed myself in the midst of everything.

To all the supportive teachers and to my amazing colleagues from Instituto Superior Técnico, we were a good batch. Everyone at Refood, who always asked how my thesis was going, and for being a safe space to escape. Everyone at Reboot, for allowing me to believe in myself again, and with whom I love to work towards a better future for all. And, last but not least, to TEDxULisboa, a place where I found happiness again, learned more about myself than I would have imagined, and where I met people who I will always keep close to my heart.

None of this would be possible without the unconditional support of my family. And while everyone has left a mark on me, I need to thank the ones that stood with me through it all. To my mother, Alice, and sister, Clara, who had to deal with my moody days and long working nights. To my sister Carmen, and my brother Tomás for bringing out my inner child and forcing me to relax. To my father Mário, who never forgets to ask if I am happy and to my grandparents Mário and Emília, for supporting me in every crossroad I have found, for taking me on fascinating trips, and for always watching over my mental health. Thank you.

Resumo

O tratamento de resíduos plásticos é uma área em crescimento e cada vez mais relevante, onde ainda são necessários estudos e desenvolvimento de tecnologias que permitam um tratamento mais eficiente destes resíduos, conducentes à sua valorização numa perspetiva de economia circular. A reciclagem química é um caminho promissor, através de processos de pirólise e gasificação. No entanto, um conhecimento detalhado da composição da matéria-prima é imprescindível, sendo este um dos grandes obstáculos a ultrapassar. Este trabalho investigou um dos mais recentemente desenvolvidos modelos mecanísticos, para estudar o efeito do comprimento da cadeia polimérica para quatro reagentes de diferentes pesos moleculares. Os resultados foram comparados com dados experimentais obtidos na bibliografia, antes de analisados com base na distribuição de produtos e radicais, elucidando a importância de cada tipo de reação incluída no modelo. Foi criada uma simples simulação virtual de um reator descontínuo, de volume fixo e em regime adiabático. Os quatro reagentes mostraram uma produção dominante de moléculas de baixo peso molecular, principalmente etileno e metano, produzidos por reações de cisão beta ou cisão homolítica de parafinas. As reações de isomerização mostraram ser responsáveis por uma maior uniformidade na produção de radicais, também produzidos nas reações de abstração de hidrogénio, que por sua vez sofrem cisão beta. O mecanismo, modelado como um polímero de 40 átomos de carbono, tetracontano, conseguiu descrever adequadamente os resultados experimentais da decomposição térmica de polietileno de alta densidade. No futuro, é necessário desenvolver melhores parâmetros cinéticos e simplificar a complexidade química das reações de pirólise.

Palavras-chave: Pirólise, modelos cinéticos, reações, polímeros, resíduos plásticos

Abstract

The study of plastic waste degradation is more than a trending topic, it is necessary to advance the knowledge and technologies to allow for proper treatment and handling of this type of waste in a more efficient way, leading to its valorization in a circular economy approach. Chemical recycling shows a promising route, through pyrolysis and gasification processes. The difficulty in accurately identifying feed composition constitutes a major problem, as it is complicated to predict the outcome of these processes, hence a better way of dealing with this is needed. This work investigated one of the most recently developed/improved detailed kinetic modeling for four hydrocarbons with different chain lengths. The results were validated against experimental data obtained in the literature and the effect of chain length was assessed. Moreover, a thorough analysis of the product and radical distributions was performed clarifying the effect of each reaction family considered. By creating an elemental virtual framework, gas-phase pyrolysis was simulated in a discontinuous reactor, with a fixed volume and adiabatic conditions. All reactants showed a marked preponderance to form light chain molecules, mainly ethylene and methane, primarily produced through $\beta - scission$ and homolytic scission reactions. Isomerization reactions are responsible for a more uniform production of radicals while many are also formed by H-abstraction which subsequently suffer $\beta - scission$. The mechanism, modeled as a 40-carbon atom hydrocarbon, tetracontane, can correctly describe the experimental results for HDPE thermal decomposition, despite substantial improvements needed regarding its complex chemistry and kinetics parameters in future developments.

Keywords: Pyrolysis, kinetic modelling, reactions, polymer, plastic waste

Table of Contents

List of figures

List of tables

List of symbols

Acronym	**Description**
.csv	*Text file*
.cti	*Cantera input file*
.ipynb	*Jupyter Notebook file*
$(CH_2)_n(CH=CH_2)_2$	*Diene general formula*
%wt	*Mass percentage*
°C	*Celsius degrees*
A	*Pre-exponential rate coefficient*
ANE	*Any chain-length alkane*
ANE:DIENE	*Ratio between alkanes and dienes*
A_ω	*Surface area of the wall*
BB:RS	*Ratio between backbiting and random scission*
β-scission	*Scission of carbon bond in beta position in relation to the radical position*
C-C	*Chemical bond between two carbon atoms*
CFD	*Computational fluid dynamics*
C_nH_{2n}	*Alkene general formula*
C_nH_{2n+2}	*Alkane general formula*
DIENE	*Any chain-length diene*
E_a	*Activation energy*
ENE	*Any chain-length alkene*
H	*Total enthalpy*
H-abstraction	*Abstraction of a hydrogen atom*
H-shifts	*Transfer of a hydrogen atom to another position in the polymer*

HCl	*Hydrochloric acid*
HDPE	*High-density polyethylene*
He	*Helium*
IUPAC	*International Union of Pure and Applied Chemistry*
K	*Kelvin degrees*
k	*Rate constant*
LDPE	*Low-density polyethylene*
LMW	*Low molecular weight*
LMWP	*Low molecular weight products*
m	*Content's mass*
MW	*Molecular weight*
PE	*Polyethylene*
PET	*Polyethylene terephthalate*
PP	*Polypropylene*
PS	*Polystyrene*
PSW	*Plastic solid waste*
PVC	*Polyvinyl chloride*
QSSA	*Quasi-steady state approximation*
R	*Perfect gas constant*
RCD	*Random chain dissociation*
RENE	*Allyl radicals*
$R_P^{\cdot}$	*Primary alkyl radicals*
‘$R_P^{\cdot}$	*Primary w-alkenyl radicals*
$R_S^{\cdot}$	*Secondary alkyl radicals*

‘$R_S^{\cdot}$	*Secondary 1-alkenyl radicals*
s	*Seconds*
T	*Temperature*
TGA	*Thermogravimetric analyses*
t_s	*Residence time*
U	*Total internal energy*
V	*Volume*

Chapter 1. Introduction

Plastic use, and thus production, has felt an overwhelming increase in the last 50 years, showing growth in consumption of 4% per year [1]. Interestingly enough, however, it has felt a decrease in the production rate of 8.5% in 2020 (Index 2015) due to COVID-19, which is only expected to reach previous numbers in 2022 at the least [2]. With high production and consumption rates, plastic wastes generation increases exponentially, calling for a more viable and sustainable treatment process. However, a large percentage (60%) of the waste is still not recovered or recycled and ends up in the environment or combustion plants or landfills (data reported between 1950 and 2015 [3]). From this polymeric waste, high-density polyethylene is the major part, making up to 20.4%.[4]

Most common plastics are made from mainly five different polymers, called the “big five”. These polymers are high-density polyethylene (HDPE), low-density polyethylene (LDPE), polypropylene (PP), polyvinyl chloride (PVC), and polyethylene terephthalate (PET) [5]. Each of these has particular characteristics that determine its production, application, and treatment, namely the branching ratio, natural contaminants, and usage either as virgin or reused plastic. Branching ratio is a measurement of the branching in the hydrocarbon backbone, *i.e.* how many times in the main chain a hydrogen atom is replaced by another covalently bonded chain of the same polymer; Natural contamination in plastic waste consists of mixed plastics of unknown compositions, organic fractions, such as food remains or paper, and even inorganic fractions, which include fillers of sodium chloride from food, for example.

Regarding the recycling of solid plastic waste (SPW) from the plastic produced and consumed globally, different alternatives have been considered to substitute the disposal in landfills. There are four main recycling methods, including re-extrusion, mechanical, chemical and energy recovery which are also called primary, secondary, tertiary, and quaternary techniques, respectively. The most appropriate method is selected based on the analysis, the waste source, composition specificities, and the purpose the polymer will serve after its processing.

Chemical recycling can take on many forms, from pyrolysis and gasification to steam and catalytic cracking. Recently, attention has been paid mainly to thermal cracking as a way of chemical treatment for SPW [6]. This method focuses on depolymerization for the recovery of valuable petrochemicals as feedstock, resulting in a very profitable and sustainable scheme for product yield. Although pyrolysis is an endothermic process, its products can be used to produce energy in the form of heat and steam with minimum waste. Energy recovery involves oxidation of the pyrolysis’ products, whether partial or complete [7]. This means it will produce heat, gaseous fuels, oils, and chars, apart from by-products that will need to be disposed of, such as ash.

However, this route for chemical recycling still lacks research and in-depth knowledge on the kinetics of the underlying processes that would allow for the proper reactor design and reaction conditions necessary to yield specific products. On the other hand, products’ energy recovery already has strong supporting research, but it falls short in terms of integration in industrial plants. These are the main reasons why the techniques are not yet considered sustainable for a scale-up process, as they will only be when the integration of waste management is implemented in the plastics' production cycle and SPW's treatment process, as a circular process.

Nonetheless, pyrolysis, as a way of thermo-chemical treatment of SPW, has gained a lot of attention since it comprises large benefits and it guarantees good results when coupled with gasification, addressing both the challenges of plastic waste management and the increasing energy demand globally. These techniques allow to cut down the amount of energy and virgin raw materials required when producing new polymers since they simultaneously eliminate SPW while generating fuels and other chemicals. All of this contributes to a circular process and economy, providing alternative solutions to landfilling and thus reducing greenhouse gases (GHG) and carbon dioxide emissions [6].

Hence, increasing interest in these techniques has led to extensive research both in the field of polymer recycling and of solid fuels for aerospace applications, as these are usually polymers, which are light and with a high heating value, to be used as fuel. Consequently, numerous papers have been published aiming to accurately predict the chemistry involved in pyrolysis reactions and their products and to estimate the time constant of this phenomenon as a function of operating conditions. Despite common efforts, still no detailed kinetic scheme, including the complicated chemistry involved, that can predict the production of by-products and HDPE consumption for thermal decomposition is available. A properly developed mechanism is of utmost importance since the applied temperature and heat transfer dynamic are deterministic for the final products obtained. Moreover, suitable kinetic parameters are imperative since these also dictate the most suitable reactor design to adopt. The numerical simulations can then be applied in a Computation Fluid Dynamics code and studied for fluid behaviour.

The mechanism serving as a reference for the present work is from Németh et al. [8] and was chosen since it can identify and quantify pyrolysis products which are necessary to study their subsequent combustion. The recent extension of the mechanism developed by Beirnaert K. [9] had to take into account a very reliable kinetic model able to describe the complex chemistry of polymer pyrolysis, which ended up having 41002 reactions and 1237 species. The reduced version of this mechanism, with only 9000 reactions, showed little to no deviation from the results of the full mechanism.

This work aims to use Beirnaert's mechanism and simulate pyrolysis reactions for four reactants with different chain lengths, all saturated hydrocarbons: decane, icosane, triacontane, and tetracontane. Varying the molecular weight from a 10-carbon atom molecule to 40, the effect of the initial substrate length is studied, alongside a brief reaction time study.

Firstly, an introduction to polymer pyrolysis is made in chapter 2 setting the basis for understanding how the reaction should be simulated. These virtual simulations can shed light on the important pathways involved and can therefore be used to optimize the process conditions for the desired products and purposes [10]. Chapter 3 is a literature review that elucidates the various modeling strategies on plastic waste pyrolysis developed up until now, showing both the benefits and limits of each model. They need to be constructed along with their thermodynamic, transport properties, and reaction rate coefficients. The majority is built on global reactions together with lumped parameters, instead of a highly detailed reaction network with individual Arrhenius' parameters. Moreover, the effects of process conditions, impurities, and mixing extent are still poorly understood [6]. Designing detailed kinetic models is essential to obtain a suitable reactor and to increase production efficiency. Levine & Broadbelt [4] and Zhou et al. [11] state that a better understanding of the kinetics is imperative for improving selectivity and desired yields for the central products.

After understanding the complexity of the process and the state-of-the-art, chapter 4 explains how the mechanism studied in this work was assembled. A reworking and extension of the Németh et al. mechanism were performed, and a new kinetic set was assumed, defined as part of Beirnaert's work [9]. The complexity of the reaction network derives from the high molecular weight and polydispersity of polymers [4]. In chapter 5 a succinct explanation is made regarding the supporting tools adopted for the development of the framework to study Beirnaert's mechanism. Chapters 6 and 7 exhibit the virtual simulation results. These are described and analyzed, which are further discussed and matched against experimental results described in the literature. A reflection is made regarding the usability of the mechanism and its ability to simulate polymer pyrolysis for different substrates, with comparable results to actual conditions where pyrolysis develops.

Chapter 2. Polymer Pyrolysis

Pyrolysis is a thermochemical conversion process that usually happens at moderate to high temperatures, atmospheric pressures, and in the absence of oxygen that converts polymers into smaller molecules. It has shown to be an interesting alternative especially for mixed and complex plastic waste feeds which cannot be mechanically separated and recycled and are, instead, incinerated in landfills [5]. In most packaging materials, polyethylene (PE) is the main component, because it is the one that ensures the structural integrity and bulkiness of common packages [5]. However, different layers with different components are used to ensure the correct application and purpose of packaging [12]. This means that mechanical recycling is not suitable to ensure the polymer's re-usage. Pyrolysis is a technology that sustains highly contaminated and highly heterogeneous feed, making it a very desired way of treating complex polymer feeds [6]. It is important to stand out that while polymer recycling is one attractive usage of pyrolysis' advantages, aerospace applications have shown an increasing interest in this process consuming polymers to be used as solid fuel [13].

SPW's pyrolysis products can be separated into three categories: gas, liquid, and solid residue. Different polymer's composition gives rise to a very distinctive product range, which depends on their predominant decomposition pathway and reaction conditions. Attention should be headed to the contamination level of the feed because this is what will have the most impact on product distribution. As an example, if the polymer contains any oxygenates, then methanol or formaldehyde can be formed, jeopardizing the recycling scheme, and possibly corroding the process equipment. This uncertainty, plus a large number of reactions that pyrolysis entitles, are the main problems to tackle since they define how the outcome should be handled. Not to mention the complexity in designing a trustworthy and complete kinetic mechanism that can reproduce, with precision, the reactional scheme [6].

Nowadays [5], distillation has presented itself to be the chosen separation technique that allows for the purification of the obtained monomers and liquids. Since pyrolysis is only economically viable when carried out in large volumes, large distillation towers are also needed, implying high costs due to the demanding cooling duties. To avoid the formation of common contaminants such as polyvinylchloride (PVC) and hence hydrochloric acid (HCl), lower temperature pyrolysis has been suggested by a few authors, where a pre-pyrolysis reactor is considered, and 98 wt% chlorine removal has been achieved [14,15]. Calcium and sodium carbonates or oxides can be added to neutralize the remaining 2 wt% chlorine. As of now, the separation approaches are not sophisticated enough to be able to treat these hazardous components, which leads to environmental constraints such as a larger number of waste streams, which are still unavoidable if the goal is to obtain a suitable and usable petrochemical fuel [5].

As for the reactor design, the fluidized bed reactor is widely accepted, mainly due to advantages like the uniformization of products and high conversion rates. It is already a mature and extensively studied reactor design, easing the process around how heat and mass transfer occur in the reactor which helps in the prediction of reaction conditions [16]. Heat and mass transfer strongly affect thermal degradation so although these variables for fluidized bed reactor are well established, further limitations are needed to be developed to take into account the three phases of plastic degradation: solid, liquid, and gas.

To highlight the dominant pyrolysis reaction pathways and their main characteristics, the chemical inner workings are carefully interpreted. As it is extensively proven and accepted in the literature [8,17], polymer decomposition involves free radical reaction mechanisms consisting of multistep chain reactions. Free radical mechanism implies 3 stages: initiation, propagation, and termination, which are explained hereafter.

2.1. Reaction families

Throughout the three stages, the most important reaction families consist of intermolecular H-abstraction, β-scission, and backbiting (or intramolecular H-shifts) reactions.

Intermolecular H-abstraction occurs when a radical abstracts a hydrogen atom from another neighboring molecule, transferring it from one location to another, generating thus a new radical. [18]. Both the abstracting and the product radical can be end-chain, midchain, or Low Molecular Weight (LMW) radicals [10]. It is important to note that this reaction differs from a proton transfer since the latter only involves the nucleus's transfer from the hydrogen atom.

Figure 1. Scheme of a hydrogen abstraction reaction. Adapted from [18].

In organic chemistry, β-scission reactions as the name indicates, take place when a single bond in the β position is cleaved, causing the compound to fragment into two pieces, forming a double bond between the alpha (α) and beta (β) positions and a concomitant radical specie. When it happens at the end-chain, it is a likely route to the formation of LMW radicals or Low Molecular Weight Products (LMWP). The alpha position is the position that bears the unpaired electron, making the beta position its neighboring carbon atom [10,18].

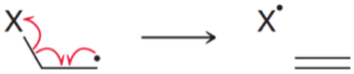

Figure 2. Scheme of a β-scission reaction. Adapted from [18].

Backbiting, isomerization, or intramolecular H-shifts occurs when the chain end curls and the radical at its end abstracts a hydrogen atom from a CH_2 group in the middle of the chain, forming a new radical position from which the chain growth continues [18]. Therefore, isomerization can happen through a 5-, 6- or 7-membered ring intermediate with a (1,4), (1,5), and (1,6) H-transfer [19].

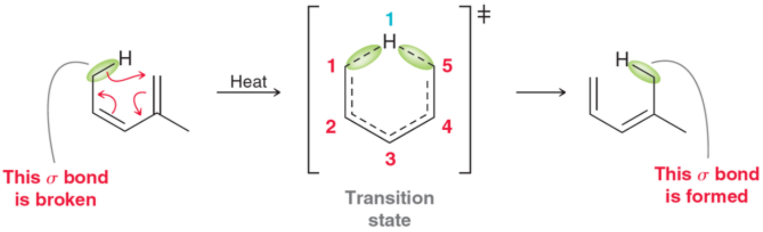

Figure 3. *Scheme of an example of a [1,5] hydrogen shift. Adapted from [18].*

Even though every reaction is important in a different reaction stage, all are necessary for the others to occur since together they form the reagents needed for the subsequent reactions.

Initiation

- Starts with the homolytic scission of C-C bonds, producing free radicals.

Propagation

- By β-scission (mid-chain), unzipping (end-chain β-scission), and intra- and inter-molecular H-abstraction, there is a production of monomers and smaller chain length molecules, respectively.

Termination

- Constitutes of recombination/disproportionation of radicals participating in the reaction mechanism. In this step, all recombination of possible radical species is taken into consideration.

Pyrolysis initiates with homolytic scissions, which are a series of random cleavage of C-C covalent bonds along the main chain of the polymer. This series of reactions is the most important first step in the process since it is what allows radical formation driving the free radical mechanism that follows. Since the bond between a hydrogen atom and a carbon atom (hydrogen bond) is stronger than between two carbons (covalent bond), the latter is not relevant for the process, and will not be considered for the reaction scheme [10,20].

The H-abstraction reactions are responsible for producing a large number of radicals that will interact with the LMWPs formed through $\beta - scission$ reactions until this latter reaction path is no longer energetically favorable. As for backbiting reactions, these are essential for the formation of LMWPs and oligomers, being the biggest contributor to the formation of products with chain lengths of 6, 10, or 14 carbon atoms [21].

In liquid phase polymerization, H-abstraction reactions are dominant over $\beta - scission$ reactions, according to the Fabuss-Smith-Satterfield mechanism [22,23]. However, when facing high temperature values and low substrate concentrations, the Rice-Kossiakoff regime applies, meaning that end-chain $\beta - scission$ reactions become the dominant reactions, producing a larger amount of LMW alkenes. These theoretical assumptions are clearly depicted in the later chapters, where the main results are discussed.

This process produces complex output streams which are very variable in content depending on reaction conditions and the feedstock composition. The products yielded will vary between liquids, as condensable vapors or oil, solids as char, and gasses, as non-condensable [6].

Taking into consideration the works of Levine & Broadbelt, and Vinu [4,10], the possible elementary reactions occurring in the pyrolysis of vinyl polymers are shown in Figure 4.

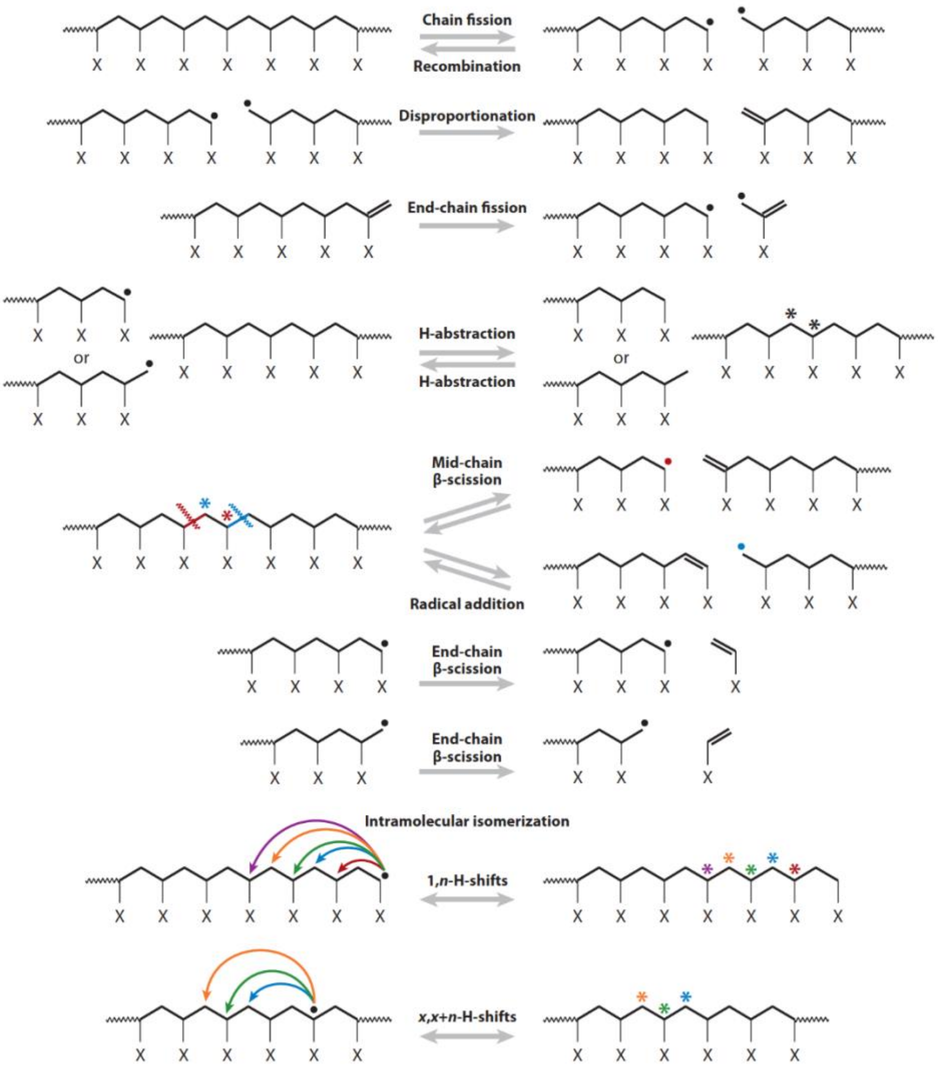

Figure 4. *Elementary reactions in pyrolysis, represented by the order in which they should occur. For intramolecular isomerization, the colours denote what position the hydrogen atom will take, after shifting. X = H, since the study is on polyethylene, and the asterisks represent the different possible radical sites. [Adapted from* [10]*].*

To approach the inner workings of this reaction scheme, several authors have developed kinetic mechanisms throughout the years attempting to predict plastic waste treatment through thermal decomposition. Numerous strategies were developed to create and implement kinetic models that simulated pyrolysis conditions, varying from very detailed models to much simplified ones [24]. For the next chapter, a literature review is made where an overview of the state-of-the-art for these models is presented and chronologically and by modeling strategy.

Chapter 3. Literature review

3.1. Introduction

In this literature review pyrolysis or thermal degradation, will be reviewed as an effective way of reducing the impact on polymer recycling. Although the most common recycling technique continues to be mechanical, both the chemical and energy recovery paths are of major interest since these are still preferred when treating complex waste feeds which are difficult to be recycled mechanically or depolymerized. This has led to a considerable amount of research in kinetic modeling on polymer pyrolysis, both thermal and catalytical. Therefore, a chronological description of different mechanisms' work and progress is presented, including the main obstacles and prospects. The strategies range from very detailed kinetic models up to a molecular level to using global kinetic models which describe the process considering few lumped reactions [24]. At the end of the chapter, a brief conclusion explains the interest in the current work, and how it aims to help in thriving the research, and practical developments, on this topic.

3.2. Kinetic Modeling Strategies for Polymer Pyrolysis

Table 1 summarizes the kinetic models covered in this chapter. The detailed reviews are divided into modeling strategies from global kinetic modeling, method of moments, to kinetic Monte Carlo. For each modeling strategy, the works presented are organized chronologically.

Table 1. *Overview of the modelling strategies used in the development of kinetic models for polymer pyrolysis.*

MODELING STRATEGY	YEAR	FEED TYPE	VALIDATION RANGE	APPLICATIONS
PROBABILISTIC GLOBAL MODELING	Westerhout et al.[16] 1997	Branched alkane with malleable MW	$T < 450°C$ TGA	Production of valuable Chemicals; Polymer Recycling
DETERMINISTIC, METHOD OF MOMENTS	Bockhorn et al.[25] 1999	Linear polymer, accounting for polydispersity	$T < 400°C$ TGA	Polymer Recycling
PROBABILISTIC MONTE CARLO	Poutsma[26] 2003	Alkane with malleable MW	$T \leq 780°C$	-
DETERMINISTIC, METHOD OF MOMENTS WITH QSSA	Marongiu et al.[19] 2007	Linear polymer, accounting for polydispersity	$300 \leq T \leq 800ºC$ TGA	Production of valuable Chemicals; Polymer Recycling
DETERMINISTIC GLOBAL MODELING	Mastral et al.[24] 2007	Linear alkane	$500 \leq T \leq 1000ºC$	Polymer Recycling
DETERMINISTIC MONTE CARLO	Németh et al.[8] 2007	Tetracontane	Low conversion 500°C	Polymer Recycling
DETERMINISTIC, METHOD OF MOMENTS	Levine & Broadbelt [4] 2009	Linear polymer, accounting for polydispersity	420 °C	Energy Recovery; Polymer Recycling
DETERMINISTIC MONTE CARLO	Gascoin et al.[27] 2012	Tetracontane	$427 \leq T \leq 927°C$ $1 \leq p \leq 100$ bar	Hybrid Rocket Technology

3.2.1. Global Kinetic Models

Westerhout et al. (1997)

The work from Westerhout et al. [16] was published in 1997, alongside the works from Ranzi et al. [28], included in the section below. A few things differentiate the two works, starting from the modeling strategy implemented.

Westerhout et al. aimed to experimentally determine the kinetic data for the pyrolysis of PE, PP, and PS. The thermogravimetric analysis of the experiments was performed at temperatures below 450°C. The thermal degradation of these compounds is relevant in the production of valuable chemicals such as ethylene, propene, butene, and styrene that can be useful in producing new polymers or sold for other purposes. The authors used an RCD, random chain dissociation, approach. The method takes into consideration both physical and chemical influence in the kinetic scheme, namely in the polymer chain bond cleavage, since this cleavage doesn't mean that all the products will evaporate because of the volatilization of a compound strongly depends on the length of the fragment, and the temperature applied. To take this into account, the model considers the polymer as represented in Figure 5.

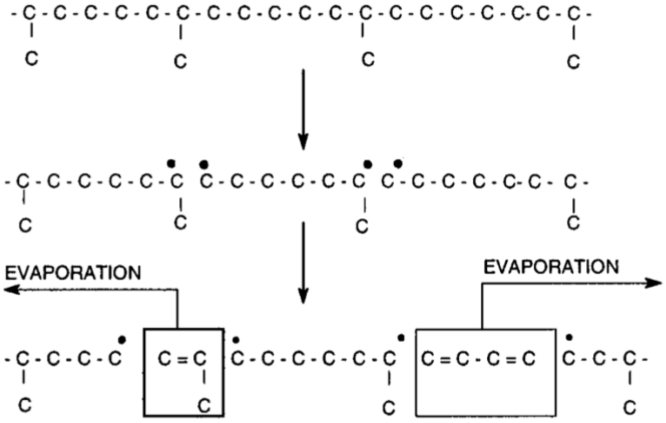

Figure 5. Polymer chain representation for the RCD method implemented in modeling pyrolysis for PE, PP, and PS initial substrates. Adapted from [16].

The breakage rate for different bond types will differ, giving rise to different values of pre-exponential values, and activation energies, which were considered in the model, as well as the chain length and the level of branching. The branches considered are methyl, ethyl, propyl, and benzyl groups assumed to be distributed evenly over the main chain. Experimentally, it was found that the conversion rate increases in the order HDPE < LDPE < PP < PS, explained by the stability of the free radicals produced for each initial substrate.

Although some of the older kinetic models proposed were very complex, they have far limited practical use due to the short range of conditions studied. On the other hand, the work of Westerhout et al. [16] is a valuable description of the process since it can be applied to larger ranges of conditions, but it is too simplified when it comes to having a complete description of the gas phase composition. Moreover, it is not possible to "derive an analytical representation of the pyrolysis kinetics".

Mastral et al. (2007)

Ten years later, in 2007, two other studies were published by two different research groups. The one by Mastral et al. [24] also implemented a global kinetic modeling strategy to describe the reaction's kinetics.

This research focused on theoretical validation, and it considered pyrolysis of high-density polyethylene, represented by a global Arrhenius law. The authors aimed to show how the temperature and residence time affected its product distribution, which was studied in a fluidized bed reactor for intervals of 500 – 1000 °C and 0.52 – 2.07 s, respectively. A mechanistic model was used and followed a radical mechanism, which seems to be a unanimous approach for several models, developed by different research groups. Here, besides alkanes, olefins, and diolefins, aromatics were also included as relevant species, although one of the main results showed that they were only relevant at higher residence times. The installation was designed to account for different reactor volumes, allowing to study a broad range of residence times, indispensable to further analyze this variable and its effect on the system, particularly in the development of secondary reactions.

Throughout the decomposition process, three reactions compete for intermediate products: $\beta - scission$, hydrogen transfer, and termination reactions. If on the one hand, fast $\beta - scission$ increases the cracking process, thus producing large amounts of olefins and diolefins, on the other hand, hydrogen transfer stimulates the growth of paraffin and diolefins, which are also enhanced during the termination stage. At this point, olefins' production decreases, due to the reduction of cracking reactions, which happens when the overall concentration of radicals diminishes. Considering aromatics, these are only relevant at temperatures of 800°C or higher since their formation greatly depends on temperature.

At intermediate cracking levels, gas production (C_1-C_4) is relatively high, while products C_5-C_{12} show a minimum weight percentage, and C_{19}-C_{32} represent a maximum production, resulting in the cracking of intermediate fractions towards lighter compounds. At high residence times and moderate temperature, C_1-C_4 products are overestimated, because the isomerization reactions from hydrogen transfer and $\beta - scission$ are considered to have the same probability. In practice, isomerization mostly generates gaseous products, which indicates that the way the model is built, will output gas fractions that exceed the experimental results.

One of the downsides of the model is that to have more detailed information on the concentration of intermediate species created, a steady-state assumption is not made, increasing the computational time, which can be analyzed to understand if it is a reasonable choice, or if the disadvantages surpass the advantages. Furthermore, the model does not allow multi-species formation and consumption. Future work should include alternative kinetic schemes for polyaromatics to improve the quantitative result of this fraction, other relevant gaseous species, and aromatic intermediate compounds.

3.2.2. Method of Moments

Bockhorn et al. (1999)

The work of Bockhorn et al. [25] focused on polystyrene but was chosen to be included here due to the interesting insights it brought to the field. The main goal was to deliver a quantitative estimation of the bias in the overall kinetic parameters assessing both pillars, heat transport effects, and complex reaction mechanisms.

Since polymers are very long-chain molecules, a temperature gradient is likely to occur when dynamic heating is applied to the material that itself, is already a poor heating conductor. Thus, a common method in determining kinetic parameters is to perform both isothermal and dynamic experiments, delineate conversion curves, and adapt kinetic models to these curves. When developing a more detailed kinetic scheme (which should be analyzed in more detail in the respective paper [25]), the method of moments was employed, to solve the rate equations for the polydisperse species.

For polystyrene, isothermal and dynamic experiments were made considering a range of temperature from 200°C to 400°C, in TGA experiments. It was found that using small heating rates and smaller sample weights, the deviations for both the activation energy and the pre-exponential value would become irrelevant, showing that the temperature non-uniformity only causes small deviations when considering working in the conditions presented. Further developments were envisioned considering a more detailed mechanism, while still assuming a single reaction step for the kinetic scheme.

Ranzi et al., Faravelli et al., and Marongiu et al. (1997, 1999, 2007)

In 1997, several researchers from Politecnico di Milano were the main precursors in the field and developed a mechanistic kinetic model to predict the radical mechanism of liquid hydrocarbon pyrolysis. The work was under revision and development for ten years, with an enhanced work published in 2007. Hereafter are described the progress and tests carried out over the years.

Ranzi et al. (1997)

Thermal degradation was simulated for polyethylene and polypropylene, and the mechanism was validated against experimental data for both molecules. A defined heating rate of $10°Cmin^{-1}$ was established for all TGA experiments, from 300°C to 500°C, maintaining the reaction isothermal and at atmospheric pressure. The end criterion chosen was the helium molar fraction, which should reach values close to 1, the point when the reaction would be considered finished.

A numerical, single-step Arrhenius approach was assumed for the rate of equations that describes the apparent kinetics. The kinetic parameters were based on gas-phase values, since no other suitable values were available to estimate the reaction, hinting this to be a possible source for errors or inconsistencies in the results. This did not appear to be a problem for propagation and termination stages, while it seemed to be for initiation. Thus, after classifying the C-C bond cleavage based on the different types of the formed radicals, some corrections would be made to take into account the kinetic discrepancy.

The relevant reactions in the model include homolytic cleavage of C-C bonds, hydrogen abstraction, scission, and radical recombination. The model makes use of the random scission hypothesis to predict the reaction pathways. This means that intramolecular H-abstractions are only considered in a pre-determined portion of the reacting chains when these are a target for backbiting reactions in a defined dt.

One of the downsides of this method is that using a single step Arrhenius approach does not work for a wide range of heating rates, conversion, or temperature values, falling short of the usability the mechanism could have in different scenarios, and preventing it from being used outside this scope of the study. Furthermore, at the time, the information available on the topic was not specific in the amount of polymer used in the experiments neither on heating rates for the evaluation of possible mass nor heat limitations, which led to the need of producing new data on polyolefins thermal degradation. This also meant that scaling of the process could not be achieved. Lastly, considering the most common reaction families and pathways in pyrolysis, one very important type of reaction was not considered in the model, the backbiting reactions. This means that a considerable number of products were not considered to form in theory as well as the physical aspects of the degradation process [21]. This mechanistic model served as the first draft and attempt in describing polymer pyrolysis, being a big breakthrough in the field, that promoted enhanced research from different research groups throughout the years. However, results show a discrepancy when compared to experimental data, which is something that the work of Faravelli et al. [21] aimed to correct, and that is explained below.

Faravelli et al. (1999)

As a means to improve the kinetic scheme implemented in the first draft by Ranzi et al. [28], additional suppositions were made such as neglecting heat transfer limitations and assuming that the polymer melt temperature is constant. Since this study was performed under the conditions of a bubbling reactor, the mass transfer was considered to be the controlling factor, meaning that the Fick equation was introduced. At the same time, the most relevant modification was the addition of backbiting reaction steps to the already assumed random scission hypothesis. This change allowed the model to correctly predict relative and absolute amounts of the different chain length species, revealing peaks for lighter products which are typically formed in backbiting reactions (oligomers with 6, 10, and 14 carbon atoms), and a decreasing trend for heavier products formed in cracking reactions before the gas phase.

To simplify the large number of species, present during PE pyrolysis, the intermediate steady-state hypothesis was adopted, assuming that the concentration of intermediate species, radicals, remains constant throughout the reaction. Thus, they are consumed at the same rate as they are produced. This is a reasonable assumption since radicals are unstable compounds that tend to disappear very quickly, existing only transiently between the reactants and products.

The product distribution depends on two factors: the type of C-C bonds and the relative amount of the different types of radical chains. In the former (already discussed in [28]), the position of the beta carbon in the chain determines the formed radical which will, in turn, determine the resulting product. For example, propylene formation is favored when an allyl position is involved during $\beta - scission$. The latter, which was a development in the model, has to do with probability, since if radicals appear in certain positions more than in others, then the products formed will derive from this, and not from other radicals in different positions, tendentially. Some reaction steps like intramolecular H-abstractions do not show an effect on the total concentration of radical species, but they do affect their distribution.

An insistent problem continues to be the lack of basic knowledge on technologies for large scale processes, which still require research towards “thermal efficiency, operational problems, and pollutant emission control” [21]. The future work involved the further development of the model, which was done by the same research group, culminating in a published article in 2007 by Marongiu et al. [19].

Marongiu et al. (2007)

In this work, besides PE and PP, polystyrene (PS) was also analyzed, aiming to unify the thermal degradation process for these three vinyl polymers in the liquid state, based on a defined set of radical reactions. The kinetic parameters were considered to be very similar to the ones estimated for the gas phase [28]. Here, both discrete approaches and the method of moments were implemented to solve the numerical equations from the large reactions’ kinetic scheme.

Both works previously reviewed failed to account for the differences in the starting material and in describing the reaction process over wide ranges of operating conditions. In Faravelli et al. [21] a very good fit was achieved between the resulting product distribution and respective experimental studies.

In Marongiu et al. [19] the method of moments was studied, aiming to overcome the struggles the last works encountered. This method models the average properties of the polymers and the distinction between species is based on the chemical structure of the polymeric chain. It shows that backbiting reactions become less relevant as pyrolysis proceeds, unlike random scission reactions, which become more important as pyrolysis progresses. The method also takes advantage of the quasi-steady-state approximation (QSSA) to estimate the workings of radical’s propagation. If a lumped reduction method were to be implemented, then a reduction in the system’s overall size could be achieved, if discrete sections for the long-chain molecules were assumed [29].

Three different numerical approaches were analyzed and compared, focusing on describing the main reaction classes and on the definition of the intrinsic kinetic rate parameters.

1. The large balance equations' system for all species with a quasi-steady-state approximation (QSSA) for a global propagating radical.
2. The method of moments describing the statistical distribution and polymer's evolution always with QSSA.
3. The method of moments describing the statistical distribution and all the species' evolution without QSSA.

Some of the most relevant results showed that the backbiting reactions were responsible for the formation of specific products with 6, 10, and 14 carbon atoms but that random scission remains the main reaction class in the propagation stage for both PE and PP, even at high temperatures.

The conclusion of the study in both dynamic and isothermal experiments, unveiled the applicability of the model to different polymers, highlighting its flexibility. For polyethylene, pyrolysis happened at one step degradation and no char was formed. Furthermore, the results were validated over a very wide range of conditions by comparison with model predictions and measurements obtained through thermogravimetric analyses (TGA).

Levine et al. (2009)

After developing mechanistic models for the thermal degradation of polystyrene, polypropylene, and mixtures of these two main plastic polymers, in 2009 Levine & Broadbelt [4] developed another mechanistic model, this time for high-density polyethylene pyrolysis, basing their modeling framework in the previously developed works. The experimental data used to compare the model was performed by the work of De Witt et al.[30] who used Pyrex ampules and placed them in a fluidized sand bath. The main study focus was the evolution of low molecular weight products formed with time through mainly unzipping, backbiting, and random scission reactions.

As mentioned before, unzipping reactions are a succession of end-chain $\beta - scissions$ which yield a monomer from the polymer chain, thus it can be seen as the contrary of polymerization. The products from backbiting reactions (or intramolecular H-shifts) are defined as non-statistical because not all the products have the same probability of being produced, due to the steric hindrance that influences where the hydrogen transfer reactions occur, directly act on the product distribution. As for the products from random scission, these are defined as statistical, since the probability of them being produced is the same, given that each abstractable hydrogen from the main polymer chain is equally available to suffer this reaction.

The reaction pathway that presented to be the most relevant and controlling, was random scission, a conclusion made when analyzing the time evolution curves of specific LWMPs, which met the same results the Marongiu and Faravelli group reported in 2007 [19]. The backbiting pathway played a complementary role, while the unzipping pathway was not competitive at all. Especially for polyethylene, both backbiting and random scission reactions are more significant because every mid-chain hydrogen produces an equally stable secondary carbon radical. Nevertheless, not all radical types have the same chance of being produced. For specific mid-chain radicals via intramolecular hydrogen transfer, it was shown that backbiting reactions yield very specific products according to the radical position. Thus, these backbiting reactions favored an $x \rightarrow x + 4$-intramolecular hydrogen transfer giving rise to products in the range of C_8-C_{24}, both alkanes, and alkenes [10].

This kind of result is only possible to achieve and discuss since tracking of the evolution of specific species was performed. Although this is a promising mechanistic model it still presents some limitations in terms of analyzing broad product spectrum and the differences between inter and intramolecular hydrogen transfer. Moreover, the mechanism is not freely available neither for consultation nor use.

3.2.3. Kinetic Monte Carlo

Poutsma (2003)

Considering some serious data gaps on pyrolysis of PE that were imperative to understand the workings of the mechanism, Poutsma [26] compiled a series of arguments and results to enlighten about the major problems with research up to that point, what was missing, and how it affected the delay in developing a reactor design and specifications suitable for the process at hand. Some of the gaps included H:C material balances, product distribution for a wide range of operating conditions such as the conversion of initial material in isothermal closed systems, and inconsistencies in experimental analysis especially for products of lower volatility.

Taking advantage of the kinetic Monte Carlo, several simulations by formal superposition took place to find the compositions of volatiles at finite conversions, and temperature and conversion effect was also evaluated. The results found that random scission reactions should dominate at lower values of temperature, while the backbiting proportion should increase with increasing temperature. This makes the bridge with the result showing that the apparent BB:RS ratio for the volatiles should decrease with increasing conversion values, meaning that the ANE:DIENE ratio also follows the same behavior since backbiting is responsible for producing mainly alkanes and alkenes, while random scission mostly contributes to the production of dienes.

Németh (2007)

The Németh research was a breakthrough in the field since it was the first developed model ready to work with any input given, opening a path to an easier study of different polymers that pose difficulties in recycling and reuse.

The main goals were to conclude if a model for tetracontane's thermal degradation would comply with measured HDPE degradation, using a stiff differential equation solver for the numerical integration, such as Monte Carlo [10], and to determine the impact of $\beta - scission$, H-abstraction and isomerization reactions in product distribution, as well as the role of radicals through contribution analysis.

Therefore, the thermal degradation was modeled as a "detailed reaction mechanism consisting of simultaneous or subsequent H-abstraction, $\beta - scission,$ and backbiting reactions" on tetracontane, which could be described as a monodisperse polymer with 40 carbon atoms. The model assumes that all propagation reactions have the same rate constant, and to solve the reaction's balance equations, a steady-state approximation was assumed which should behave as seen in Figure 6.

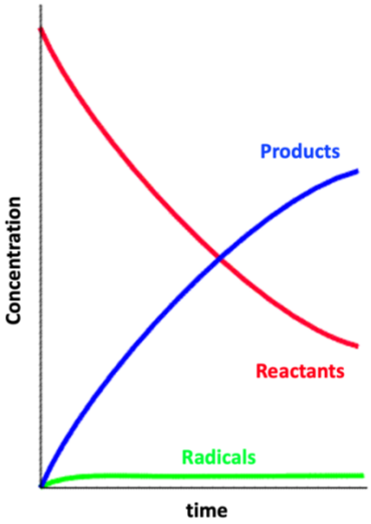

Figure 6. Typical evolution of products, reactants, and intermediates with time, when steady state is considered to obtain the solution of the differential equation system.

The experimental work was performed isothermally, at 500 °C, with a residence time of 20 s, and in a micropyrolizer reactor.

Results Deconstruction

As with any free radical mechanism, the mandatory first step is initiation, where homolytic scission of C-C bonds of the polymer occurs, producing alkyl radicals that will start the propagation step. The reaction pathway is summarized below.

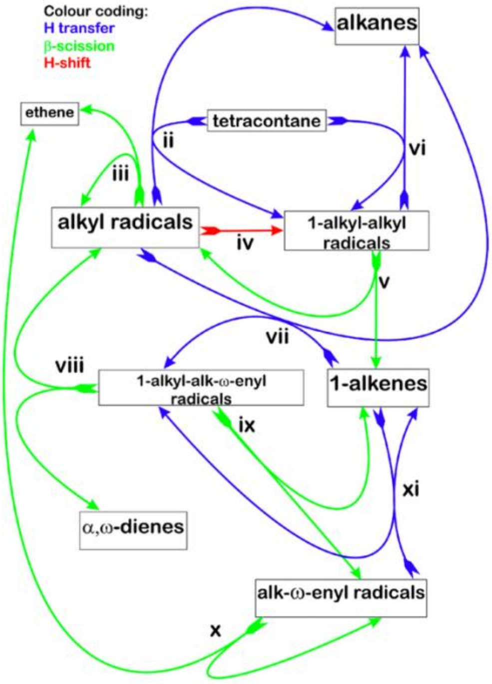

ii) H-abstraction to form *n*-alkanes (ANE) and secondary alkyl radicals ($R_S^{\bullet}$).

iii) $\beta - scission$ produces ethylene and smaller primary alkyl radicals ($R_P^{\bullet}$).

iv) Backbiting (1-4, 1-5, and 1-6 H-shifts) forms secondary alkyl radicals ($R_S^{\bullet}$), after a rearrangement to create 5-, 6- and 7- membered rings.

v) $\beta - scission$ of secondary alkyl radicals ($R_S^{\bullet}$) generates 1-alkenes (ENE) and primary alkenes radicals ($R_P^{\bullet}$).

Figure 7. *Representation of the main reaction pathways for low polymer conversion. Adapted from [8].*

vi) Secondary alkyl radicals formed in *iv)* can abstract and transfer hydrogens from the polymer.

vii) Intermediate step to produce dienes. Primary alkyl radicals ($R_P^{\bullet}$) and 1-alkenes (ENE) through H-abstraction produce secondary 1-alkenyl radicals (‘$R_S^{\bullet}$).

viii) The secondary 1-alkenyl radicals can suffer $\beta - scission$ to form α or $\omega - diene$ (DIENE), and primary alkyl radicals ($R_P^{\bullet}$), away from the existing double bond.

ix) The secondary 1-alkenyl radicals can also form 1-alkenes (ENE) and primary ω-alkenyl radicals (‘$R_P^{\bullet}$) through $\beta - scission$ in the opposite direction from the one in *viii)*.

x) Through $\beta - scission$, primary ω-alkenyl radicals (‘$R_P^{\bullet}$) produce ethylene and smaller primary ω-alkenyl radicals.

xi) H-abstraction from 1-alkenes (ENE) by primary ω-alkenyl radicals (‘$R_P^{\bullet}$) produces 1-alkene and secondary 1-alkenyl radicals (‘$R_S^{\bullet}$).

The last stage (*xii, not represented*) is termination, where recombination of all radicals occurs. The rates of the reactions included in this stage little or nothing contribute to radical consumption, independently of the radical type. Alkane production is dominated by reaction *ii)*, highlighting the importance of the reactions’ first moments. While alkanes and alkenes concentrations are most sensitive to rate constants of $\beta - scission$, dienes are more susceptible to rate constants of H-abstractions reactions. Reaction *v)* has the highest rate for all conversion values, which means that it can yield a large number of smaller alkenes, and although reaction *iv)* is only ¼ of this value, it means that processing through these two reactions will contribute significantly to the increase in the gaseous products of the pyrolysis. The overall reaction scheme of 1000 species and 7541 reactions revealed to be very sensitive to rate constants of $\beta - scission$ in primary alkyl radicals that lead to ethane production, reactions *ii)* and *iii)*. One could extrapolate, due to the results, that both $\beta - scission$ and backbiting reactions are independent of the carbon chain length of the reactants, although this conclusion calls for more reliable experimental data and extensive study. Important to note that when following the concentration evolution of alkyl radicals with time, it was possible to see that a QSS was established within the first moments of the reaction. Other assumptions worth mentioning are that alkane decomposition was not included in the reaction scheme, due to computational constraints. Therefore, the model of HDPE as tetracontane was limited to very low conversion values, H-abstraction and H-shift reactions were only considered to happen towards an outer position (towards an inner position also occurs, albeit with a lower probability).

The main obstacle in the Németh mechanism[8] is that it is only valid for conversion values up to 1%, rendering it not proper to work under larger time frames. Other weaknesses in the mechanism are the complexity of the system and the scarcity of rate constants. Certain relevant species are also absent, meaning that important reactions are automatically out of the spectrum of the ones included in the mechanism, not to mention that the exact description of the reactions included is not made and the effect of the ones left out on the accuracy of the model is not discussed [9].

Gascoin et al. (2012)

Part 1

In 2012, an extensive review on developed models for the study of polymers degradation was assessed, as an attempt to determine if any could be used and implemented, from those already openly available. This study also started unlocking the studies of this raw material for different purposes, considering implementing it in Computational Fluid Dynamics (CFD) applications.

Some of the models reviewed were also reviewed above in this section, while others weren't included since they were not found to be of relevance. The works published in 2007 by Mastral et al. [24], in 2009 by Levine and Broadbelt [4] were rendered not suitable due to the high level of simplicity or the fact that it wasn't openly available, respectively. Also, the works of Johannes et al. [31] and Elordi et al. [32] (from 2004 and 2007 respectively, not discussed here) were too simple to be able to correctly predict the reaction in the necessary conditions.

All the available mechanisms follow a single step as an Arrhenius law or a detailed kinetic mechanism with primary and secondary reaction sets, and although they were all validated against experimental data, big discrepancies were found up to a factor 7. The discrepancies might have to do with the fact that most experimental data was obtained for polymer's recycling purpose, and not for propulsion applications. As previously mentioned, one of the interests in studying HDPE pyrolysis is its application as fuel for motors in the aerospace industry.

However, one of the most difficult aspects of studying this is the uncertainty of its origin and nature, which will determine its composition and purity, besides the vast diversity in experimental conditions and pre-assumptions. Some common problems have to deal with the low ability to rapidly producing combustible gas, which is imperative for propulsion applications. A possible solution, suggested by Gascoin et al. [13] is to inflict auto-ignition delay of the products, increasing the heat release in the engine and thus the regression rates.

This review found that only six studies with single or multi-step mechanisms were developed and that from those, none considers the chemical composition of by-products with a suitable size for Computational Fluid Dynamics (CFD) applications which can only take up to 2000 reactions. This conclusion highlights the general necessity of more experiments in relevant and useful conditions to get reliable data and correct the existing mechanisms as well as proper quantification of products to assist the study on the combustion reaction with another detailed mechanism.

Nevertheless, one existing detailed kinetic mechanism was chosen to be further developed and reduced, prospecting its implementation in a CFD code. This mechanism was chosen because it was the only one capable of quantifying the gas products by each species, instead of recurring to a global approach with a single gas compound. Thus, a second paper is published by the same authors, where the reduction of the mechanism developed by Németh et al. [8] is explained and achieved.

Part 2

The biggest motivation for this work was the reduction of the Németh mechanism up to 2000 reactions and 300 species so that it could be used in CFD applications. It is important not to forget that this needs to be achieved while maintaining precision in the chemical process and the products produced, which will lead to a more realistic simulation of a real context. Moreover, if the final goal is to use this mechanism to study how this feeding type could be used in engines for rocket propulsion, then a study on the product distribution and its effect on the system must be assessed.

Different reduction methods were studied (more information available in Gascoin paper [27]), and the authors chose to combine two techniques, rendering the mechanism with 472 species and 1713 reactions. Parallelly, an analysis of the species and reactions removed was performed, which was a very important step to present trustworthy results and to bring further insights on the effects that it caused. In **Table 2**, a summary of the species and reactions reduced can be seen and will be discussed below.

Table 2. *Comparison of species and reactions included in the original mechanism [8] and in the reduced one. Adapted from [27].*

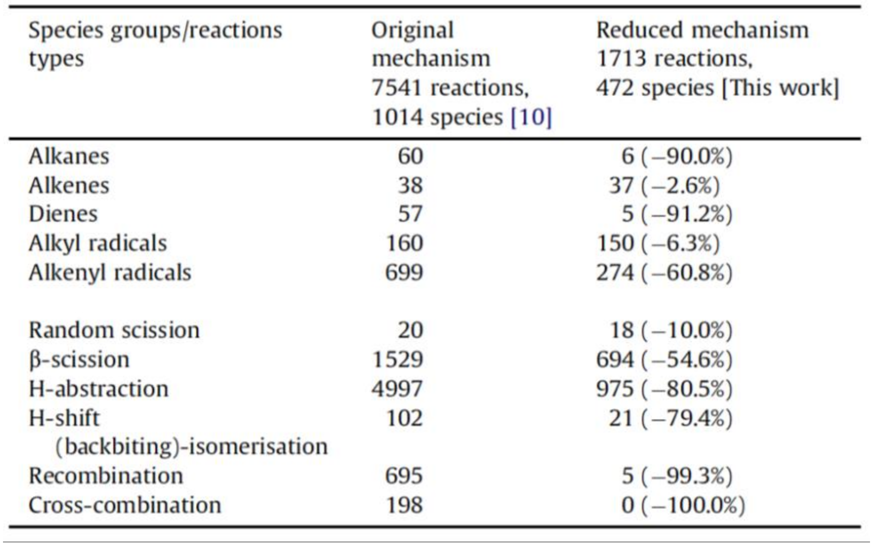

Species groups/reactions types	Original mechanism 7541 reactions, 1014 species [10]	Reduced mechanism 1713 reactions, 472 species [This work]
Alkanes	60	6 (−90.0%)
Alkenes	38	37 (−2.6%)
Dienes	57	5 (−91.2%)
Alkyl radicals	160	150 (−6.3%)
Alkenyl radicals	699	274 (−60.8%)
Random scission	20	18 (−10.0%)
β-scission	1529	694 (−54.6%)
H-abstraction	4997	975 (−80.5%)
H-shift (backbiting)-isomerisation	102	21 (−79.4%)
Recombination	695	5 (−99.3%)
Cross-combination	198	0 (−100.0%)

The most affected species were alkanes and dienes with a reduction percentage of 90% and 91.2% respectively. All alkanes from C_5 to C_{80} were removed since the most common product distribution has a majority of alkenes and small dienes, and only a very reduced distribution for alkanes for each carbon atom number which is even more prominent at higher working temperatures (above 700°C). Nevertheless, since this mechanism is thought to be coupled with their subsequent combustion, lighter alkanes were kept, as well as lighter dienes (from C_9 to C_{78} were removed) that have an important role in ethylene chemistry.

In a work published by Wampler and Levy [33], it was shown that "the distribution of dienes, alkenes, and alkanes follow a linear trend regarding the carbon atoms number", meaning that the number of alkanes can be estimated through the number of alkenes and of the carbon atoms number.

All these species reduction affects the reactions considered. As a result, all the isomerization reactions were removed, as well as the formation of alkanes from cross-combination of radicals, which was considered instead as radical lumping in this model. The transformation of alkyl radicals into dienes was also not considered due to the low importance of this species, while alkyl radicals were kept due to the importance of β-scission reactions that lead to the formation of alkenes [8,27]. Some problems with the model have been reported for 0-D computations[1], although the authors don't explain it further.

Nevertheless, this reduction allowed the authors to reduce the number of reactions and species by 77% and 53%, respectively. This lowers the computational time and already allows the kinetic mechanism to be successfully implemented in a two dimensions CFD code.

---

[1] No spatial dependency, only time dependent.

Experimental tests were performed at a temperature between 700 K and 1200 K and pressures from 1 bar to 100 bar, and they showed that the mechanism reproduced the HDPE consumption at a faster pace and kinetics, overproducing most of the species. Since this work only performed a reduction on the mechanism developed by Németh, it still lacks development in the chemical field, such as adding disproportionation reactions, hydrogen and aromatics production, and consumption and thus, the branching degree. Moreover, it is assumed that only one phase occurs throughout the process, the gas phase, while in reality, all states exist during the thermal degradation of large polymers [9].

3.3. Conclusion

The most critical conclusion is that no kinetic modeling for HDPE, or any polymer for that matter, exists that can correctly account for heat and mass transfer limitations while appropriately predicting gas-phase products in detail. Since a long-term goal of these studies is to couple gasification reactions to investigate the usability of HDPE as raw material in engine combustion, Németh's mechanism was determined as the most suitable, from the available models. It allowed quantifying the gas products by identifying each species instead of using a global approach with a single gas compound. Subsequently reduced by Gascoin et al. [27] and validated against broad experimental data, it entitled 1713 reactions and 472 species in the end.

Unfortunately, however, this mechanism was not available for further use, thus a new approach and path were decided and developed at Ghent University. Developed by Beirnaert K. [9], a new microkinetic mechanism followed the same line of thought as the Németh mechanism. The non-reduced version of this mechanism was available for research purposes thus serving as a reference even though significant changes were carried out.

In this work, Beirnaert's mechanism was used to study the effect on product distribution, as a function of the feed length, to understand the mechanism's main strengths and weaknesses. In the end, this study should support the decision of what reactions should further be included or excluded from the mechanism, as well as the assumed kinetic parameters, which should lead towards more realistic results and a more flexible mechanism to be used for any initial substrate.

Chapter 4. Cantera Mechanism File Creator - Pyrolysis of Linear Chain Alkanes (C_xH_y)

This chapter aims to explain the main differences between the micro-kinetic mechanisms developed by Németh et al. [8] and Beirnaert K.[9], as well as explain how this kinetic modeling brings advantages to the field and shows a strong potential for its implementation in the industry.

4.1. Mechanism's development

Similar to the work developed by Németh, a model compound for the polymer consisting of a linear-chain alkane with 40 carbon atoms, tetracontane, was adopted (applicable for PE without any branches). For any other linear-chain alkane model compound, the line of thought remains identical, since the mechanism is prepared to deal with different carbon length polymers, yielding the relevant reactions and products accordingly.

To understand the reactions and species considered, the important nomenclature is summarized below.

Table 3. Nomenclature and representation of the main species considered in the mechanism.

	Description	***Schematic representation***
X	Carbon number	-
Y	Radical position	-
ANEZ [2]	Linear alkanes	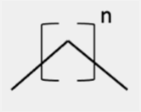
ENEZ	Linear alkenes	
DIENEZ	Linear α,ω-dienes	
RXrY	Alkane radicals (alkyl)	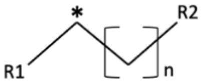
RENEXrY	Alkene radicals (allyl)	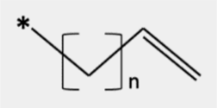

The next step is to decide on the relevant reactions to incorporate, thus **Table 4** comprises a comparison between Németh and Beirnaert's mechanisms, in terms of reactions that were considered in each case. Only the right side of the table will be explained in more detail since this is the crucial part to follow the explanations in the remaining work. It should be noted that the nomenclature is the same as the one present in Beirnaert's work, where it was used to explain how the complex chemistry of pyrolysis was broken down and introduced into coding language.

---

[2] Z is only used for the initiation and termination reactions. 1 < Z < 80.

Table 4. *Overview of all reactions included in the Németh and Beirnaert K. mechanisms* [3].

	NÉMETH [8,9]		**BEIRNAERT K.** [9]	
INITIATION	Thermal scission *(i)*	$P40 => RXr1 + R(40-X)r1$	Thermal scission *(i)* + *(i)*$_a$	$ANEZ => RXr1 + R(Z-X)r1$
	Thermal scission *(i)*$_a$	$P40 => R3r1 + R37r1$	Thermal scission *(i)* + *(i)*$_a$	$ENEZ => RENEXrX + R(Z-X)r1$
	-	-	Thermal scission *(i)* + *(i)*$_a$	$DIENEZ => RENEXrX + RENE(Z-X)r(Z-X)$
PROPAGATION	H-abstraction *(ii)*	$RXr1 + P40 => ANEX + R40rY$		
	Unzipping (β-scission) *(iii)*	$RXr1 => R(X-2)r1 + ENE2$	Unzipping (β-scission) *(iii)*	$RXr1 => R(X-2)r1 + ENE2$
	Unzipping (β-scission) *(iii)*$_{Me}$	$R3r1 => R1r1 + ENE2$	-	-
	Unzipping (β-scission) *(x)*	$RENEXr1 => RENE(X-2)r1 + ENE2$	Unzipping (β-scission) *(x)*	$RENEXrX => RENE(X-2)r(X-2) + ENE2$
	β-scission *(v)*	$R40rY => R(40-Y-1)r1 + ENE(Y+1)$	β-scission *(v)* + *(v)*$_{Me}$	$RXrY => R(X-Y-1)r1 + ENE(Y+1)$
	β-scission *(v)*	$R40rY => ENE(40-Y+2) + R(Y-2)r1$	β-scission *(v)* + *(v)*$_{Me}$	$RXrY => ENE(X-Y+2) + R(Y-2)r1$
	β-scission *(v)*$_{Me}$	$R40r3 => ENE39 + R1r1$	-	-
	β-scission *(viii)*	$RENEXrY => DIENE(Y+1) + R(X-Y-1)r1$	β-scission *(viii)* + *(viii)*$_{Me}$	$RENEXrY => DIENE(Y+1) + R(X-Y-1)r1$
	β-scission *(viii)*$_{Me}$	$RENEXr(X-2) => DIENE(X+1) + R1r1$	-	-
	β-scission *(ix)*	$RENEXrY => ENE(X-Y+2) + RENE(Y-2)r1$	β-scission *(ix)*	$RENEXrY => ENE(X-Y+2) + RENE(Y-2)r(Y-2)$
	Backbiting 1,4 (H-shift) *(iv)*$_{14}$	$RXr1 => RXr4$	Backbiting 1,4 (H-shift) *(iv)*$_{14}$	$RXr1 => RXr4$
	Backbiting 1,5 (H-shift) *(iv)*$_{15}$	$RXr1 => RXr5$	Backbiting 1,5 (H-shift) *(iv)*$_{15}$	$RXr1 => RXr5$
	Backbiting 1,6 (H-shift) *(iv)*$_{16}$	$RXr1 => RXr6$	Backbiting 1,6 (H-shift) *(iv)*$_{16}$	$RXr1 => RXr6$
	-	-	Backbiting 1,4 (H-shift)	$RENEXrX => RENEXr(X-4)$
	-	-	Backbiting 1,5 (H-shift)	$RENEXrX => RENEXr(X-5)$
	-	-	Backbiting 1,6 (H-shift)	$RENEXrX => RENEXr(X-6)$

---

[3] *(i) – (xii)* are the reaction pathways defined in Németh et al. [8]

	-	-	Backbiting x+4 (H-shift)	$RXrY => RXr(Y+4)$
	-	-	Backbiting x+5 (H-shift)	$RXrY => RXr(Y+5)$
	-	-	Backbiting x+6 (H-shift)	$RXrY => RXr(Y+6)$
	-	-	Backbiting x+4 (H-shift)	$RENEXrY => RENEXr(Y+4)$
	-	-	Backbiting x+5 (H-shift)	$RENEXrY => RENEXr(Y+5)$
	-	-	Backbiting x+6 (H-shift)	$RENEXrY => RENEXr(Y+6)$
	H-transfer (inter) *(vi)*	$RXrZ + P40 => ANEX + R40rY$	H-transfer (inter) *(vi)*	$RXrZ + ANEK => ANEX + RKrY$
	-	-	H-transfer (inter) *(vi)*	$RENEXrZ + ANEK => ENEX + RKrY$
	H-transfer (inter) *(vii)*	$ENEX + R1r1 => ANE1 + RENEXrY$	H-transfer (inter) *(vii)*	$RXrZ + ENEK => ANEX + RENEKrY$
	H-transfer (inter) *(vii)*	$ENEX + R2r1 => ANE2 + RENEXrY$	-	-
	H-transfer (inter) *(vii)*	$ENEX + R3r1 => ANE3 + RENEXrY$	-	-
	H-transfer (inter) *(xi)*	$ENEX + RENEZr1 => ENEZ + RENEXrY$	H-transfer (inter) *(xi)*	$RENEXrZ + ENEK => ENEX + RENEKrY$
TERMINATION	Recombination *(xii)*	$2\,RXrZ => C(2X)$ $2\,RXrZ => P40$ $2\,RXrZ => ANE(2X)$	Recombination *(xii)*	$RXrY + RZrK => ANE(X+Z)$
	Recombination *(xii)*	$2\,RENEXrY => CENE(2X)$ $2\,RENEXrY => DIENE(2X)$	Recombination *(xii)*	$RENEXrY + RENEZrK => DIENE(X+Z)$
	-	-	Recombination *(xii)*	$RXrY + RENEZrK => ENE(X+Z)$

As it can be observed from **Table 4**, some reactions were not considered in the new mechanism, while others were added. A few of the decisions had to do with the assumed kinetic parameters but the most propelling reason was to adapt for any polymeric chain length thus considering all alkane radicals possible. Two other main differences between the models are the species allowed to initiate and the decision on branched species. While branched species are considered in the Németh mechanism (they follow the same reaction paths and take on the same kinetic values as non-branched species), they were not included in Beirnaert's mechanism. On the other hand, this mechanism allows for all species to initiate the free-radical mechanism, including saturated species, which enables the usage of this mechanism for higher conversion values. Moreover, all reaction types are included for every species, hence the higher number of reactions on the right side of **Table 4**. For backbiting reactions, more possibilities were added including backbiting of primary alkene radicals and secondary backbiting reactions. Considering hydrogen transfer reactions, H-abstraction from saturated alkane species by 1-alkene radicals was also added. The final stage of the mechanism, termination, also evaluates the recombination of two primary 1-alkene radicals as an alternative to form α,ω-dienes.

All these additions make the mechanism heavier, which consequently increases the computational time. While the reduced Németh mechanism entitles 1713 reactions and 472 species, the reduced form of Beirnaert's mechanism was only able to reduce to 9000 reactions and 8965 species. It should be noted that the reduction method applied for this mechanism is based on a simplistic mechanism approach from Cantera [34] that focuses on the reduction of reactions, meaning that the reduction in species is only a secondary effect.

For a clearer understanding of the reaction path, **Figure 8** should be considered.

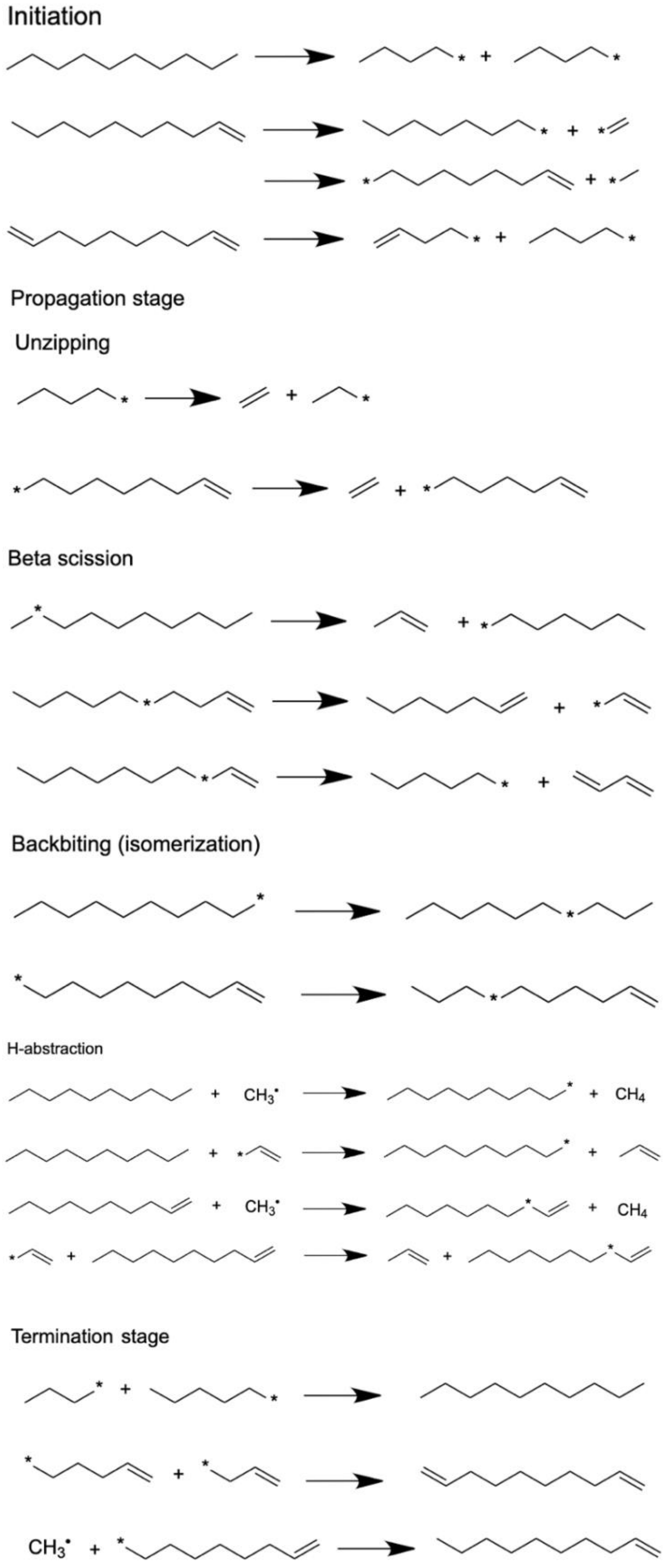

__Figure 8__. Reaction path considered for Beirnaert's mechanism [9] and present work.

4.2. Construction of the Mechanism

To start developing the mechanism, three different initial substrates are considered – alkanes (ANE), alkenes (ENE), and α, ω-alkedienes (DIENE) – which are the main components produced after the C-C homolytic reaction undergone by the polymer.

The products obtained when considering each of these substrates will vary, hence the need for 3 different sets of code, each nested for loops. Within each of these sets of code, the respective values of the pre-exponential factor and activation energy are accessed from an available .csv file which is read accordingly. A brief explanation of each of these components and their characteristics will be made to help to understand the mechanism in this study.

Alkanes

Alkanes are hydrocarbons with simple C-C bonds, with the general formula - C_nH_{2n+2}. Alkyl radicals are alkanes that have lost 1 hydrogen atom.

Alkenes

Alkenes are unsaturated hydrocarbons that contain a C-C double bond with the general formula C_nH_{2n}. Important to note that if there is more than one C-C double bond then we start talking about alkedienes. Alkenes have two hydrogen atoms less than the corresponding alkane with the same carbon number and the simplest alkene is ethylene (C_2H_4), or ethene by IUPAC [35]. Allyl radicals are constituted of a methylene bridge (-CH_2-) attached to a vinyl group (-$CH=CH_2$).

Alkedienes

Alkedienes are compounds that contain two double bonds between two carbon atoms. α,ω-alkedienes have the general formula $(CH_2)_n(CH=CH_2)_2$. Two double bonds are located at each end of the molecule.

To shed some light on the basis upon which the mechanism is developed, **Figure 9** should be taken into consideration. Also consider **Figure** A 1 in the appendix to have a broader understanding of the kinetic modeling structure.

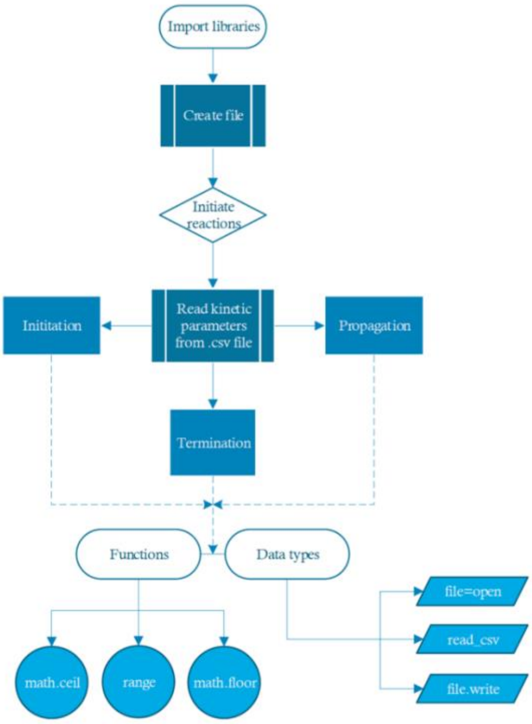

Figure 9. *Flowchart explaining the tools used in developing the kinetic reaction mechanism.*

Before starting, in python language (or any other programming languages), it is important to import libraries that are going to be used and referred to: In this case, libraries such as *math* and *pandas*. The file created and opened is a mechanism file and includes every relevant reaction considered, *n*. The used functions, as well as the data type of simple commands and actions, are also schematized. As explained before, three sets of code are developed, each for every stage of the free radical mechanism. Inside these sets of code, three functions are used, range, math.ceil, and math.floor. *math* calls for mathematical functions included in this library, imported at the beginning. The range function returns a sequence of numbers that start from 0 and increments by 1 ending at a specified number (End-Start+Step). [36]

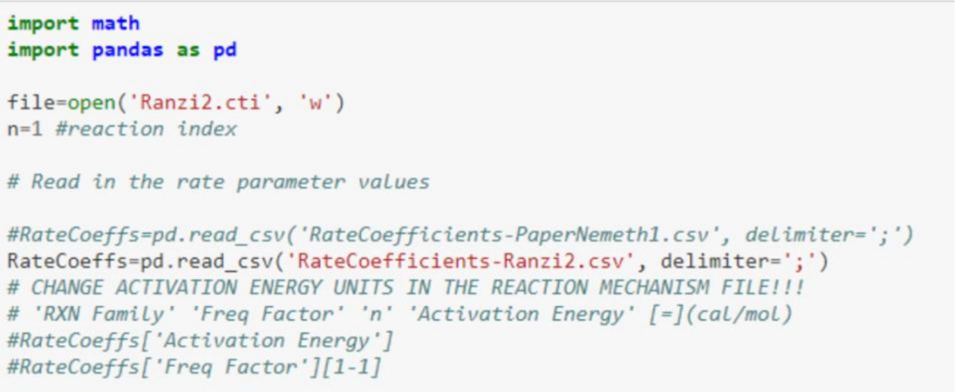

```
import math
import pandas as pd

file=open('Ranzi2.cti', 'w')
n=1 #reaction index

# Read in the rate parameter values

#RateCoeffs=pd.read_csv('RateCoefficients-PaperNemeth1.csv', delimiter=';')
RateCoeffs=pd.read_csv('RateCoefficients-Ranzi2.csv', delimiter=';')
# CHANGE ACTIVATION ENERGY UNITS IN THE REACTION MECHANISM FILE!!!
# 'RXN Family' 'Freq Factor' 'n' 'Activation Energy' [=](cal/mol)
#RateCoeffs['Activation Energy']
#RateCoeffs['Freq Factor'][1-1]
```

Figure 10. *Start of the algorithm.*

Initialization

Alkane

The simplest form of an alkyl radical is the methyl radical ($CH_3^{\bullet}$) which means that the lowest molecule obtained will have a minimum of 1 carbon atom.

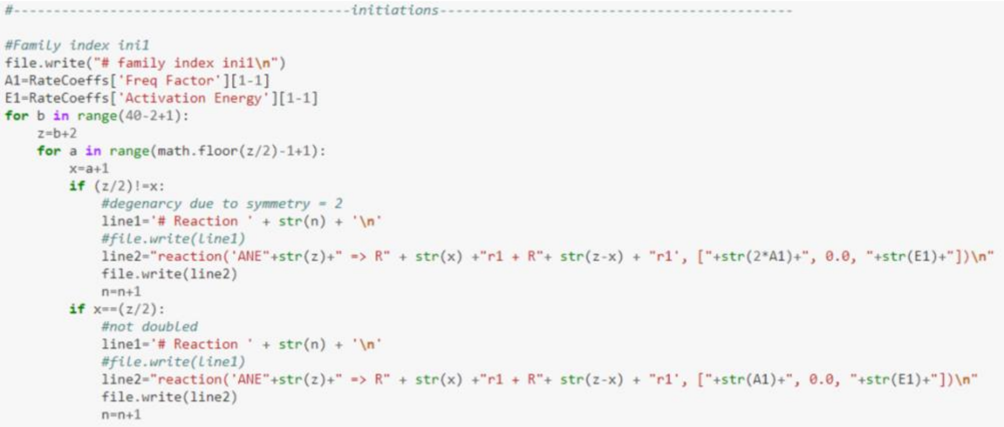

```
#------------------------------------------initiations------------------------------------------

#Family index ini1
file.write("# family index ini1\n")
A1=RateCoeffs['Freq Factor'][1-1]
E1=RateCoeffs['Activation Energy'][1-1]
for b in range(40-2+1):
    z=b+2
    for a in range(math.floor(z/2)-1+1):
        x=a+1
        if (z/2)!=x:
            #degenarcy due to symmetry = 2
            line1='# Reaction ' + str(n) + '\n'
            #file.write(line1)
            line2="reaction('ANE"+str(z)+" => R" + str(x) +"r1 + R"+ str(z-x) + "r1', ["+str(2*A1)+", 0.0, "+str(E1)+"])\n"
            file.write(line2)
            n=n+1
        if x==(z/2):
            #not doubled
            line1='# Reaction ' + str(n) + '\n'
            #file.write(line1)
            line2="reaction('ANE"+str(z)+" => R" + str(x) +"r1 + R"+ str(z-x) + "r1', ["+str(A1)+", 0.0, "+str(E1)+"])\n"
            file.write(line2)
            n=n+1
```

Figure 11. *Initiation reaction for alkanes.*

The first for loop means that every compound will be coursed through, from #C=2 until #C=40. Within this first for loop, a second for loop is implemented. The intent is to take into account the symmetry of the alkane chain, i.e, a chain with a radical on the first carbon atom is identical to a chain with a radical on the last carbon atom meaning that the output reaction will be the same. In this way only the chain length from 1 carbon atom until 20 carbon atoms will be looked for, decreasing the complexity of the algorithm.

Inside both for loops a conditional statement is written to look for degeneracy states. Degeneracy states have the same energy and typically result from the molecule symmetry. Thus, when going through the code, the first time when z/2=x, it means that there is no degeneracy. When it finds repeated values then z/2 is no longer equal to x, and degeneracy happens. This is a doubled degeneracy (symmetry axis in the center of the molecule) so the pre-exponential factor needs to be counted twice. For better comprehension and visualization of this concept, **Figure 12** should be used as a reference.

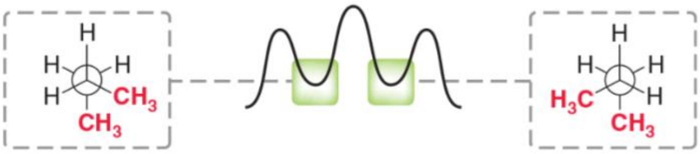

Figure 12. *Two staggered conformations that exhibit degenerate interactions. Adapted from* [18].

When every linear chain is run through for a specific reaction, then the next reaction for the same substrate (alkane in this case) can be evaluated.

Thus, every reaction will be written in the output file as follows:

$$\text{ANE}_{Z} \Rightarrow \text{R}_{X}\text{r1} + \text{R}_{Z\text{-}X}\text{r1}, [\text{A1}, 0.0, \text{E1}]$$

In conclusion, since this reaction family is constructed for end-chain alkyl radicals (r1), the scission results in a radical with X carbon numbers and the remaining chain is left with (Z-X) carbon numbers.

Alkenes

A similar line of thought as to what was explained for alkanes was considered to populate the reaction mechanism, although with some differences worth mentioning. The first difference is that adding to the formation of alkyl radicals, there will also be the formation of allyl radicals. Thus, the respective pre-exponential factor and activation energy need to be considered, explaining the two lines used:

A1 = RateCoeffs[‘Freq Factor’][1-1][4]
A2 = RateCoeffs[‘Freq Factor’][2-1]

The smallest allyl radical possible to form has 3 carbon atoms. Then, when starting the for loop, the range function courses through molecules with #C=3 until #C=39.

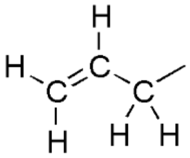

Figure 13. *Representation of the smallest allyl radical possible.*

Note

Range function going only until carbon length 39 can be explained based on the fact that C40 reactions cannot happen in a single step.

The second for loop means to ascertain the radical position. If (Z-X) =3, then an allyl radical is formed.

Here, we need to assess the radical position hence the way to write the reaction on the output file:

---

[4] A1 for alkyl radicals and A2 for allyl radicals.

```
Line2= “reaction(‘ENE” + str(z) + “=> RENE” + str(x) + “r” + str(x) + “ +R” + str(z-x) + “r1’,
[“str(A1)+”,0.0,”+str(E1)+”]\n”
```

Depending on where the double C-C bond is located in the alkene, the radical position will vary.

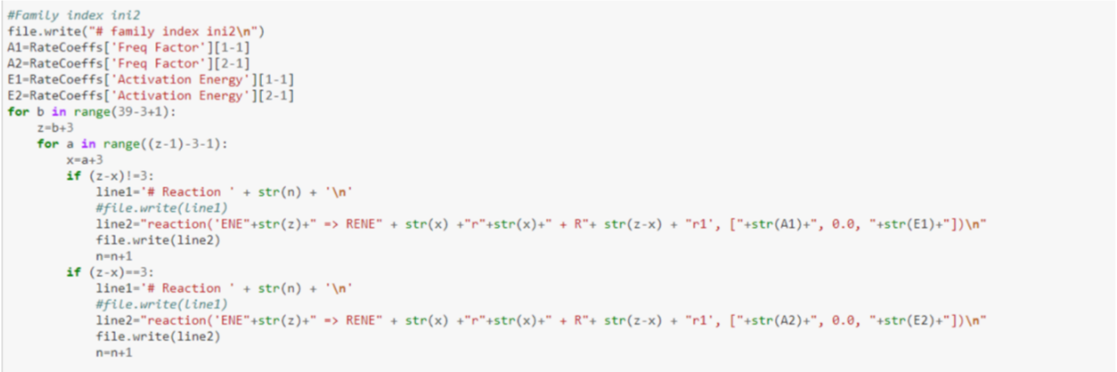

```
#Family index ini2
file.write("# family index ini2\n")
A1=RateCoeffs['Freq Factor'][1-1]
A2=RateCoeffs['Freq Factor'][2-1]
E1=RateCoeffs['Activation Energy'][1-1]
E2=RateCoeffs['Activation Energy'][2-1]
for b in range(39-3+1):
    z=b+3
    for a in range((z-1)-3-1):
        x=a+3
        if (z-x)!=3:
            line1='# Reaction ' + str(n) + '\n'
            #file.write(line1)
            line2="reaction('ENE"+str(z)+" => RENE" + str(x) +"r"+str(x)+" + R"+ str(z-x) + "r1', ["+str(A1)+", 0.0, "+str(E1)+"])\n"
            file.write(line2)
            n=n+1
        if (z-x)==3:
            line1='# Reaction ' + str(n) + '\n'
            #file.write(line1)
            line2="reaction('ENE"+str(z)+" => RENE" + str(x) +"r"+str(x)+" + R"+ str(z-x) + "r1', ["+str(A2)+", 0.0, "+str(E2)+"])\n"
            file.write(line2)
            n=n+1
```

Figure 14. *Initiation reaction for alkenes.*

<u>Alkedienes</u>

The scission of alkedienes results in two alkene molecules which will then form an alkyl and an allyl radical. Thus, both values for the pre-exponential factor (A1 and A2) and the activation energy (E1 and E2) are needed as input.

To go through every chain length, we start in #C=39 until #C=6, because that is the minimum carbon atoms possible to have in alkedienes.

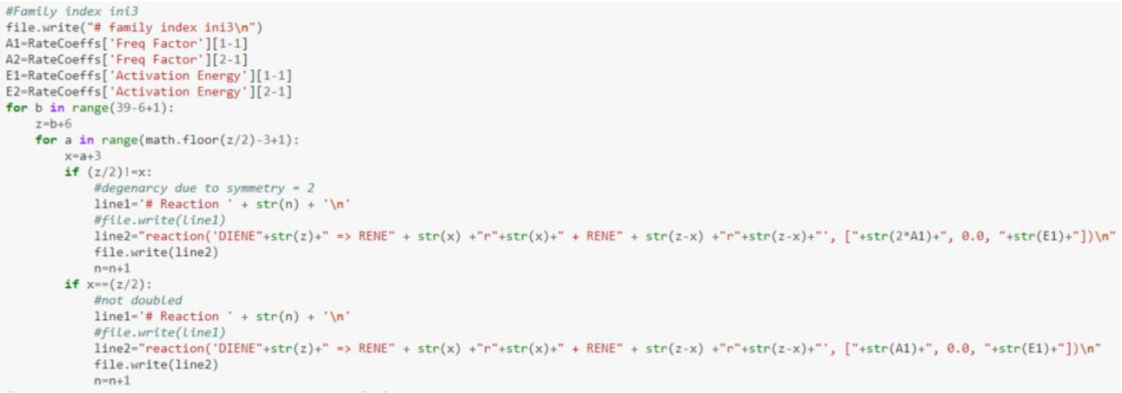

```
#Family index ini3
file.write("# family index ini3\n")
A1=RateCoeffs['Freq Factor'][1-1]
A2=RateCoeffs['Freq Factor'][2-1]
E1=RateCoeffs['Activation Energy'][1-1]
E2=RateCoeffs['Activation Energy'][2-1]
for b in range(39-6+1):
    z=b+6
    for a in range(math.floor(z/2)-3+1):
        x=a+3
        if (z/2)!=x:
            #degenarcy due to symmetry = 2
            line1='# Reaction ' + str(n) + '\n'
            #file.write(line1)
            line2="reaction('DIENE"+str(z)+" => RENE" + str(x) +"r"+str(x)+" + RENE" + str(z-x) +"r"+str(z-x)+"', ["+str(2*A1)+", 0.0, "+str(E1)+"])\n"
            file.write(line2)
            n=n+1
        if x==(z/2):
            #not doubled
            line1='# Reaction ' + str(n) + '\n'
            #file.write(line1)
            line2="reaction('DIENE"+str(z)+" => RENE" + str(x) +"r"+str(x)+" + RENE" + str(z-x) +"r"+str(z-x)+"', ["+str(A1)+", 0.0, "+str(E1)+"])\n"
            file.write(line2)
            n=n+1
```

Figure 15. *Initiation reaction for alkedienes.*

The two alkene radicals formed are referred to as RENE. One with as many carbon numbers as the radical position X and the other with as many carbon numbers as the total Z minus the radical position X, which is indicated in the line of code as,

```
RENE+str(x) + r+str(x)+ + RENE+str(z-x) + r+str(z-x)+
```

As many carbon numbers as the carbon number where the radical is.

Total carbon numbers – carbon number where the radical is.

Similarly to what was explained for alkanes, when degeneracy is a possibility, the pre-exponential factor is doubled. To ascertain the degeneracy, one can think of an alkediene as two units of alkenes, which means that by finding the integer number of z/2 (math.floor(z/2)) two alkenes are obtained. Since the minimum number of carbons in an alkene is 3, the respective line of code will be:

```
for a in range (math.floor(z/2)-3+1)
```

Propagation

*Unzipping (*End-chain *β-scission)*

Unzipping reactions are end-chain β-scission reactions that produce monomers and smaller radicals. The first step is to assess if the reaction is happening to an alkane or alkene radical. These two types have to be treated separately since the product is different.

Alkanes

To go through each chain length a for loop is implemented. If the free radical is in the carbon number three then, upon reaction, a methyl radical will form, separating itself from the remaining chain. If not, then it will form another primary alkane radical (alkyl). The input values are A2 and E2 for the methyl radical and A1 and E1 for the alkyl, respectively. Ideally the corresponding rate coefficient for every carbon length molecule would be known and accessed in the file to reproduce truer and more reliable results.

Alkenes

For alkenes, instead of a methyl radical, a 1-alkene radical will form. Here the for loop implemented aims to go through every chain from carbon atom number 5 until 39.

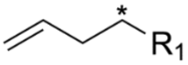

Figure 16. *Representation of an alkene with five carbon atoms.*

In both cases, the radicals will have 2 fewer carbon atoms which give rise to the monomer.

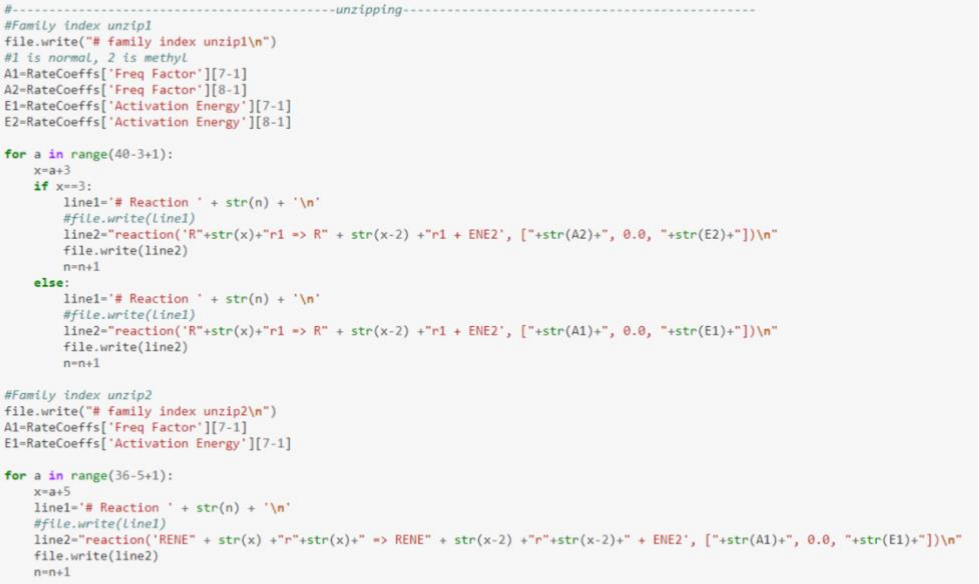

```
#--------------------------------------------unzipping----------------------------------------------
#Family index unzip1
file.write("# family index unzip1\n")
#1 is normal, 2 is methyl
A1=RateCoeffs['Freq Factor'][7-1]
A2=RateCoeffs['Freq Factor'][8-1]
E1=RateCoeffs['Activation Energy'][7-1]
E2=RateCoeffs['Activation Energy'][8-1]

for a in range(40-3+1):
    x=a+3
    if x==3:
        line1='# Reaction ' + str(n) + '\n'
        #file.write(line1)
        line2="reaction('R"+str(x)+"r1 => R" + str(x-2) +"r1 + ENE2', ["+str(A2)+", 0.0, "+str(E2)+"])\n"
        file.write(line2)
        n=n+1
    else:
        line1='# Reaction ' + str(n) + '\n'
        #file.write(line1)
        line2="reaction('R"+str(x)+"r1 => R" + str(x-2) +"r1 + ENE2', ["+str(A1)+", 0.0, "+str(E1)+"])\n"
        file.write(line2)
        n=n+1

#Family index unzip2
file.write("# family index unzip2\n")
A1=RateCoeffs['Freq Factor'][7-1]
E1=RateCoeffs['Activation Energy'][7-1]

for a in range(36-5+1):
    x=a+5
    line1='# Reaction ' + str(n) + '\n'
    #file.write(line1)
    line2="reaction('RENE" + str(x) +"r"+str(x)+" => RENE" + str(x-2) +"r"+str(x-2)+" + ENE2', ["+str(A1)+", 0.0, "+str(E1)+"])\n"
    file.write(line2)
    n=n+1
```

Figure 17. *Propagation reaction for alkanes and alkenes* – unzipping.

Mid-chain β*-scission (Beta 1 – Beta 4)*

Beta 1: The difference between unzipping and this reaction, although both are β-scission reactions, is that unzipping happens at the end-chain while this β-scission reaction happens at mid-chain.

To start, every chain length starting at 2 carbon atoms is browsed and within them, a radical position is looked for only in the first half of the molecule since the second half is the mirror of the first one. By going through every one of the values:

```
For b in range (math.floor(x/2)-2+1)
```

This scission will give rise to two compounds, an alkyl radical and an alkene. It is worth mentioning that in this set of code it is not considered the specific formation of methyl radicals since this was done in the next set of code. These compounds will have *#C=x-y-1* and *#C=y+1,* respectively (see example).

Example

Note

X is the number of carbon atoms right before the scission reaction occurs and Y is the position number of the radical (as described in **Table 4**).

```
#--------------------------------------------beta scissions-----------------------------------------------
#Family index Beta1
file.write("# family index Beta1\n")
A1=RateCoeffs['Freq Factor'][5-1]
E1=RateCoeffs['Activation Energy'][5-1]
for a in range(40-5+1):
    x=a+5
    for b in range(math.floor(x/2)-2+1):
        y=b+2
        if x-y >1:
            line1='# Reaction ' + str(n) + '\n'
            #file.write(line1)
            line2="reaction('R" + str(x)+ "r"+str(y) + " => R" + str(x-y-1) + "r1" + " + ENE" + str(y+1) + "', ["+str(A1)+", 0.0, "+str(E1)+"])\n"
            file.write(line2)
            n=n+1
```

Figure 18. *Propagation reaction producing an alkyl radical and an alkene through* mid-chain *β-scission*.

Beta 2: the formation of methyl radicals is taken into account. First, we need to determine if the radical position is within the length of the molecule. If this is true, then the molecule is run through to assess its degeneracy.

```
If math.ceil(x/2)==y and x/2!=y
```

Afterward, a differentiation about the β-scission type is made. Depending on this, the reaction will output either an alkyl radical and an alkene or a methyl radical and an alkene. Both the activation energy and the pre-exponential factor present different values, depending on the type of reaction. A methyl radical will form when the radical appears in the third carbon atom.

```
#Family index Beta2
file.write("# family index Beta2\n")
A1=RateCoeffs['Freq Factor'][5-1]
A2=RateCoeffs['Freq Factor'][6-1]
E1=RateCoeffs['Activation Energy'][5-1]
E2=RateCoeffs['Activation Energy'][6-1]
for a in range(40-5+1):
    x=a+5
    for b in range(math.ceil(x/2)-3+1):
        y=b+3
        if x-y >0:
            line1='# Reaction ' + str(n) + '\n'
            #file.write(Line1)
            if math.ceil(x/2)==y and x/2!=y:
                #double A due to degenaracy (symmetry)
                if y-2!=1:
                    line2="reaction('R"+str(x)+"r"+str(y)+" => ENE"+str(x-y+2)+" + "+"R"+str(y-2)+"r1"+"', ["+str(2*A1)+", 0.0, "+str(E1)+"])\n"
                if y-2==1:
                    #Methyl
                    line2="reaction('R"+str(x)+"r"+str(y)+" => ENE"+str(x-y+2)+" + "+"R"+str(y-2)+"r1"+"', ["+str(2*A2)+", 0.0, "+str(E2)+"])\n"
            else:
                if y-2!=1:
                    line2="reaction('R"+str(x)+"r"+str(y)+" => ENE"+str(x-y+2)+" + "+"R"+str(y-2)+"r1"+"', ["+str(A1)+", 0.0, "+str(E1)+"])\n"
                if y-2==1:
                    #Methyl
                    line2="reaction('R"+str(x)+"r"+str(y)+" => ENE"+str(x-y+2)+" + "+"R"+str(y-2)+"r1"+"', ["+str(A2)+", 0.0, "+str(E2)+"])\n"
            file.write(line2)
            n=n+1
```

Figure 19. *Propagation reaction producing either an alkyl or a methyl radical and an alkene through* mid-chain β*-scission*.

For the remaining reactions, the line of thought remains similar, so an extensive explanation will not be made here. Reference [9] should be accessed for further understanding.

4.3. Kinetic Parameters

To simulate a chemical reaction, it is necessary to have proper kinetic parameters that allow for the correct simulation to happen. **Figure 10** shows that the kinetic values are based on the Dipartimento di Chimica at Politecnico di Milano research, and the values are denoted in Marongiu et al. [19]. Besides PE, PP and PS have also been the target of extensive studies, and all rate parameters found are based on a very limited set of reference values, deduced from the available research concerning the analogous gas-phase reactions. Thus, the parameters used for each reaction type are described in **Table 5**.

Table 5. *Kinetic parameters for every reaction type present in the mechanism.*

Reaction Families	***Rate coefficient units***	***Kinetic Parameters*** [19]	
		A	**E_a (kcal/mol)**
Thermal Scission	s^{-1}	$8.00 \cdot 10^{14}$	78.0
Thermal Scission (Allyl formation)	s^{-1}	$8.00 \cdot 10^{14}$	73.2
Unzipping	s^{-1}	$3.50 \cdot 10^{14}$	30.1
$\boldsymbol{\beta - scission}$	s^{-1}	$1.50 \cdot 10^{14}$	30.1
H-abstraction (end chain)	$L \cdot mol^{-1} \cdot s^{-1}$	$3.00 \cdot 10^{11}$	11.9
H-abstraction (mid chain)	$L \cdot mol^{-1} \cdot s^{-1}$	$3.00 \cdot 10^{11}$	12.0
1,4 Hydrogen shift	s^{-1}	$1.00 \cdot 10^{11}$	20.6
1,5 Hydrogen shift	s^{-1}	$1.60 \cdot 10^{10}$	14.4
1,6 Hydrogen shift	s^{-1}	$5.00 \cdot 10^{9}$	20.6
x→x + 3 Hydrogen shift	s^{-1}	$1.00 \cdot 10^{11}$	20.6
x→x + 4 Hydrogen shift	s^{-1}	$1.60 \cdot 10^{10}$	14.4
x→x + 5 Hydrogen shift	s^{-1}	$5.00 \cdot 10^{9}$	20.6
Recombination	$L \cdot mol^{-1} \cdot s^{-1}$	$3.87 \cdot 10^{10}$	6.0

The Arrhenius equation can be written as follows.

$$k = AT^n e^{-\frac{E_a}{RT}} \tag{1}$$

$$k = A e^{-\frac{E_a}{RT}} \tag{2}$$

The Arrhenius equation is commonly used in the form of equation (2, but a modified version, seen in (1, can be advantageous in certain cases. Equation (2 represents the dependence of the rate coefficient A of a reaction on the absolute temperature T, whereas equation (1 is an extension where A is proportional to T^n, with $-1 < n < 1$ [37]. Although it is assumed in most cases that $n = 0$, the recombination reactions suppose a value of $n = 1$, as a way to take into consideration the temperature effect, in particular the influence of the heating rate.

To simulate polymer pyrolysis, the mechanism needs to access these kinetic values, which are in a .csv file. Besides this, another file with thermodynamic and transport data of all the species and the reactions included is needed, this is the initial .cti file. After running the mechanism, a different .cti file will be created, where the output of the reactions will be written as seen in **Figure 20**.

```
# family index inil
reaction('ANE2 => R1r1 + R1r1', [800000000000000.0, 0.0, 78000])
reaction('ANE3 => R1r1 + R2r1', [1600000000000000.0, 0.0, 78000])
reaction('ANE4 => R1r1 + R3r1', [1600000000000000.0, 0.0, 78000])
reaction('ANE4 => R2r1 + R2r1', [800000000000000.0, 0.0, 78000])
reaction('ANE5 => R1r1 + R4r1', [1600000000000000.0, 0.0, 78000])
reaction('ANE5 => R2r1 + R3r1', [1600000000000000.0, 0.0, 78000])
reaction('ANE6 => R1r1 + R5r1', [1600000000000000.0, 0.0, 78000])
reaction('ANE6 => R2r1 + R4r1', [1600000000000000.0, 0.0, 78000])
reaction('ANE6 => R3r1 + R3r1', [800000000000000.0, 0.0, 78000])
reaction('ANE7 => R1r1 + R6r1', [1600000000000000.0, 0.0, 78000])
reaction('ANE7 => R2r1 + R5r1', [1600000000000000.0, 0.0, 78000])
reaction('ANE7 => R3r1 + R4r1', [1600000000000000.0, 0.0, 78000])
```

Figure 20. *Organization of the new .cti file created when running the mechanism where the output reactions are written.*

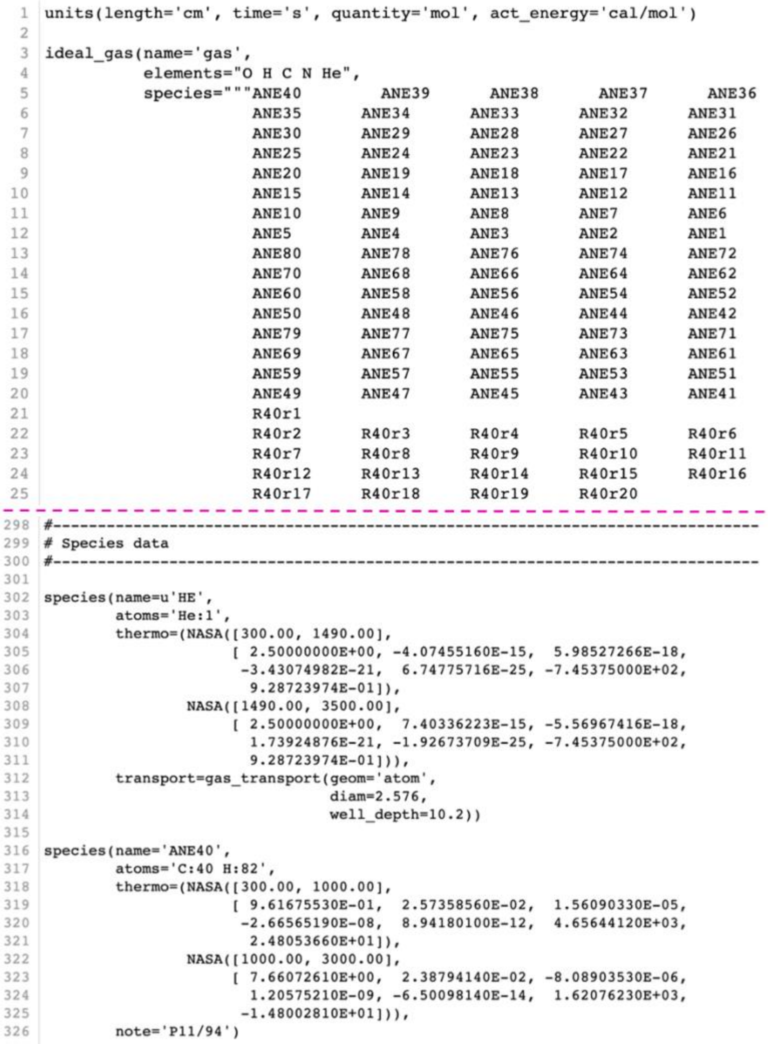

```
units(length='cm', time='s', quantity='mol', act_energy='cal/mol')

ideal_gas(name='gas',
          elements="O H C N He",
          species="""ANE40       ANE39      ANE38      ANE37      ANE36
                     ANE35       ANE34      ANE33      ANE32      ANE31
                     ANE30       ANE29      ANE28      ANE27      ANE26
                     ANE25       ANE24      ANE23      ANE22      ANE21
                     ANE20       ANE19      ANE18      ANE17      ANE16
                     ANE15       ANE14      ANE13      ANE12      ANE11
                     ANE10       ANE9       ANE8       ANE7       ANE6
                     ANE5        ANE4       ANE3       ANE2       ANE1
                     ANE80       ANE78      ANE76      ANE74      ANE72
                     ANE70       ANE68      ANE66      ANE64      ANE62
                     ANE60       ANE58      ANE56      ANE54      ANE52
                     ANE50       ANE48      ANE46      ANE44      ANE42
                     ANE79       ANE77      ANE75      ANE73      ANE71
                     ANE69       ANE67      ANE65      ANE63      ANE61
                     ANE59       ANE57      ANE55      ANE53      ANE51
                     ANE49       ANE47      ANE45      ANE43      ANE41
                     R40r1
                     R40r2       R40r3      R40r4      R40r5      R40r6
                     R40r7       R40r8      R40r9      R40r10     R40r11
                     R40r12      R40r13     R40r14     R40r15     R40r16
                     R40r17      R40r18     R40r19     R40r20
#-------------------------------------------------------------------------------
# Species data
#-------------------------------------------------------------------------------

species(name=u'HE',
        atoms='He:1',
        thermo=(NASA([300.00, 1490.00],
                     [ 2.50000000E+00, -4.07455160E-15,  5.98527266E-18,
                      -3.43074982E-21,  6.74775716E-25, -7.45375000E+02,
                       9.28723974E-01]),
                NASA([1490.00, 3500.00],
                     [ 2.50000000E+00,  7.40336223E-15, -5.56967416E-18,
                       1.73924876E-21, -1.92673709E-25, -7.45375000E+02,
                       9.28723974E-01])),
        transport=gas_transport(geom='atom',
                                diam=2.576,
                                well_depth=10.2))

species(name='ANE40',
        atoms='C:40 H:82',
        thermo=(NASA([300.00, 1000.00],
                     [ 9.61675530E-01,  2.57358560E-02,  1.56090330E-05,
                      -2.66565190E-08,  8.94180100E-12,  4.65644120E+03,
                       2.48053660E+01]),
                NASA([1000.00, 3000.00],
                     [ 7.66072610E+00,  2.38794140E-02, -8.08903530E-06,
                       1.20575210E-09, -6.50098140E-14,  1.62076230E+03,
                      -1.48002810E+01])),
        note='P11/94')
```

Figure 21. *Sample of Cantera input (initial .cti file) to paste in the new .cti file created, before implementing in the 1-D framework.*

In **Figure 21** it's possible to see that both thermodynamic and transport specifications for each species are written. The thermal data is inserted via NASA-polynomials [38], but the origin of the coefficients is not mentioned in the reference articles [8,28,39] nor the mechanism file. Note that this data is not chain-length specific. The NASA-polynomials have fourteen coefficients, the first seven for the upper-temperature interval, and the last seven for the lower temperature interval.

Although the kinetic parameters assumed are from the knowledge in the gas phase reactions, polymer pyrolysis occurs in all phases, solid, liquid, and gas. For He, helium, the inert feed gas, the transport parameters are considered. **Table 6** shows how the information is usually available [40].

Table 6. *Example of how the transport data is organized in a file.*

Species	***Molecular Index***	***L-J potential well depth***	***L-J collision diameter***	***Dipole moment***	***Polarization ability***	***Rotational relaxation collision number***
He [41]	0	10.2	2.576	0	0	0

In theory, if the kinetic parameters of the gas and liquid phase are considered the same, a sterical hindrance in the liquid phase is likely to occur, meaning that some rotations of segments in the polymer cannot happen and are inhibited. On the other hand, H-abstraction reactions are extremely faster in the liquid phase, thus $\beta - scission$ reactions define the step rate for temperatures between 600 - 800 K [28].

Significant improvements are necessary for the development of kinetic models used in polymer pyrolysis simulation. Beirnaert's work showed that the modeled conversion is highly sensitive to the kinetic set, especially for higher molecular weight products estimation.

4.4. Conclusion

The thought process explained here can be extrapolated for any new reaction to being implemented in the reaction scheme. Thus, preliminary knowledge of organic chemistry and chemical bonds is required. It is crucial to understand how the molecule breaks down into smaller molecules and monomers and when degeneracy should be considered. Once this is done, taking into consideration how the free-radical mechanism works, a mechanism can be developed. To start, a study of every possible reaction path should be performed and transformed into a modeling language. Afterward, this language should be reproducible and should help in further understanding the mechanism. To put the knowledge into practice, the mechanism was implemented in a 1-D framework, and the process is explained in the following chapter.

Chapter 5. 1-D framework creation

After understanding how the kinetic mechanism works, it’s necessary to understand how to use it and implement it in a 1-D framework. This is the tool that will allow the study of HDPE pyrolysis in pre-defined conditions. This chapter explains how the framework was built and how it uses the mechanism as an input.

Note

Deterministic models can be classified dimensionally as 0D, 1D, 2D, or 3D. The difference lies in the number of independent variables from which the system is a function of.

Figure 22 below shows the complete developed framework. The concepts, assumptions, and functions used are explained in the sub-chapters.

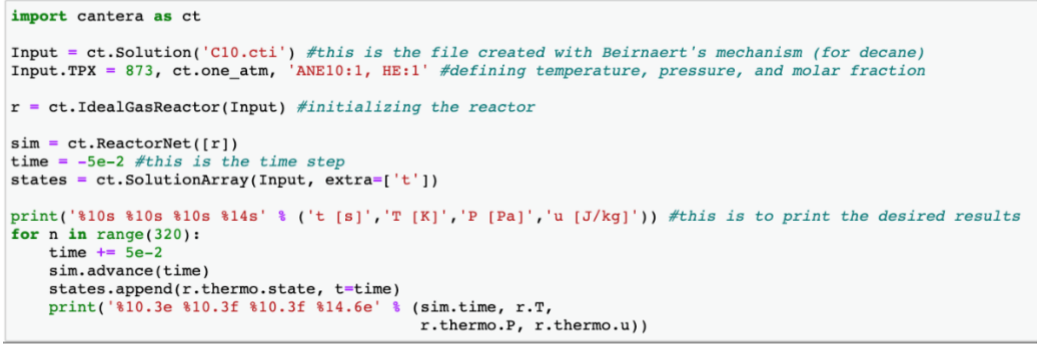

```
import cantera as ct

Input = ct.Solution('C10.cti') #this is the file created with Beirnaert's mechanism (for decane)
Input.TPX = 873, ct.one_atm, 'ANE10:1, HE:1' #defining temperature, pressure, and molar fraction

r = ct.IdealGasReactor(Input) #initializing the reactor

sim = ct.ReactorNet([r])
time = -5e-2 #this is the time step
states = ct.SolutionArray(Input, extra=['t'])

print('%10s %10s %10s %14s' % ('t [s]','T [K]','P [Pa]','u [J/kg]')) #this is to print the desired results
for n in range(320):
    time += 5e-2
    sim.advance(time)
    states.append(r.thermo.state, t=time)
    print('%10.3e %10.3f %10.3f %14.6e' % (sim.time, r.T,
                                           r.thermo.P, r.thermo.u))
```

Figure 22. *Pyrolysis’ simulation in a discontinuous reactor for 16 s at 873 K and 1 atm. Equimolar feedstock of n-decane (ANE10) and helium (HE).*

5.1. Cantera

Cantera is defined as “an open-source suite of tools for problems involving chemical kinetics, thermodynamics, and transport processes”, which can also solve transient systems and be used in steady-state conditions [42]. Therefore, it was decided to be used and to adopt its built-in functions, libraries, and reaction data, to take advantage of its main attack points: automation, object-oriented, multiple interfaces, and broad applications. It can be used in diverse languages, from Python and MATLAB to C++ and Fortran 90, and is currently used for applications such as combustion, electrochemical energy conversion and storage, batteries, aqueous electrolyte solutions, and thin film deposition [43].

All calculations made in Cantera require an input file that describes the properties of the relevant phases [44]. The input file we will use is the one that results from the mechanism developed by Beirnaert K. [9] after it runs in the sought conditions.

To investigate a reaction network, there is a general path necessary to follow:

1. Define **Solution** objects for your feed to flow through your reactor network;
2. Define the reactor type(s), as well as the reservoir(s);
3. *[Optional]* Set up the boundary conditions between your reactor(s) and reservoir(s);
4. *[Only when building a reactor network]* Define the reactor network that contains all the reactors created in 2.
5. Advance the simulation in time, typically with a `for-loop`;
6. Analyze the data.

Class **Solution** represents a substance with thermodynamic, kinetics, and transport properties. The substance can be any of any type, from a gas mixture to a liquid or solid solution. Usually, it's initiated by using a phase definition, species, and reactions pre-defined in a `.cti` input file. The input parameters are the contents, name, and energy, in the following way [45].

```
Input = ct.Solution ('contents', 'name', 'energy')
```

If the contents are not specified, then it is assumed the reactor is initially empty and the same line of thought is applied for the energy parameter, which if not specified, the energy equation will be solved, by default.

A Cantera Reactor simulates a chemically reacting system with a defined control volume, V. All states are a function of time and thermodynamic equilibrium is assumed in every point of the reactor at all time instants. By default, all reactors are closed (no inlets or outlets), with fixed volume and adiabatic, with chemically inert walls. The zero-dimensional reactor implies that the concentration inside the reactor is the same at every point, i.e., there is no concentration gradient.

The state variables defined for Cantera's reactor models are:

- Content's mass, m;
- Reactor volume, V (when the volume is a fixed parameter);
- Reactor energy, as the total internal energy, U, total enthalpy, H, or temperature, T;
- Mass fraction for each species, Y_k[5].

When analyzing how a homogeneous system evolves in terms of chemical composition with time, a batch reactor can be used. It can be either a rigid vessel with variable pressure or a varying volume with a fixed pressure value. Since the goal of the present study is to understand

---

[5] k = number of species

how product distribution varies with temperature and with the chain length of the fuel, a batch reactor is a simple and fast way to study the content's fraction with time. For this purpose, an Ideal Gas Reactor was simulated, with a fixed volume and under adiabatic conditions. Important to note that this reactor only considers ideal gas phases. Further details on the detailed balances used by Cantera can be found in Cantera's manual [42].

The behavior of the solution is simulated for a single reactor created (**Figure 22**). For the defined simulation time, the value of temperature, pressure, and total internal energy was saved for each time step also defined in the framework. Hereafter, a brief description of the Jupyter Notebook is made.

5.2. Jupyter Notebook

The server chosen as the working interface was Jupyter Notebook. This is an open-source server-client application that allows editing and running notebook documents via a web browser. This document is saved with the `.ipynb` extension, which can be shared with others without needing to install the Jupyter Notebook. It also includes a "Dashboard" that acts as a control panel where you can choose the notebooks you wish to open and where you can also visualize and shut down its kernels. Since a single Jupyter Notebook app allows to open multiple notebooks, it is not recommended to have various copies of the app [46,47].

The notebooks are documents produced in the Jupyter Notebook app, that contain the computer code (in a specific programming language) and text elements like equations, figures, links, etc (taking advantage of libraries and packages like `matplotlib` and `pandas` [48,49]). These documents are both human-readable and executable, meaning that they include the data description and also its analysis, available after running the code. The kernel is automatically started, and it is the "computational engine" that puts into action the commands written in the notebook. For this work, the default kernel, *ipython,* was used meaning that it executes python code, chosen language to develop this framework. In such a manner, the kernel is responsible for completing the computation and producing the results, consuming CPU and RAM [50].

Common uses of this server include data cleaning and transformation, statistical modeling, data visualization, numerical simulation, and machine learning. One of its main advantages is that it allows the user to work on a computational problem in pieces. Related ideas are written in a single cell and the user can move forward once the previous parts are working correctly. This means that it is unnecessary to break the computation into scripts that must be executed together, which is especially important in parts that take a long time to run [51].

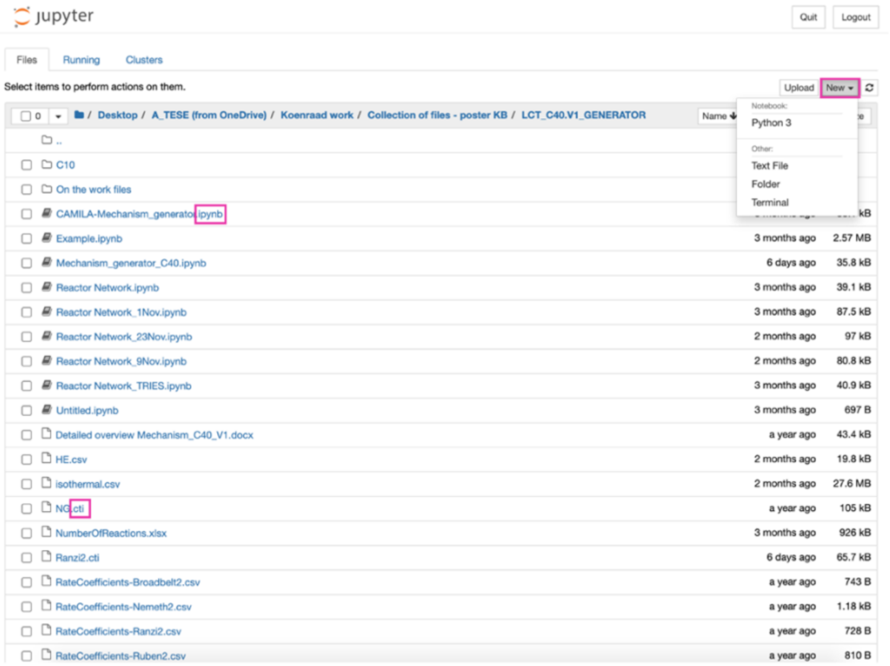

Select items to perform actions on them.

/ Desktop / A_TESE (from OneDrive) / Koenraad work / Collection of files - poster KB / LCT_C40.V1_GENERATOR

..		
C10		
On the work files		
CAMILA-Mechanism_generator.ipynb	[illegible]	[illegible] kB
Example.ipynb	3 months ago	2.57 MB
Mechanism_generator_C40.ipynb	6 days ago	35.8 kB
Reactor Network.ipynb	3 months ago	39.1 kB
Reactor Network_1Nov.ipynb	3 months ago	87.5 kB
Reactor Network_23Nov.ipynb	2 months ago	97 kB
Reactor Network_9Nov.ipynb	2 months ago	80.8 kB
Reactor Network_TRIES.ipynb	3 months ago	40.9 kB
Untitled.ipynb	3 months ago	697 B
Detailed overview Mechanism_C40_V1.docx	a year ago	43.4 kB
HE.csv	2 months ago	19.8 kB
isothermal.csv	2 months ago	27.6 MB
NG.cti	a year ago	105 kB
NumberOfReactions.xlsx	3 months ago	926 kB
Ranzi2.cti	6 days ago	65.7 kB
RateCoefficients-Broadbelt2.csv	a year ago	743 B
RateCoefficients-Nemeth2.csv	a year ago	1.18 kB
RateCoefficients-Ranzi2.csv	a year ago	728 B
RateCoefficients-Ruben2.csv	a year ago	810 B

Figure 23. *Illustration of the Jupyter Notebook's dashboard. On the top right button, a new notebook can be created. .cti files can be accessed, but only .ipynb files can be edited and run.*

As a global conclusion, after all the concepts here present are understood, then **Figure 22** should be revisited. A more in-depth and familiarity with the knowledge of the command lines, as well as their functionality, should now be clearer. It should be explicit the inner workings of the tools implemented and how they interact with the other.

The next chapter will cover the simulations performed and enlighten on the results obtained. A discussion on the mechanism's assumption [9], as well as in the framework developed will take place.

Chapter 6. Discussion of Results

The mechanism will be tested in different sets of conditions to assess its behaviour and to understand the results at a chemical and kinetic level. In the course of the work, two questions were at the center of the analysis.

1. What are the most relevant reactions in hydrocarbon pyrolysis?
2. How do chain length and kinetics affect the results?

These questions are imperative when studying the inner workings of a mechanism, since they will show if the assumptions made need revising and, therefore, if improvements are necessary. To develop the most realistic mechanism possible, reaction chemistry is a key part of the analysis.

For this purpose, the microkinetic mechanism developed by Beirnaert K. [9] was chosen to study how close to reality the model could predict HDPE thermal decomposition.

The first objective was to compare its prediction ability to experimental results available in the literature. Two main works were considered for this purpose, Faravelli et al. [21] and Levine & Broadbelt [4]. Although the work of Németh et al. [8] is of utmost importance, the experimental results were not reliable either by lacking information about the reactant's characteristics, initial reaction conditions, or heating rate. These inconsistencies rendered the work untrustworthy for experimental comparison studies, highlighting once again the necessity of further intelligible experimental research and tests.

On the contrary, the tests performed by both authors aforementioned happened under known conditions also published alongside the main results, hence the decision to use these references. However, the experiments were performed with HDPE with variable molecular weight, while this study considered tetracontane as the species for the modeling strategy. A tetracontane reference was not chosen since there is no thermal decomposition study published or available to use.

6.1. Mechanism's Evaluation Against Experimental Conditions from Literature

6.1.1. Faravelli et al. [21]

The simulations performed with Beirnaert K. [9] mechanism, allowed to have the resulting product distribution for all carbon numbers which is something not yet widely or publicly available. Although this is an advantage, it becomes difficult to find experimental data to compare to, since relevant information is missing. Faravelli's works here disclosed, do not discern alkene products below five carbon atoms and do not show results for chains larger than 25 carbon atoms. Hence, the comparisons are molded by the available experimental results.

Faravelli's reaction was also performed at isothermal conditions, with 100% vaporization of the sample at the end of the defined time. Other characteristics are shown in the table below.

Table 7. *Faravelli's experimental conditions for HDPE thermal decomposition.*

Reaction characteristics	T (°C)	600
	p[6] (Pa)	101325
	Carrier gas	Helium
	Reactor type	Pyroprobe 2000 CDS
	Residence time, t_s (s)	15
HDPE characteristics	Quantity (mg)	0.53
	Density (g/cm^3)	0.96
	Melting point (°C)	128
	Number average molecular weight (Mn)	15100
	Critical ratio (Mw/Mn)	5.55

The figures below show the simulation results obtained from the 1-D framework developed and the experimental and theoretical results from Faravelli, respectively.

---

[6] The pressure value is assumed atmospheric since it is not mentioned in the reference paper.

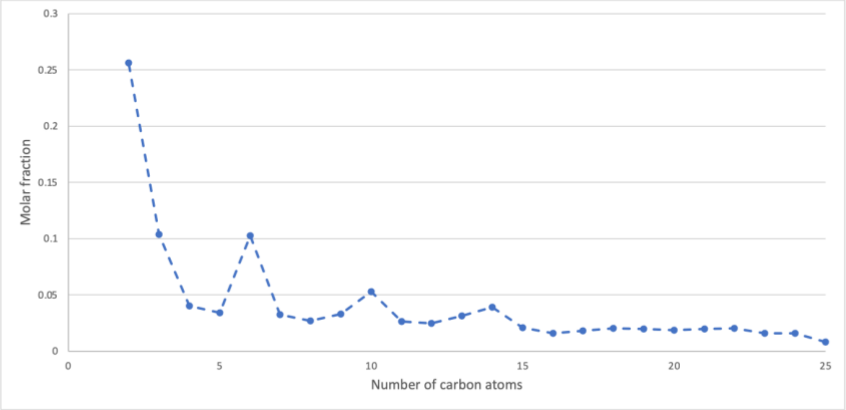

Figure 24. *Alkene product distribution from modeled pyrolysis of tetracontane at 600°C.*

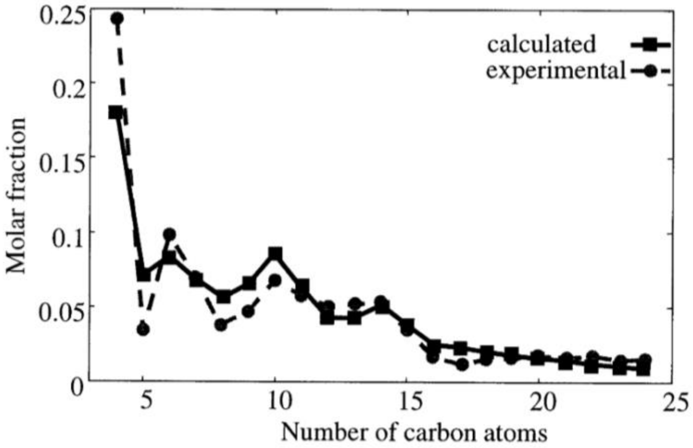

Figure 25. *Alkene product distribution from isothermal pyrolysis of HDPE at 600°C. Comparison between experimental and calculated (modeled) results. Adapted from [21].*

When analysing both figures, it is clear that Beirnaert's modeled pyrolysis follows the experimental data behaviour, obtained by Faravelli. Nonetheless, both models show a good prediction for the amounts of the different chain length species. The revealed peaks are typical of backbiting reactions [19], as well as the gradually decreasing amounts of longer chain products, which happen due to the cracking reactions before the gas phase [21].

According to **Figure 24**, the most abundant product from the lighter chain products is ethylene. In **Figure 25** it's not possible to distinguish the yield of the lighter products. However, the smallest experimental alkene molar fraction value rounds up to around 0.25, while Faravelli's calculated value is close to 0.20. When compared to the value obtained in **Figure 24**, it amounts to 0.27, which although is an overestimation, more accurately predicts the final value. Therefore, the error of the prediction of experimental value decreased from 20% to a mere 8%.

As for the kinetic parameters in Faravelli et al., these were estimated applying the method of moments. The method creates functions for the parameters of interest based on sample results, and the equations are solved as a mean point estimation for the defined parameters. For the simulations with the Beirnaert K. mechanism, the same values were assumed. Not despising other statistic methods, the method of moments was rendered reliable to predict results close to reality, thus the decision to make use of the pre-calculated kinetic values.

6.1.2. Levine & Broadbelt [4]

Similar to Faravelli, the only data available to evaluate was the alkene distribution. **Table 8** shows the experimental conditions simulated.

Table 8. *Levine's experimental conditions for HDPE thermal decomposition.*

Reaction characteristics	T (°C)	420
	p (Pa)	Low values
	Carrier gas	Argon
	Reactor type	Pyrex ampules
	Residence time, t_s (min)	30 - 240
HDPE characteristics	Quantity (mg)	12.3 – 27.8
	Melting point (°C)	mild enough that no degradation was observed
	Molecular Weight (Mw)	125000

To assist in the comparison of experimental and simulated results, **Figure 26** should be considered.

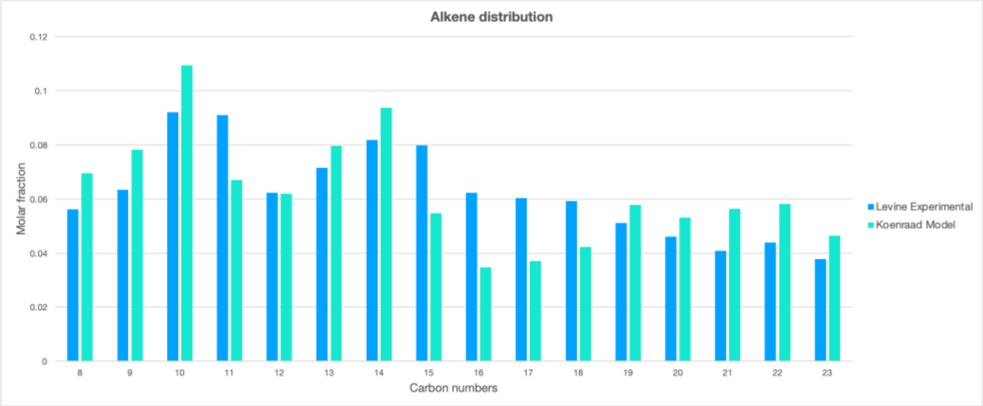

Figure 26. *Alkene distribution comparison between experimental results from Levine et al. [4] and simulation from the developed framework.*

Similar behaviour can be observed in the distribution for different carbon numbers between experimental and theoretical results. This shows, once again, the applicability of Beirnaert's mechanism to a different set of experimental conditions. However, it also shows that it has a tendency to overestimate the values, with error values up to 44% for product C16.

The peaked values appear again for products C10 and C14, as already expected. A simple comparison with the paper allows us to conclude once more the overestimation that this model produces. In **Table 9** below these values are discriminated.

Table 9. Molar yield value for peaked species. Calculated as the average molar yield of the species one carbon above and below the peaked species.

C10	Levine	1.23
	Simulation	1.53
C14	Levine	1.10
	Simulation	1.44

To quantify the peaked effect, Levine & Broadbelt [4] averaged the molar yield of the neighboring products (a carbon number lower and higher) of the desired species. The results were considered for three different reaction times and their behaviour attenuated with time, highlighting the loss of importance of the backbiting pathway with time.

A study was also performed which enabled the authors to derive conclusions about the results of backbiting reaction, in particular $x, x+4-shifts$. When analysing the net rate during pyrolysis, it was found that this reaction was responsible for forming mid-chain radicals, that when undergoing β – scission, form a range of C_8-C_{24} alkanes and alkenes [10]. Alkenes C10 and C14 are products of a series of $x, x+4-shifts$, which is a reaction less favored than the 5 and 6 shifts, due to the presence of extra strain energy. However, from the entropic point of view, it is a much more favored pathway [21], increasing the fraction of products that derive from this reaction, explaining the peaked values for C10 and C14.

It is important to emphasize that both works showed three peak values, for C6, C10, and C14. As previously described, the main reactions happening during pyrolysis, in the propagation stage, are intermolecular H-abstraction, $\beta-scission$, and backbiting (or intermolecular H-shifts). Although every type of reaction is responsible, in part, for the formation of LMWPs, the most relevant one is backbiting. This reaction had already been introduced in the Faravelli modeling strategy as an addition to the random scission hypothesis (assumed by Ranzi et al. [28]), and it allowed a more accurate prediction of these specific products' yield. Moreover, this addition produced decreasing values for the formation of heavier compounds before the gas phase [21], depicting a closer estimation to reality.

Another author, Poutsma [26], hypothesizes that the longer the reaction time, the less relevant become these peaked values. This happens because the likelihood to form LMWPs from the combination of intermolecular H-abstraction and mid-chain $\beta-scission$ decreases as the fuel molecular weight also decreases. This behaviour is specific for random scission pathways since the backbiting pathway is not affected by the molecular weight [4]. Therefore, it is a strong reason to further corroborate the assumed random scission hypothesis proposed in the models.

6.2. Mechanism Results: Evolution with Time

All the simulations were run in a discontinuous batch reactor at constant volume and adiabatic conditions. Varying only the initial substrate chain length, this subchapter will first analyze conversion and temperature evolution with time for all the different reagents. Afterward, an evaluation of the products and intermediates (radicals) distribution with time will be performed. For the simulation, **Table 10** should be considered for reaction conditions.

Table 10. *Reaction conditions for pyrolysis virtual simulation.*

Reaction characteristics (initial)	T (°C)	600
	p (Pa)	101325
	Carrier gas	Helium
	Reactor type	Discontinuous
	Residence time, t_s (s)	15
Polymer characteristics	Carbon length	10, 20, 30, and 40

In this case, all substrates were subjected to the same experimental conditions, namely temperature and reaction time. They were all assumed to work in adiabatic conditions in a discontinuous reactor, with the same assumed kinetic parameters.

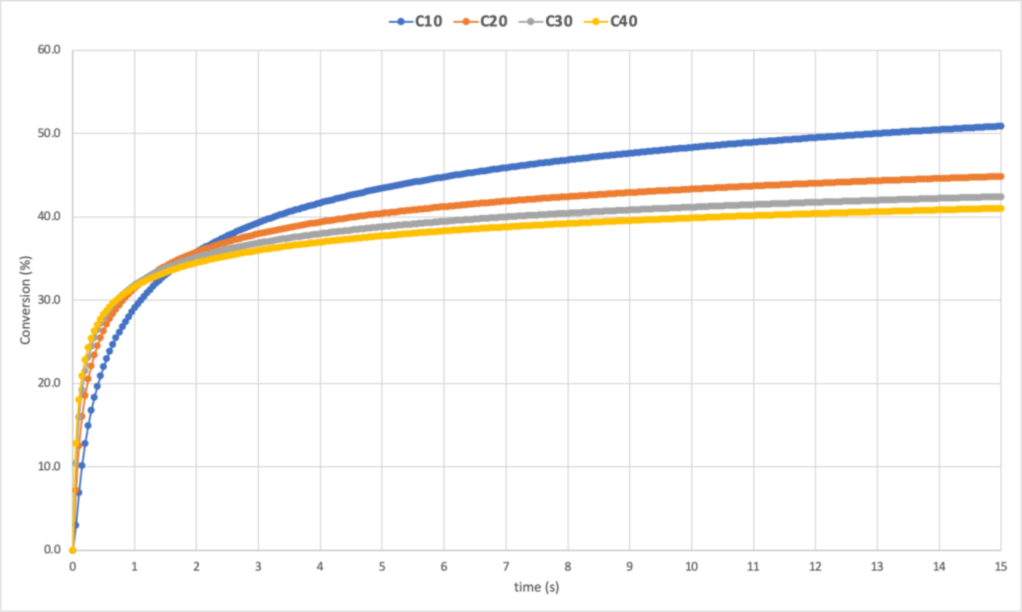

Figure 27. *Conversion evolution for all substrates with reaction time.*

Since C10, or decane, is the smallest hydrocarbon, it was expected that it would achieve a higher conversion value sooner than the other substrates. Observing the figure above, it's possible to observe that this assumption was correct, although with some discrepancies. Decane does reach higher conversion values, however, it shows the smallest growth line in the first instances (until 1s), where the heaviest hydrocarbon (C40) shows the greatest growth. Worth mentioning that despite this, the three heaviest hydrocarbons have very similar growth lines.

Overall, conversion values shift between a minimum of 41% and a maximum of 51%. Although all the curves continually show an ascending behaviour, the growth rate is extremely slow, and very close to zero for C40, especially reaching the end of reaction at 15s.

To understand how reaction time affected these values, the same experiment was simulated for 100s for C10, yielding a value of 60% conversion which is only a rise in 10% of the value for 15s. (please refer to **Figure A 2** in appendix). Thus, no further assessments were made regarding reaction time, and it was decided to maintain all simulations running for 15s since the additional conversion gained was not significant for the results.

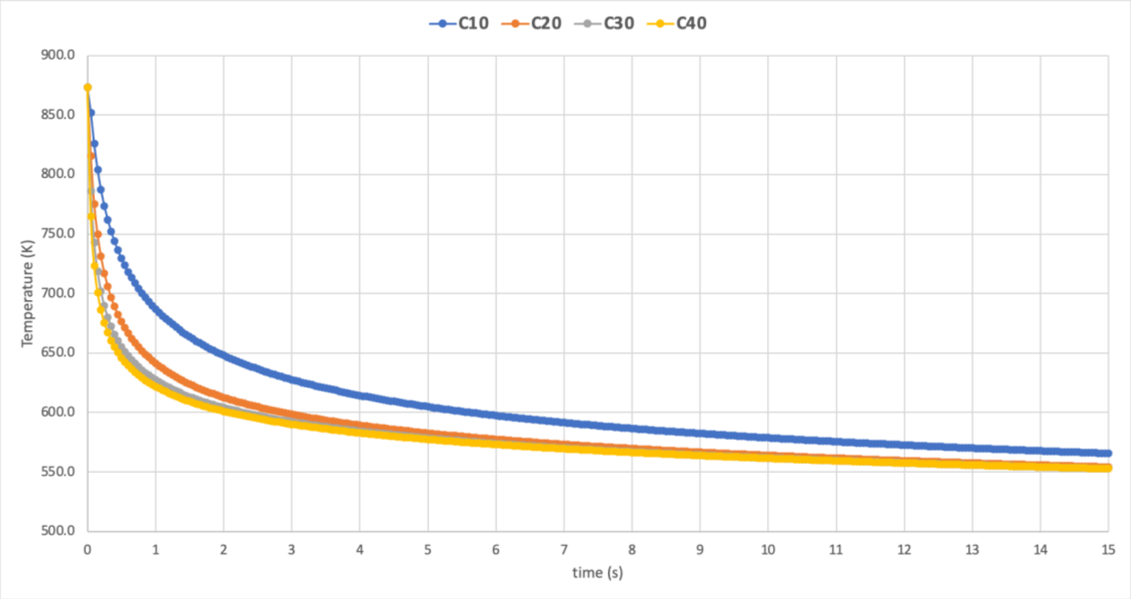

Figure 28. *Temperature evolution for all substrates along reaction time.*

Analysing **Figure 28**, the temperature is set at 873 K but rapidly decreases to a value 200 K below just in the first 2 seconds. At the end of reaction time, it reaches around 550 K, or 277°C, for all substrates. Regarding the curves' behaviour, pyrolysis is an endothermic process, which means that in adiabatic conditions, it will decrease its temperature as reactions take place. For C10, the temperature shows a slower reduction which happens because, being a shorter molecule, it has fewer breakable bonds, thus requiring less energy which in turn results in a slower decrease in temperature. However, the temperature reached at the end of the 15s is very similar for all substrates, indicating that while the initial instances are more sensitive to the chain length [21], all substrates have analogous tendencies when reaching the end of the reaction.

With this initial analysis made, a closer look into each substrate and its products' distribution is made in the following pages.

6.2.1. Product Distribution

As explained in previous chapters, the products yielded during hydrocarbon pyrolysis are alkanes, alkenes, and dienes which are all linked together. These products' production at the end of reaction time is presented below, divided into four figures, each for one of the four studied polymers (the results for the intermediates can be found in appendix figures **Figure A 3**, **Figure A 4**Figure **A 5**Figure A **6**). Afterward, the results are organized by substrate and type of product, where a 3D column graphic can be found, showing the carbon number on the horizontal axis, molar fraction on the vertical axis, and time, in seconds, in the depth axis.

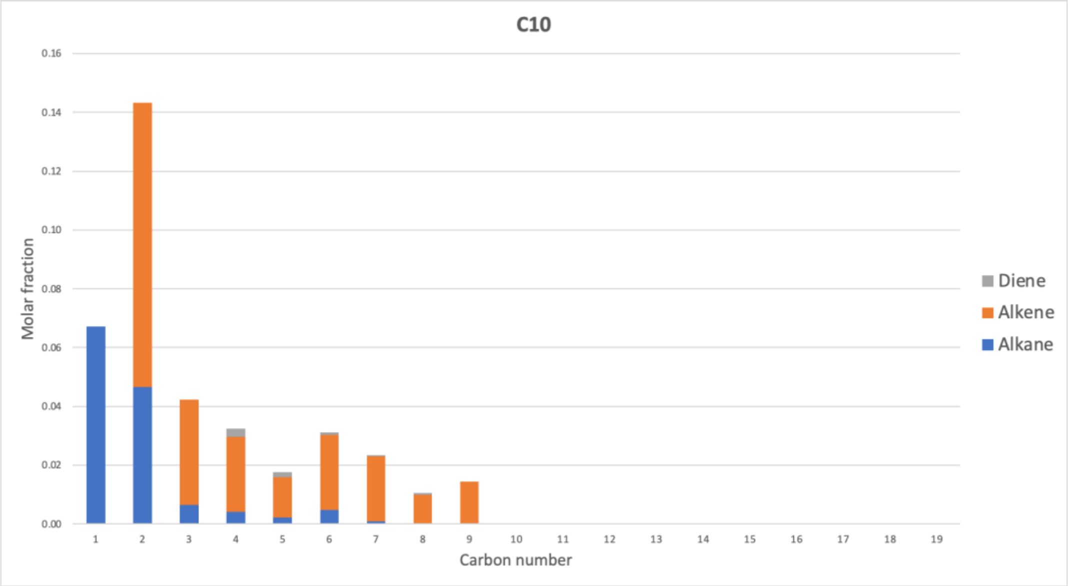

Figure 29. *Product distribution (alkanes, alkenes, and dienes) for the pyrolysis of decane, at 15s.*

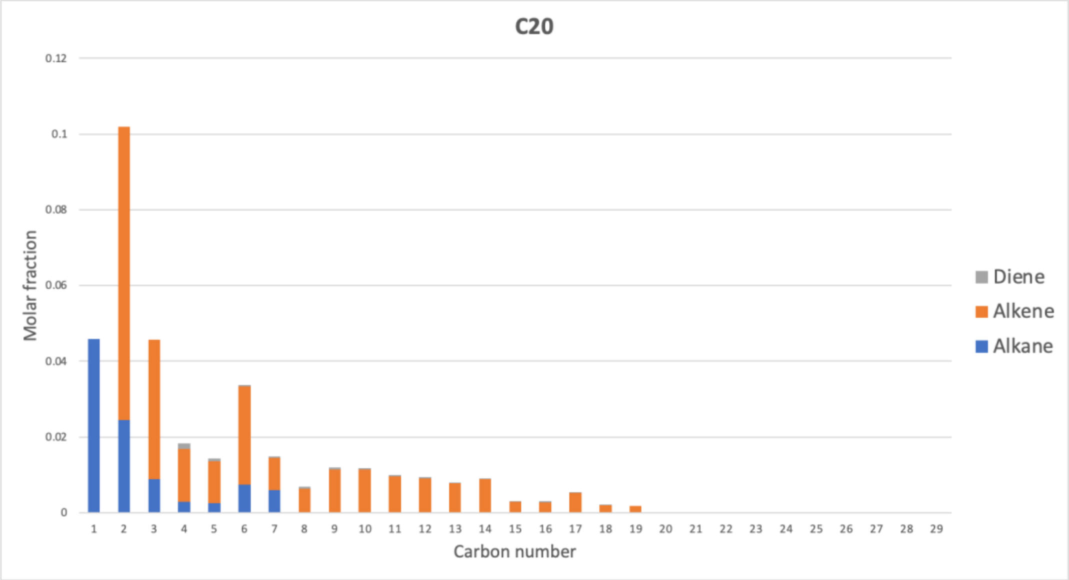

Figure 30. *Product distribution (alkanes, alkenes, and dienes) for the pyrolysis of icosane, at 15s.*

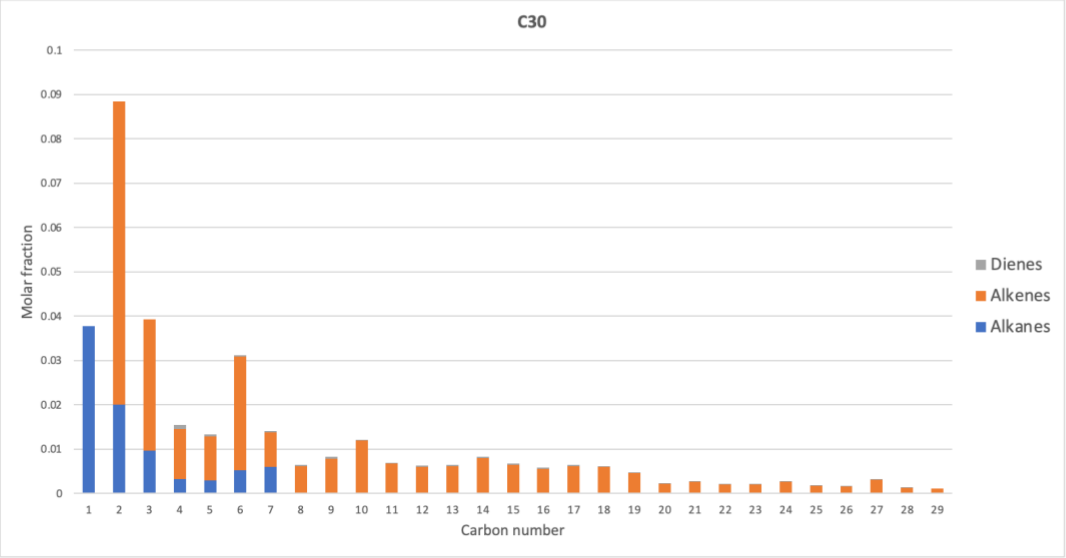

Figure 31. *Product distribution (alkanes, alkenes, and dienes) for the pyrolysis of triacontane, at 15s.*

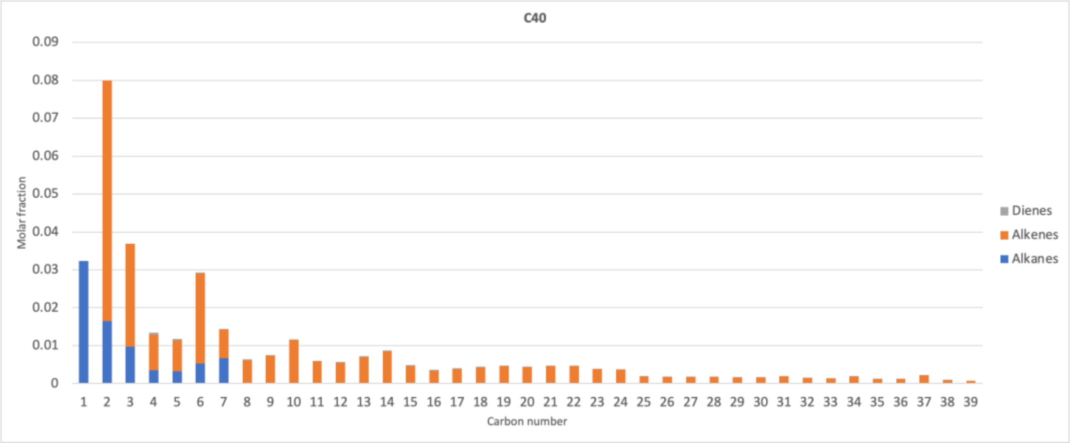

Figure 32. *Product distribution (alkanes, alkenes, and dienes) for the pyrolysis of tetracontane, at 15s.*

This broad overview aims to show the distribution's behaviour for all substrates and the relative quantitative values for the different family type products before diving into the details of the analysis.

Decane (C10)

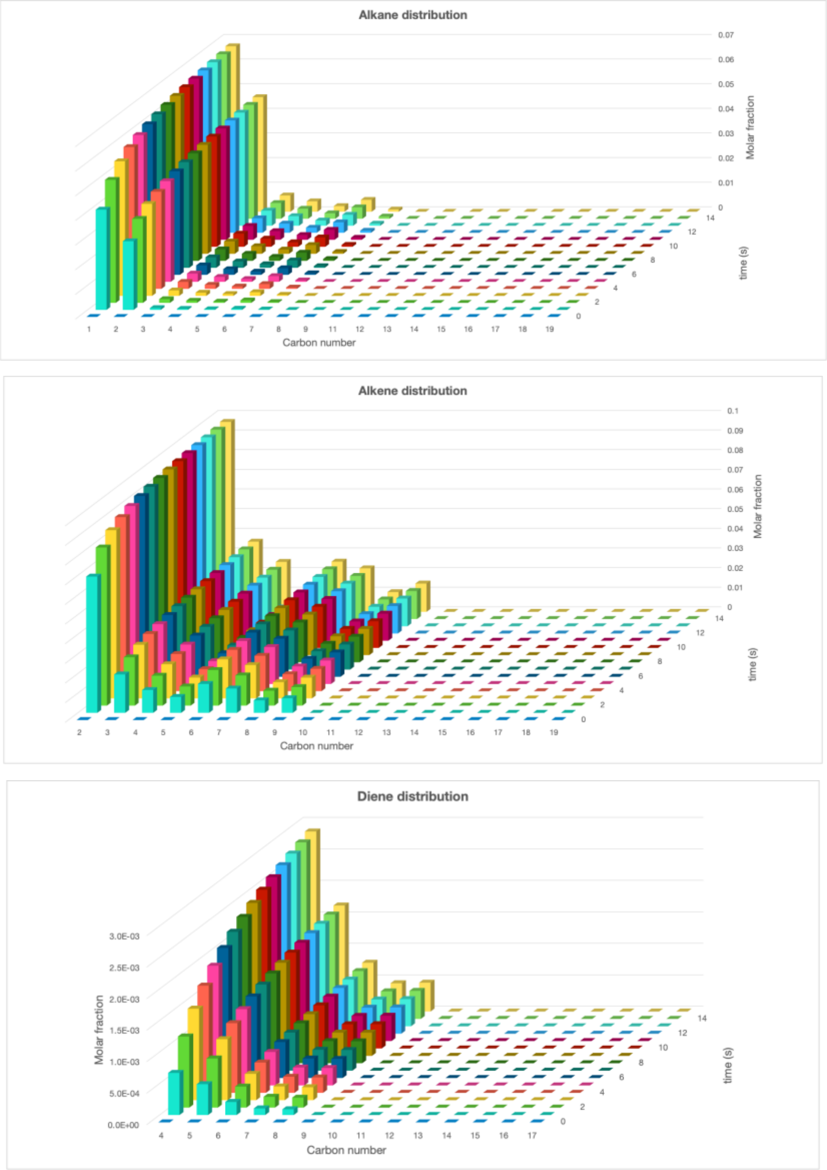

Figure 33. *Alkane, alkene, and diene distribution for the pyrolysis of decane.*

Icosane (C20)

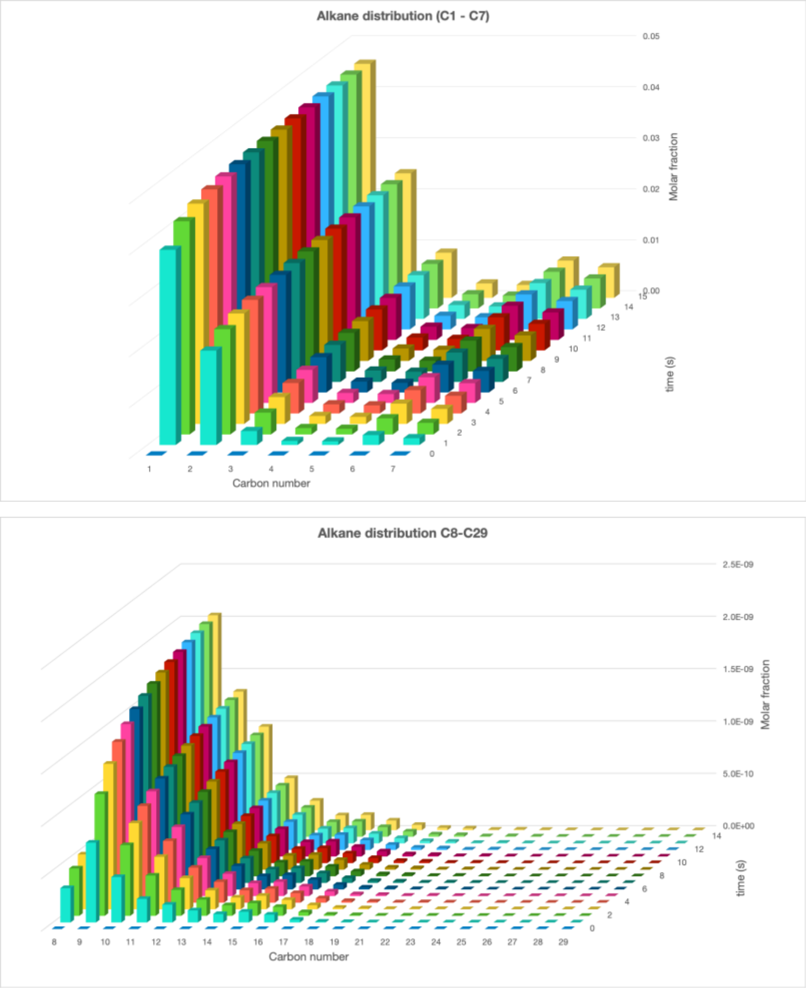

Figure 34. *Alkanes distribution for the pyrolysis of icosane.*

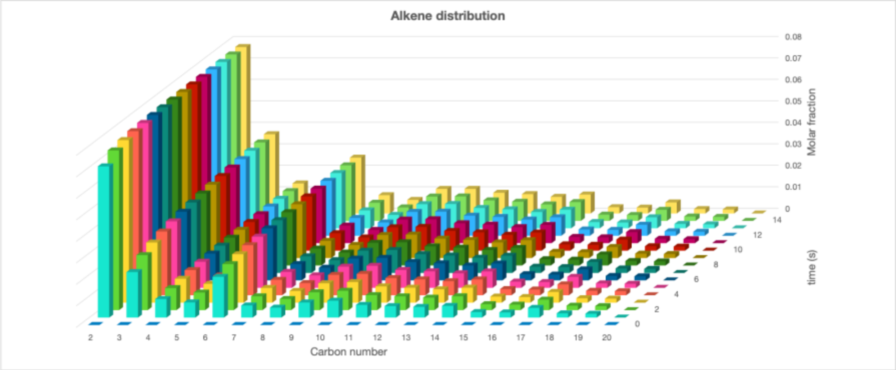

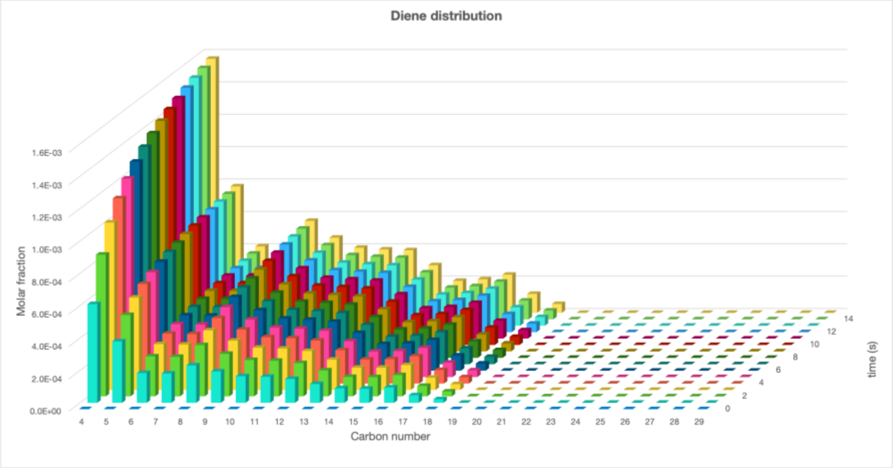

Figure 35. *Alkenes and dienes distribution for the pyrolysis of icosane.*

Triacontane (C30)

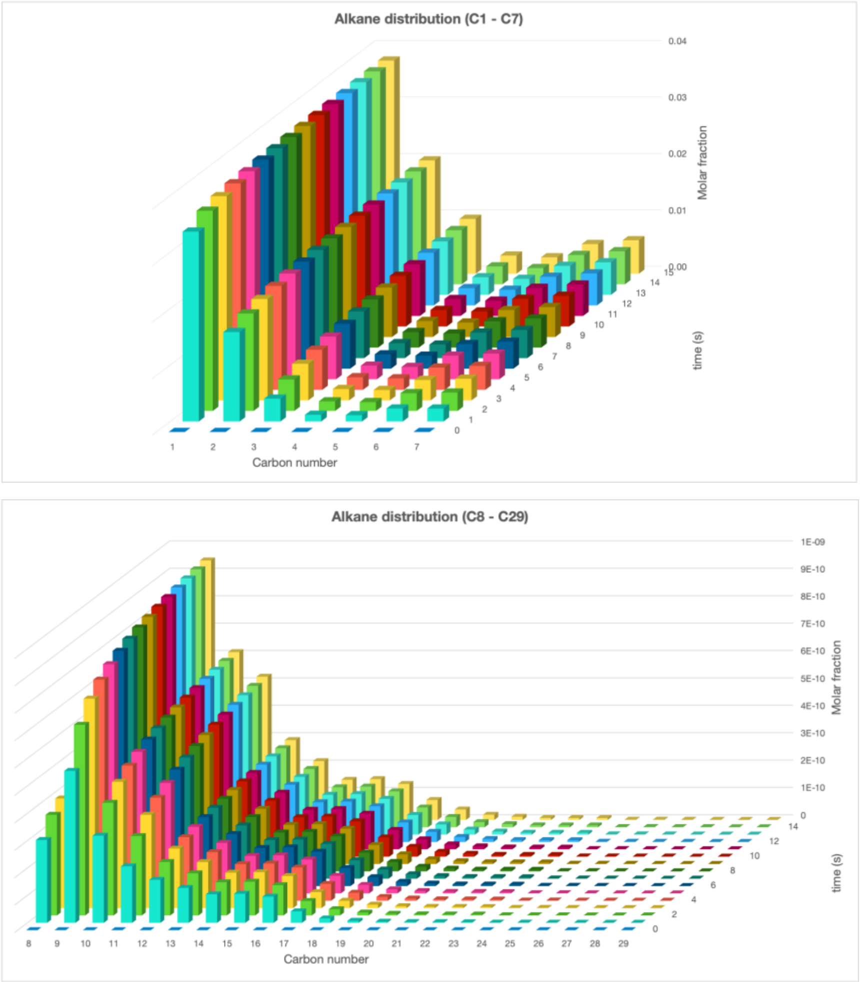

Figure 36. *Alkanes distribution for the pyrolysis of triacontane.*

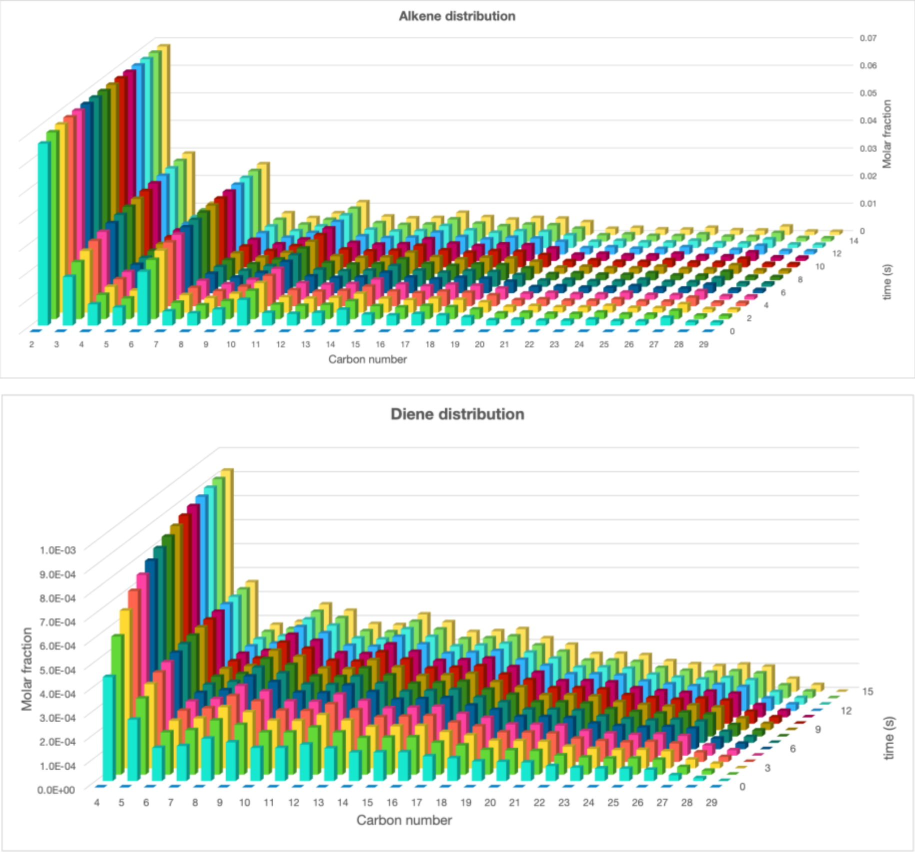

Figure 37. *Alkenes and dienes distribution for the pyrolysis of triacontane.*

Tetracontane (C40)

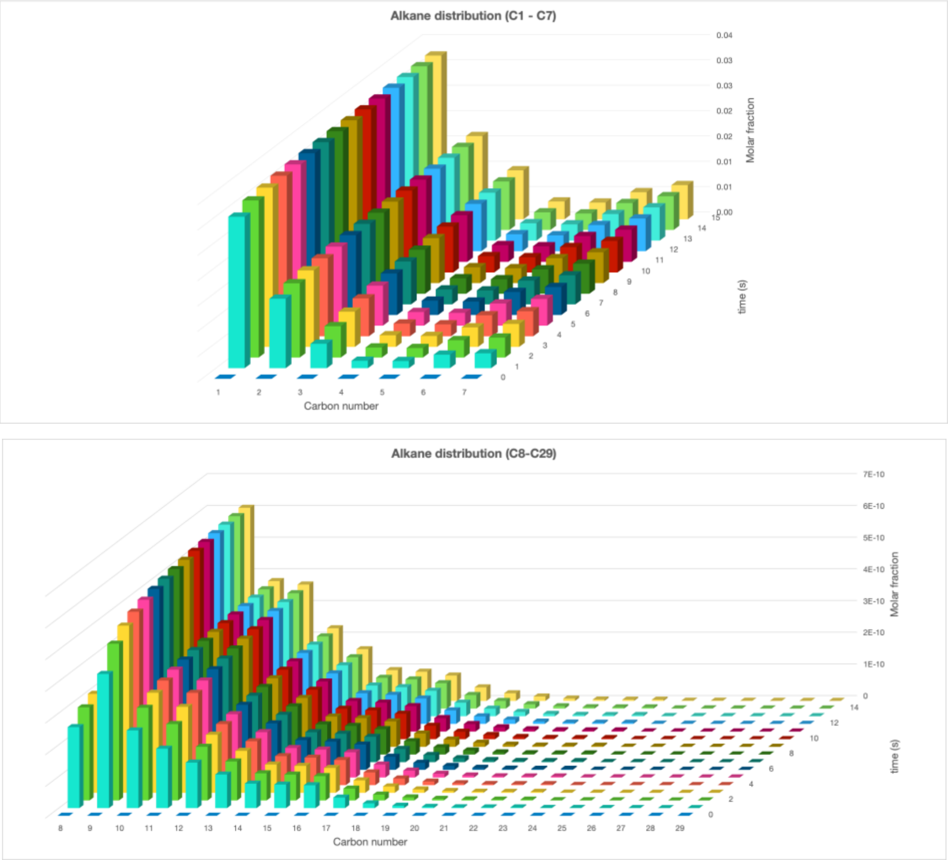

Figure 38. *Alkanes distribution for the pyrolysis of tetracontane.*

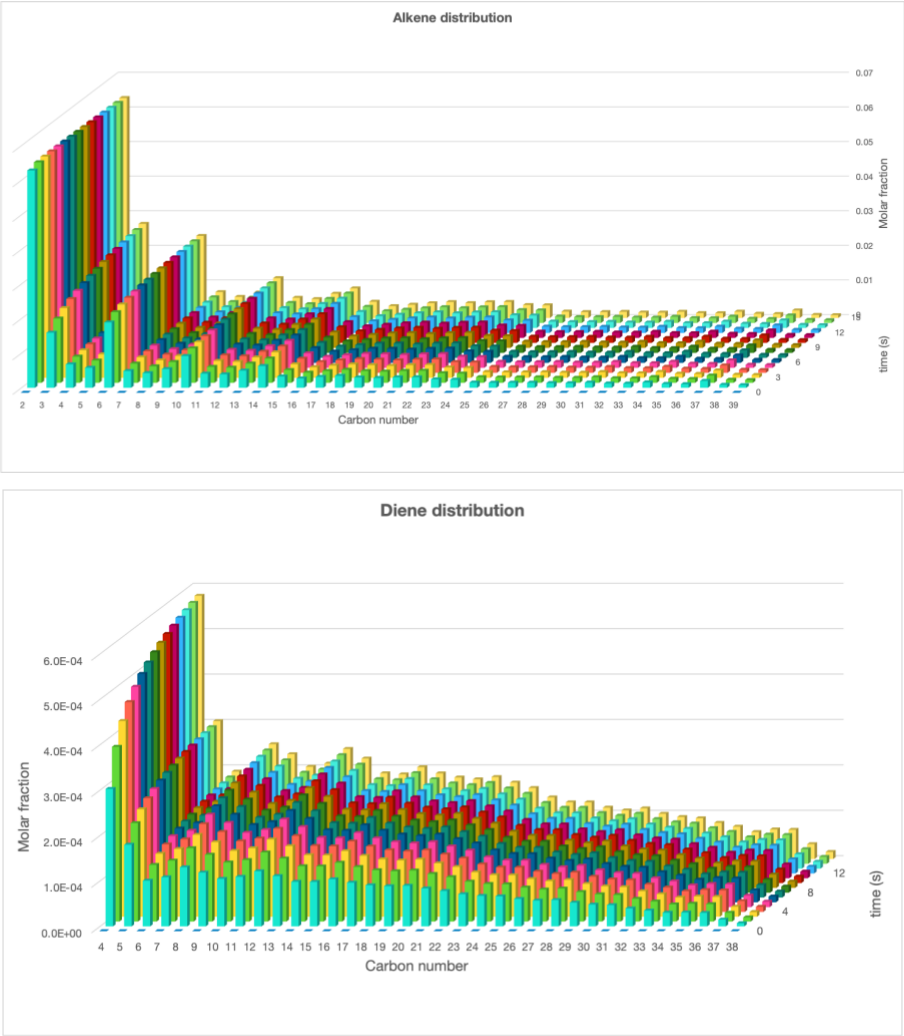

Figure 39. *Alkenes and dienes distribution for the pyrolysis of tetracontane.*

6.2.2. Discussion

An instantaneous conclusion, which is also in line with the literature, is that decane is the substrate that breaks down into smaller molecules at a faster pace, thus also showing a higher molar fraction value for the products formed, with the highest value of 0,1 for ethylene (**Figure 33**).

Taking into consideration figures **Figure 33Figure 34**, **Figure 36**, and **Figure 38** for alkane molecules production, methane shows the highest molar fraction value, compared to all the yielded molecules, while ethane places itself as the second most produced product. For decane, these two show values of 0.07 and 0.05 respectively. Propane is the third most produced molecule, although for decane its value is 10 times smaller than for methane and ethane. However, with increasing chain length, this deviation decreases. If **Figure 38** for tetracontane is considered, propane shows a molar fraction value close to 0.01 while ethane and methane's values are 0.02 and 0.03 respectively. This can indicate the increasing importance of this product for longer chain lengths, although this was not a tested hypothesis.

Regarding other lighter products for figures **Figure 34**, **Figure 36**, and**Figure 38** all reveal a peak for nonane, a chain with nine carbon atoms, while butane and pentane, chains with four and five carbon atoms respectively, are the least produced molecules. Heavier alkane chains, in particular, longer than eighteen carbon atoms, despite being produced, do not have significant production values for any initial substrate, indicating once more the preponderance of lighter chain products for pyrolysis reaction.

Concerning figures **Figure 33**, **Figure 35**,**Figure 37**, and **Figure 39** for alkenes, all show ethylene as the most produced molecule, followed by propene and hexene. With decane as the initial substrate, ethylene has the highest molar fraction value of all products for all substrates, close to 0.1. This is explained since ethylene is produced in the first instances of the propagation stage, through unzipping reactions. Heavier alkenes follow a similar tendency as heavier alkanes. While still formed for every initial substrate, their relevance is considerably lower than lighter molecules formed [21]. This effect is very accentuated for decane, **Figure 33**, since a single axis does not allow proper visualization of the negligible values for longer chain alkenes (more than ten carbon atoms).

Meanwhile, for the same figures diene distribution seems to work in a particular way. For decane, the longest carbon chain molecule produced is constituted by 8 carbon atoms, for icosane only 18 and so on. To understand this, it's important to take an attentive look at the reaction path (**Figure 8**) since it is what stipulates the relevance of each reaction type and thus, of each product, and to **Figure 40**.

Figure 40. $\beta - scission$ *reaction to an allyl radical forming a diene molecule and an alkyl radical.*

Dienes are formed from allyl radicals that suffer $\beta - scission$ to yield both dienes and alkyl radicals. Since allyl radicals are the product of alkene radicalization, if the initial alkene has ten carbon atoms, then the allyl radicals formed will only have up to nine carbon atoms. When these suffer $\beta - scission$, the products can only have up to eight carbon atoms, result seen in **Figure 33**. However, this is an observation made for all substrates thus according to this rule, produced dienes can only have up to *(n-2)* carbon atoms, *n* being the number of carbon atoms of the initial substrate.

It should be noted that the mechanism only takes into account the production of linear dienes, with double bonds at opposite terminal positions. For all substrates, the most relevant product is 1,3-Butadiene, followed by 1,4-Pentadiene.

6.2.3. Radical Distribution

For this sub-chapter, the analysis of each figure will be made right below the respective, instead of at the end as in the previous sub-chapter. The information is also organized by substrate and type of radical on 3D column graphics.

Decane (C10)

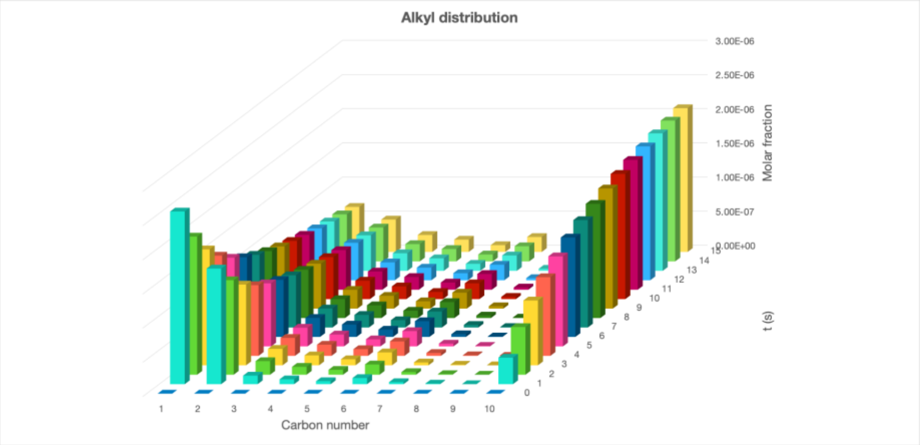

Figure 41. *Alkyl radicals' distribution for the pyrolysis of decane.*

The radicals formed in the initiation stage, and in the propagation stage through backbiting reactions (isomerization) are crucial for the progress of the reaction. While radicals with seven to nine carbon atoms are produced during unzipping reactions, they are consumed in the following $\beta - scission$ reactions, giving rise to shorter radicals and new alkenes. In later reactions, namely in H-abstraction, alkyl radicals with ten carbon atoms are produced as the outcome of the reaction between decane and alkyl or allyl radicals, hence why it has a preponderant expression increasing with time. This is the explanation for the radicals' distribution shown above, which can also be extended for the other studied substrates, despite a few differences.

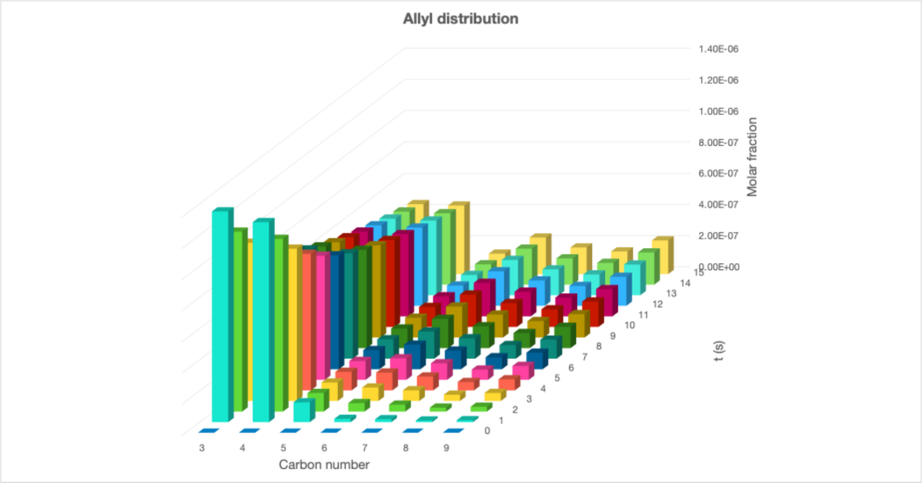

***Figure 42**. Allyl radicals' distribution for the pyrolysis of decane.*

Since decane is a saturated hydrocarbon, during the initiation stage no allyl radicals are formed. Therefore, these are only produced in the last reaction of the propagation stage, H-abstraction, as an outcome of the reaction between alkyl radicals and smaller alkanes. Since the mechanism is not sequential, meaning that if a molecule is only formed in the defined last reaction in the propagation stage, it can still go through all of the beforehand defined reactions. This is the case for allyl radicals, which mainly form chains from six to nine carbon atoms through H-abstraction which then undergo $\beta - scission$ reactions yielding smaller allyl radicals. During the termination stage, allyl radicals are consumed to form farther alkenes. All these combined results in the distribution shown above, where propyl and butyl radicals show the highest molar fraction value, around 8.7×10^{-7}.

One point that still needs further investigation is the understanding of the non-uniformity of the distribution of the products. **Figure 42** shows that higher production of chain lengths of six and nine carbons, which means that these are either preferred to the other ones or less susceptible of being consumed.

Icosane (C20)

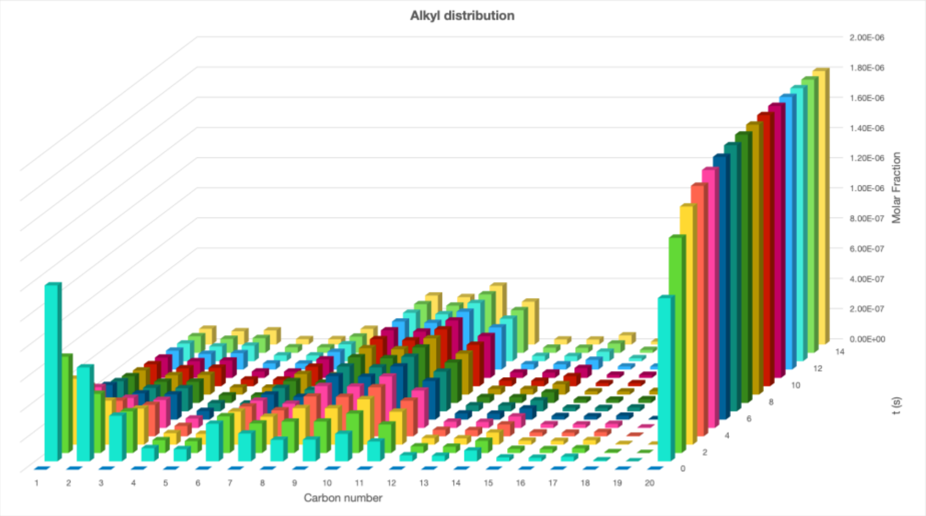

Figure 43. *Alkyl radicals' distribution for the pyrolysis of icosane.*

As a general rule, lighter radicals show the highest molar fraction values, apart from the alkyl radical with the same number of carbon atoms as the respective initial substrate which is produced in H-abstraction reactions. The significant synthesis of lighter radicals is a direct effect of the importance of $\beta - scission$ reactions in the pyrolysis' scheme, identified in the above figure and all below.

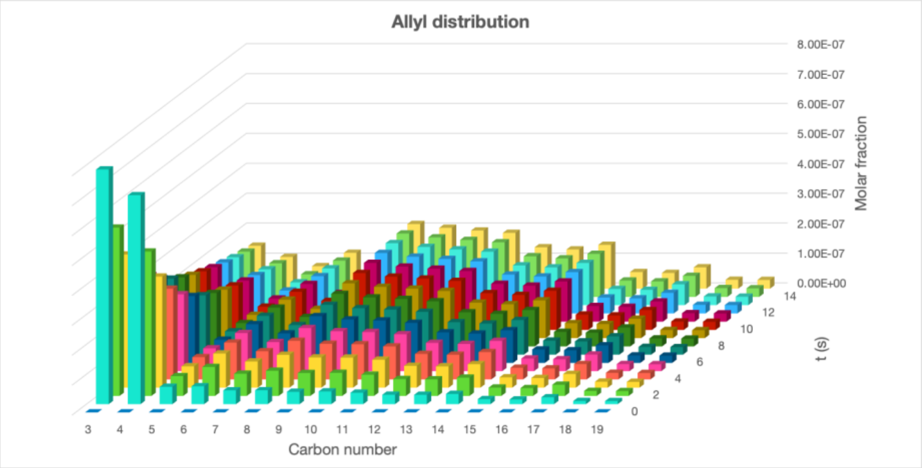

Figure 44. *Allyl radicals' distribution for the pyrolysis of icosane.*

Similar to decane, lighter chain molecules show a greater production in the early stages of the reaction, which will then convert into longer chains, from eight to fourteen carbon atoms, stabilizing at the end of reaction time.

The results for triacontane and tetracontane will not be discriminated since both have the same distribution behaviour. The respective figures can be found in appendix figures **Figure A 7** to**Figure A 10**.

Chapter 7. Alkyl Radical Distribution: Discussion

7.1. Introduction

With the intent of understanding the distribution of radicals without any other variable, a virtual experiment was performed for the two substrates in each end, decane and tetracontane. This is an experiment only possible to perform as a simulation since cracking reactions cannot be manipulated to this extent in real conditions. The goal is to deconstruct the pyrolysis reaction path by reaction type to follow how the products evolve and to answer the question: how does the chain length affect these results? Or in other words, how far do the isomerization reactions go? The aim is to have a much clearer understanding of the purpose of each reaction and how they all interconnect.

7.2. Analysis

The first substrate analyzed was decane, C10, which considered the reactions shown in **Figure 45** (the full list can be consulted in **Figure A 11** in appendix). The following figures show how the conversion of decane evolves with time and how the produced radicals distribute amongst themselves.

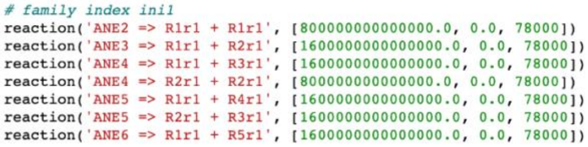

```
# family index ini1
reaction('ANE2 => R1r1 + R1r1', [8000000000000000.0, 0.0, 78000])
reaction('ANE3 => R1r1 + R2r1', [16000000000000000.0, 0.0, 78000])
reaction('ANE4 => R1r1 + R3r1', [16000000000000000.0, 0.0, 78000])
reaction('ANE4 => R2r1 + R2r1', [8000000000000000.0, 0.0, 78000])
reaction('ANE5 => R1r1 + R4r1', [16000000000000000.0, 0.0, 78000])
reaction('ANE5 => R2r1 + R3r1', [16000000000000000.0, 0.0, 78000])
reaction('ANE6 => R1r1 + R5r1', [16000000000000000.0, 0.0, 78000])
```

Figure 45. *Small section of the reaction scheme with initiation and isomerization reactions for decane.*

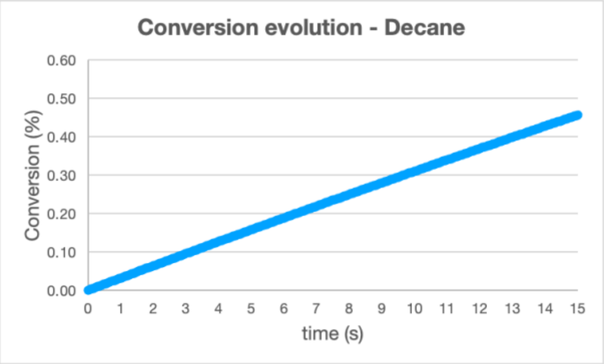

Figure 46. *Conversion evolution of decane when only subjected to initiation and isomerization reactions.*

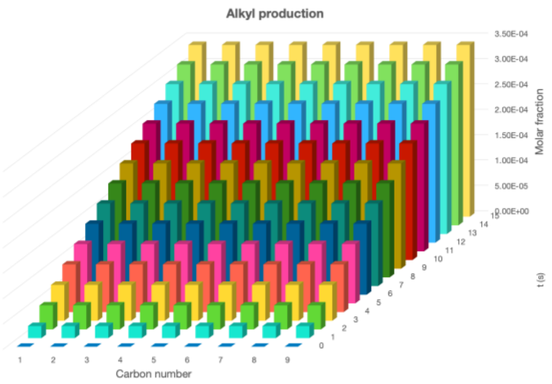

Figure 47. *Alkyl radicals' distribution for decane.*

Since decane is a linear, saturated hydrocarbon, only alkyl radicals are yielded. For every carbon number, the radical production follows a uniform pattern, and the molar fraction increases with time, up to a value of $3.50\ 10^{-4}$. This uniform behaviour results from the assumption for the activation energy values, which are kept at the same value according to **Table 5** in chapter 4. Since a fixed value was considered, the production probability of all radicals is the same, with an equivalent growth rate.

However, there is no formation of radicals with 10 carbon atoms, which is the main radical produced in pyrolysis. When starting with a substrate with 10 carbon atoms, denominated *ANE10* in the mechanism, the maximum possible to yield are radicals with 9 carbon atoms. When considering the actual cracking of the molecule discussed in the previous chapter, radicals with 10 carbon atoms will form through H-abstraction reactions which will later be useful during termination reactions to produce larger hydrocarbon chains, which can be seen further down in this analysis.

Regarding tetracontane or C40, the results for the conversion evolution and radicals' distribution under the same set of conditions are shown in the figures below.

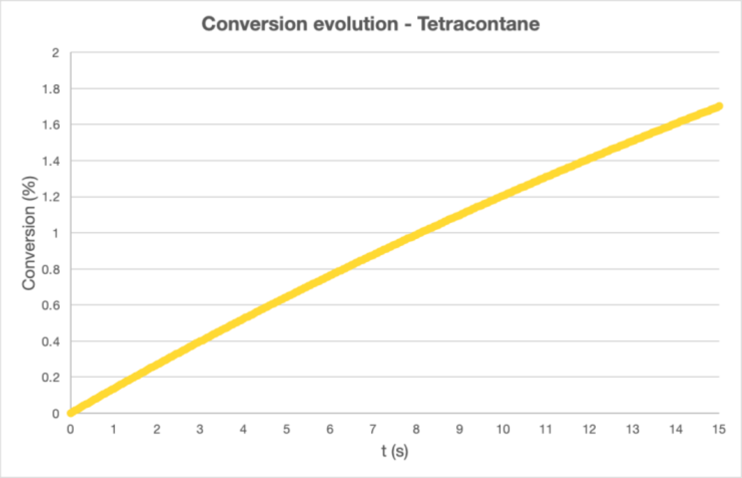

__Figure 48.__ Conversion evolution of tetracontane when only subjected to initiation and isomerization reactions.

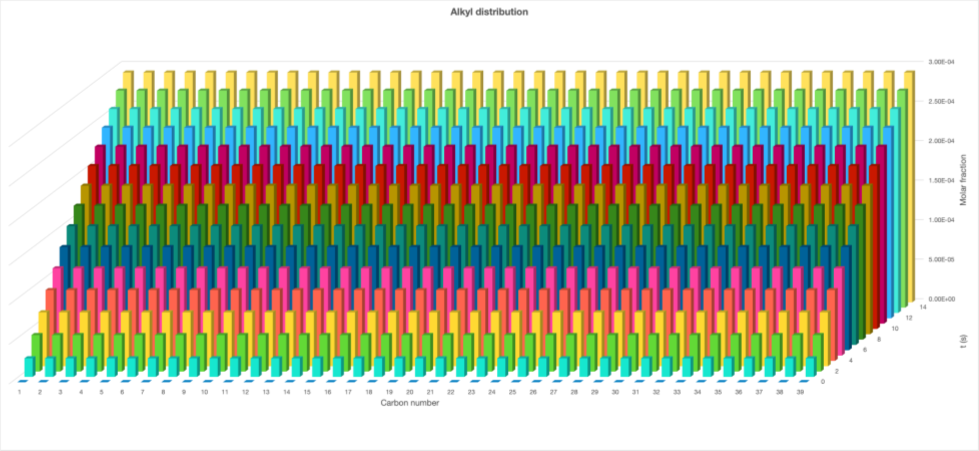

__Figure 49.__ Alkyl radicals' distribution for decane.

For this case, although still to an irrelevant extent, a higher conversion value is achieved when compared to decane. This is expected since a bigger molecule is more susceptible to random breakage when subjected to high temperature values, thus creating further products or radicals in this case. For the radicals' distribution, it is also interesting to note that the maximum molar fraction value attained is close to $3.00\ 10^{-4}$, positioning itself below the value achieved with decane. Since a larger number of radicals are produced, and of higher molecular weight, the chemical mixture is more prompt to reacting, thus less stable [17].

After analysing figures **Figure 47Figure 49**, isomerization reactions seem to be independent of the chain length, which was already a conclusion made in the previous chapter about backbiting reactions. Whether radicals with nine or thirty-nine carbon atoms are formed, will give rise to an identical pattern of distribution. This pattern is uniform in time since all products increase their molar fraction with time and at the same rate regardless of the number of carbon atoms. With the model at hand, no radical has a stronger probability of being formed. Thus, isomerization reactions are not the source of different results for each initial substrate when undergoing the same surrounding conditions.

Icosane and triacontane are not exhibited here since their analysis would not be of use for further conclusions, placing themselves in between the results for decane and tetracontane. To clarify the mechanism approach in terms of reaction type and relevance, a step-by-step study of each reaction type is made hereafter.

After the initiation stage, the propagation stage initiates with unzipping reactions, or end-chain $\beta - scission$.

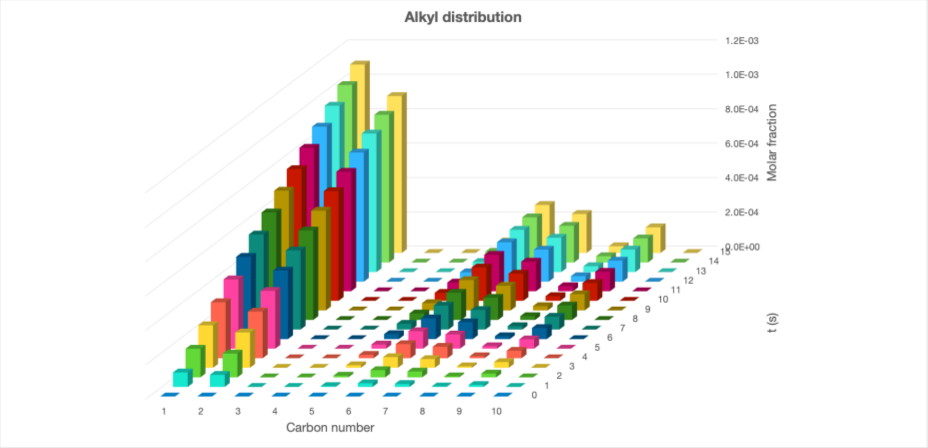

Figure 50. *Alkyl distribution for unzipping reactions for decane.*

As observed in **Figure 47**, during the initiation stage decane is divided into complimentary radicals, at a balanced amount. When the mixture undergoes unzipping reactions which are end-chain $\beta - scissions$, every alkyl will output a smaller alkyl and an ethylene molecule. Thus, in **Figure 50**, it could be expected that the complementary pairs, such as C9 and C1 would have similar values. However, through unzipping reactions, heavier radicals are consumed giving rise to more stable smaller products.

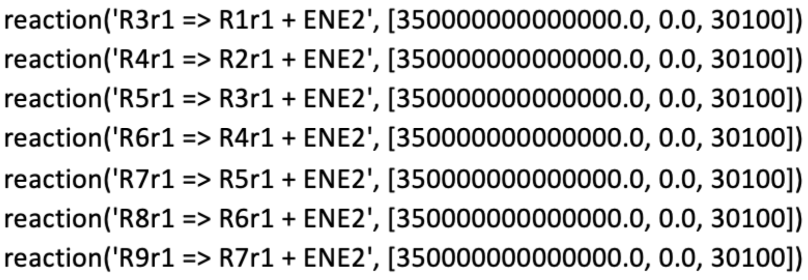

```
reaction('R3r1 => R1r1 + ENE2', [350000000000000.0, 0.0, 30100])
reaction('R4r1 => R2r1 + ENE2', [350000000000000.0, 0.0, 30100])
reaction('R5r1 => R3r1 + ENE2', [350000000000000.0, 0.0, 30100])
reaction('R6r1 => R4r1 + ENE2', [350000000000000.0, 0.0, 30100])
reaction('R7r1 => R5r1 + ENE2', [350000000000000.0, 0.0, 30100])
reaction('R8r1 => R6r1 + ENE2', [350000000000000.0, 0.0, 30100])
reaction('R9r1 => R7r1 + ENE2', [350000000000000.0, 0.0, 30100])
```

Figure 51*. Unzipping reactions for decane.*

C1 and C9 should have the same values at the exact moment the chemical bond is broken. To try and find this instance another simulation was run for 1s and 0.1s. However, this result was not visible for any experiment, thus no further analysis on this is made from this point forward. For the moment, it was assumed that this instance is too brisk to be noticed and that C9, and heavier radicals alike, immediately react to form smaller molecules.

Subsequently, mid-chain $\beta - scission$ and backbiting (isomerization) reactions were simulated.

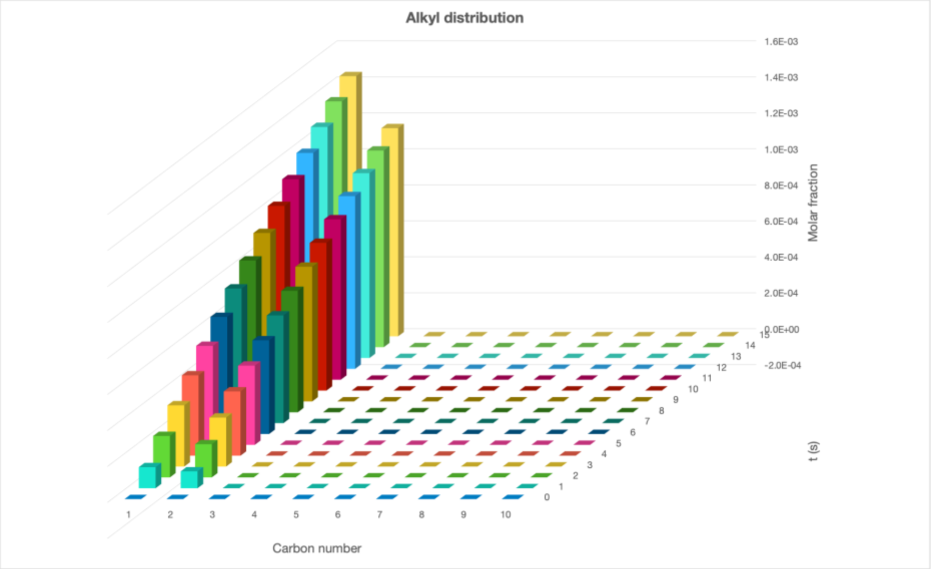

Figure 52. *Alkyl distribution for unzipping, $\beta - scission$, and backbiting reactions for decane.*

Through $\beta - scission$ reactions, all heavier radicals are consumed to form mainly methyl and ethyl radicals, as shown above. This successive follow-up allows for the visualization of the importance of each reaction type. $\beta - scission$ reactions are essential for the formation of light intermediates and products, indicating that all others are mainly products from other reaction types, namely from H-abstraction. In fact, the figure below already considers the contribution of this reaction, which is almost the exact result obtained when pyrolysis is simulated in full, as discussed in the previous chapter.

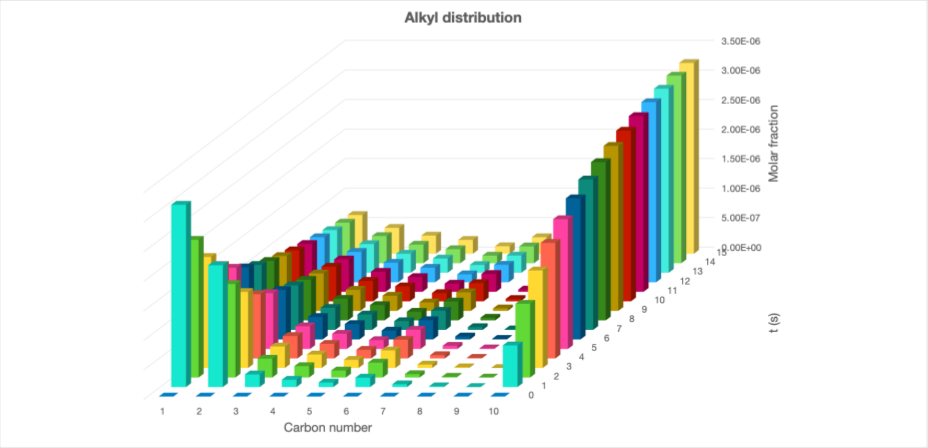

Figure 53. *Alkyl distribution for unzipping,* $\beta - scission$*, backbiting, and H-abstraction reactions for decane.*

Adding termination reactions will not change the overall distribution but will diminish the molar fraction value for every radical since they are consumed as reagents to form alkenes and dienes in the last pyrolysis stage.

At this point, the role and relevance of each reaction should be clearly depicted. By simulating only initiation and isomerization reactions for these two substrates, it was possible to visualize that hydrocarbon molecules with higher molecular weight are more reactive and less tolerant of ambient changes. If the right conditions are laid out, these molecules will spontaneously react towards a more stable and less energy-consuming product [10].

This short study helped in understanding that isomerization and homolytic scission reactions are indispensable and independent of chain length at the same time. These are the reactions that launch pyrolysis net of reactions, enabling the decomposition of plastic waste.

Chapter 8. Conclusion and Future Work

The aim of the study presented was to understand how the chain length of the initial hydrocarbon substrate influences the pyrolysis reaction rate and product distribution and if the chosen mechanism could correctly describe the thermal decomposition independently of polymer length, based on the reactions considered and its correspondent kinetics.

The mechanism was able to closely predict two different sets of experimental data for HDPE's thermal decomposition, showing that it can accurately be used as a first evaluation of the product distribution. Although it was designed to account for saturated and unsaturated feedstock, the simulations were only performed starting from saturated hydrocarbons which also means that all alkene products derive from the assumed reactions in the modeling strategy.

In line with published literature, even though with a certain degree of overestimation, the simulations demonstrated the relevance of light chain products, which are produced to a greater extent when compared to heavier chain products. These results are intrinsically connected to the improved network of reactions included in this mechanism and the associated kinetic parameters. Keeping this in mind, T**able 11** below shows the ratio of light chain products both alkanes and alkenes for decane and tetracontane to summarize the relevance of each reaction family and the effect of chain length on yielded results.

*T**able 11**. Ratio between alkanes and alkenes produced for decane and tetracontane after 15s with 2, 3, and 6 carbon atoms.*

Product chain length	Decane (C10)	Tetracontane (C40)
C2	0.48	0.26
C3	0.19	0.36
C6	0.19	0.23

All ratios are below 0.5, indicating that alkene products show preponderance over alkanes, independently of the length of the produced molecule. Unzipping reactions, which are the first reactions occurring after the initiation stage, are responsible for producing large amounts of alkenes, in particular ethylene, being the main contributor to these results. The relative values for propene and propane show the greater importance of $\beta - scission$ reactions when compared to H-abstraction reactions since the former only produces alkenes, which includes propene, while the latter yields both alkanes and alkenes. Higher production of propane is found for tetracontane, which can be explained due to the increased amount of alkyl radicals produced during initiation, which are later used as reagents in H-abstraction reactions. Despite a smaller discrepancy, this is also the explanation for hexane and hexene, which are produced through H-abstraction reactions, and show a slight increase in ratio's value for tetracontane.

To account for the distribution of low molecular alkenes, $\beta - scission$ are the most important reactions to consider, while H-abstraction reactions are mainly responsible for producing alkanes and many radicals. Both generate higher fractions of light chain products even though H-abstraction is responsible for most of the heavier chain products yielded. Backbiting reactions might seem less relevant but are the ones that consume longer chain radicals, thus generating smaller units that subsequently disappear when subjected to the other reaction families. The role of each reaction family is greatly dependent on the chemical kinetics assumed. The implemented method of moments in Beirnaert's mechanism allowed to estimate the parameters based on the chemical structure of the polymer, discerning the species considered. This method reveals the variation in the relative importance of reaction families, showing that backbiting becomes less relevant with time while $\beta - scission$ becomes the dominating pathway.

Future work includes, firstly, a validation of the model with suitable experimental datasets which does not exist, for the time being. Considering the available experimental results, the mechanism can acceptably predict pyrolysis results. However, due to the long reactions and species list included, it is still too large to be implemented in a 1-D CFD code. Moreover, improvements in the reaction network are necessary since a considerable amount of intermediates, alkyl and allyl radicals, are not consumed, appearing at the end of reaction time. It is also essential to take into account many important reactions such as hydrogen and aromatics production and branched species. Thus, further development of the mechanism is necessary, also followed by reduction work, before coupling combustion reactions. Crucial improvements are necessary for developing more accurate kinetic parameters, as well as enhanced models which consider heat and mass transfer limitations. Polymer degradation needs to consider three phases (gas, liquid, and solid) that interact together and influence each other. For this, new approaches are required which should consider having a more accurate knowledge of the initial substrate's composition, since this is determinant for the subsequent reactions and products yielded. Techniques such as chromatography or photoionization mass spectrometry can be used for this purpose. As for computational simulations, more detailed kinetic models should be considered, namely kinetic Monte Carlo and heterogeneous models [6].

Even though there is still a long way before the present mechanism can be adopted, the current work showed that it's possible to build a flexible model able to predict thermal decomposition for different feedstocks, if suitable kinetic parameters are available, and relevant reactions are considered.

Bibliography

1. Mastral, J. F., Berrueco, C. & Ceamanos, J. Theoretical prediction of product distribution of the pyrolysis of high density polyethylene. *J. Anal. Appl. Pyrolysis* **80**, 427–438 (2007).
2. PlascticEurope-Association of Plastics Manufactures. Plastics – the Facts 2020. *PlasticEurope* 1–64 (2020).
3. Geyer, R., Jambeck, J. R. & Law, K. L. Production, use, and fate of all plastics ever made. *Sci. Adv.* **3**, e1700782 (2017).
4. Levine, S. E. & Broadbelt, L. J. Detailed mechanistic modeling of high-density polyethylene pyrolysis: Low molecular weight product evolution. *Polym. Degrad. Stab.* **94**, 810–822 (2009).
5. Ragaert, K., Delva, L. & Van Geem, K. Mechanical and chemical recycling of solid plastic waste. *Waste Management* vol. 69 24–58 (2017).
6. Dogu, O. *et al.* The chemistry of chemical recycling of solid plastic waste via pyrolysis and gasification: State-of-the-art, challenges, and future directions. *Prog. Energy Combust. Sci.* **84**, (2021).
7. Feldman, D. International plastics flammability handbook, 2nd ed., J. Troitzsch, (Ed.), Hanser Publishers, Munich, Vienna, New York, 1990, 531 pp. Price: D.M. 278, US $165.00, £110.00. *J. Polym. Sci. Part A Polym. Chem.* **29**, 292 (1991).
8. Németh, A., Blazsó, M., Baranyai, P. & Vidóczy, T. Thermal degradation of polyethylene modeled on tetracontane. *J. Anal. Appl. Pyrolysis* **81**, 237–242 (2008).
9. Beirnaert, K. Static Chamber Vortex Unit (SCVU): from theory to applications. (Ghent University, 2020).
10. Vinu, R. & Broadbelt, L. J. Unraveling Reaction Pathways and Specifying Reaction Kinetics for Complex Systems. *Annu. Rev. Chem. Biomol. Eng.* **3**, 29–54 (2012).
11. Zhou, X., Broadbelt, L. J. & Vinu, R. Chapter Two - Mechanistic Understanding of Thermochemical Conversion of Polymers and Lignocellulosic Biomass. in *Thermochemical Process Engineering* (ed. Van Geem, K. M. B. T.-A. in C. E.) vol. 49 95–198 (Academic Press, 2016).
12. Ügdüler, S. *et al.* Towards closed-loop recycling of multilayer and coloured PET plastic waste by alkaline hydrolysis. *Green Chem.* **22**, 5376–5394 (2020).
13. Gascoin, N., Navarro-Rodriguez, A., Gillard, P. & Mangeot, A. Kinetic modelling of high density polyethylene pyrolysis: Part 1. Comparison of existing models. *Polym. Degrad. Stab.* **97**, 1466–1474 (2012).
14. Okuwaki, A. Feedstock recycling of plastics in Japan. *Polym. Degrad. Stab.* **85**, 981–988 (2004).
15. Sadat-Shojai, M. & Bakhshandeh, G.-R. Recycling of PVC wastes. *Polym. Degrad. Stab.* **96**, 404–415 (2011).
16. Westerhout, R. W. J., Waanders, J., Kuipers, J. A. M. & Van Swaaij, W. P. M. Kinetics of the low-temperature pyrolysis of polyethene, polypropene, and polystyrene modeling, experimental determination, and comparison with literature models and data. *Ind. Eng.*

Chem. Res. **36**, 1955–1964 (1997).

17. Depolymerization. *polymerdatabase.com* http://polymerdatabase.com/polymer chemistry/Depolymerization.html.
18. Klein, D. *Organic Chemistry*. *Wiley* (Johns Hopkins University, 2015). doi:10.1007/bfb0050135.
19. Marongiu, A., Faravelli, T. & Ranzi, E. Detailed kinetic modeling of the thermal degradation of vinyl polymers. *J. Anal. Appl. Pyrolysis* **78**, 343–362 (2007).
20. H. Petrucci, R., S Harwood, W., Herring, F. G. & D. Madura, J. *General Chemistry: Principles and Modern Application & Basic Media Pack*. (Pearson College Div, 2007).
21. Faravelli, T. *et al.* Gas product distribution from polyethylene pyrolysis. *J. Anal. Appl. Pyrolysis* **52**, 87–103 (1999).
22. Poutsma, M. Fundamental reactions of free radicals relevant to pyrolysis reactions. *J. Anal. Appl. Pyrolysis* **54**, 5–35 (2000).
23. Savage, P. Mechanisms and Kinetics Models for Hydrocarbon Pyrolysis. *J. Anal. Appl. Pyrolysis - J ANAL APPL PYROL* **54**, 109–126 (2000).
24. Mastral, J. F., Berrueco, C. & Ceamanos, J. Modelling of the pyrolysis of high density polyethylene. Product distribution in a fluidized bed reactor. *J. Anal. Appl. Pyrolysis* **79**, 313–322 (2007).
25. Bockhorn, H., Hornung, A., Hornung, U. & Jakobströer, P. Modelling of isothermal and dynamic pyrolysis of plastics considering non-homogeneous temperature distribution and detailed degradation mechanism. *J. Anal. Appl. Pyrolysis* **49**, 53–74 (1999).
26. Poutsma, M. L. Reexamination of the Pyrolysis of Polyethylene: Data Needs, Free-Radical Mechanistic Considerations, and Thermochemical Kinetic Simulation of Initial Product-Forming Pathways. *Macromolecules* **36**, 8931–8957 (2003).
27. Gascoin, N., Navarro-Rodriguez, A., Fau, G. & Gillard, P. Kinetic modelling of High Density PolyEthylene pyrolysis: Part 2. Reduction of existing detailed mechanism. *Polym. Degrad. Stab.* **97**, 1142–1150 (2012).
28. Ranzi, E. *et al.* Kinetic modeling of polyethylene and polypropylene thermal degradation. *J. Anal. Appl. Pyrolysis* **40**–**41**, 305–319 (1997).
29. Faravelli, T. *et al.* Thermal degradation of polystyrene. *J. Anal. Appl. Pyrolysis* **60**, 103–121 (2001).
30. De Witt, M. J. & Broadbelt, L. J. Binary interactions between high-density polyethylene and 4-(l-naphthylmethyl)bibenzyl during low-pressure pyrolysis. *Energy and Fuels* **14**, 448–458 (2000).
31. Johannes I, Tamvelius H, T. L. A step-by-step model for pyrolysis kinetics of polyethylene in an autoclave under non-linear increase of temperature. *J. Anal. Appl. Pyrolysis* 72:113–9 (2004).
32. Elordi, G., Lopez, G., Olazar, M., Aguado, R. & Bilbao, J. Product distribution modelling in the thermal pyrolysis of high density polyethylene. *J. Hazard. Mater.* **144**, 708–714 (2007).
33. Wampler, T. P. & Levy, E. J. Effect of heating rate on oxidative degradation of polymeric

materials. *J. Anal. Appl. Pyrolysis* **8**, 153–161 (1985).

34. “mechanism_reduction.py | Cantera.” *[Online]* https://cantera.org/examples/python/kinetics/mechanism_reduction.py.html.
35. IUPAC. *[Online]* https://iupac.org/.
36. Python range() Function. *[Online]* https://www.w3schools.com/python/ref_func_range.asp.
37. KEITH J. LAIDLER. A GLOSSARY OF TERMS USED IN CHEMICAL KINETICS, INCLUDING REACTION DYNAMICS. *Pure Appl. Chem.* **68**, 149–192 (1996).
38. NASA-polynomials. *[Online]* http://combustion.berkeley.edu/gri_mech/data/nasa_plnm.html.
39. TSUCHIYA Y & SUMI K. Thermal Decomposition Products of Poly. *J Polym Sci Part A-1 Polym Chem* **7**, 3131–3138 (1969).
40. Kaisare, N. Chemkin Tutorial. *[Online]* http://che.iitm.ac.in/~nkaisare/courses/CHEMKIN_tutorial.pdf (2007).
41. W. K. Metcalfe, S. Burke, H. J. C. Combustion Chemistry Centre. *[Online]* http://www.nuigalway.ie/media/researchcentres/combustionchemistrycentre/files/mechanismdownloads/AramcoMech_1.3_tran.dat.
42. Cantera, D. Reactors and Reactor Networks. *[Online]* https://cantera.org/science/reactors.html (2021).
43. Cantera, D. Cantera. *[Online]* https://cantera.org/ (2021).
44. Cantera, D. Working With Input Files. *[Online]* https://cantera.org/tutorials/input-files.html (2021).
45. Cantera, D. Objects Representing Phases. *[Online]* https://cantera.org/documentation/docs-2.4/sphinx/html/cython/importing.html#cantera.Solution (2021).
46. What is the Jupyter Notebook? *[Online]* (2015).
47. Project Jupyter. Jupyter. *[Online]* https://jupyter.org/ (2021).
48. Hunter, J., Dale, D., Firing, E. & Droettboon, M. Matplotlib: Visualization with Python. *[Online]* https://matplotlib.org/.
49. Team. Pandas. *[Online]* https://pandas.pydata.org/ (2021).
50. Melendez, S. What is the Difference Between CPU Usage & RAM? *Techwalla [Online]* (2018).
51. Jupyter Team. The Jupyter Notebook. *[Online]* https://jupyter-notebook.readthedocs.io/en/stable/notebook.html (2015).

Appendix

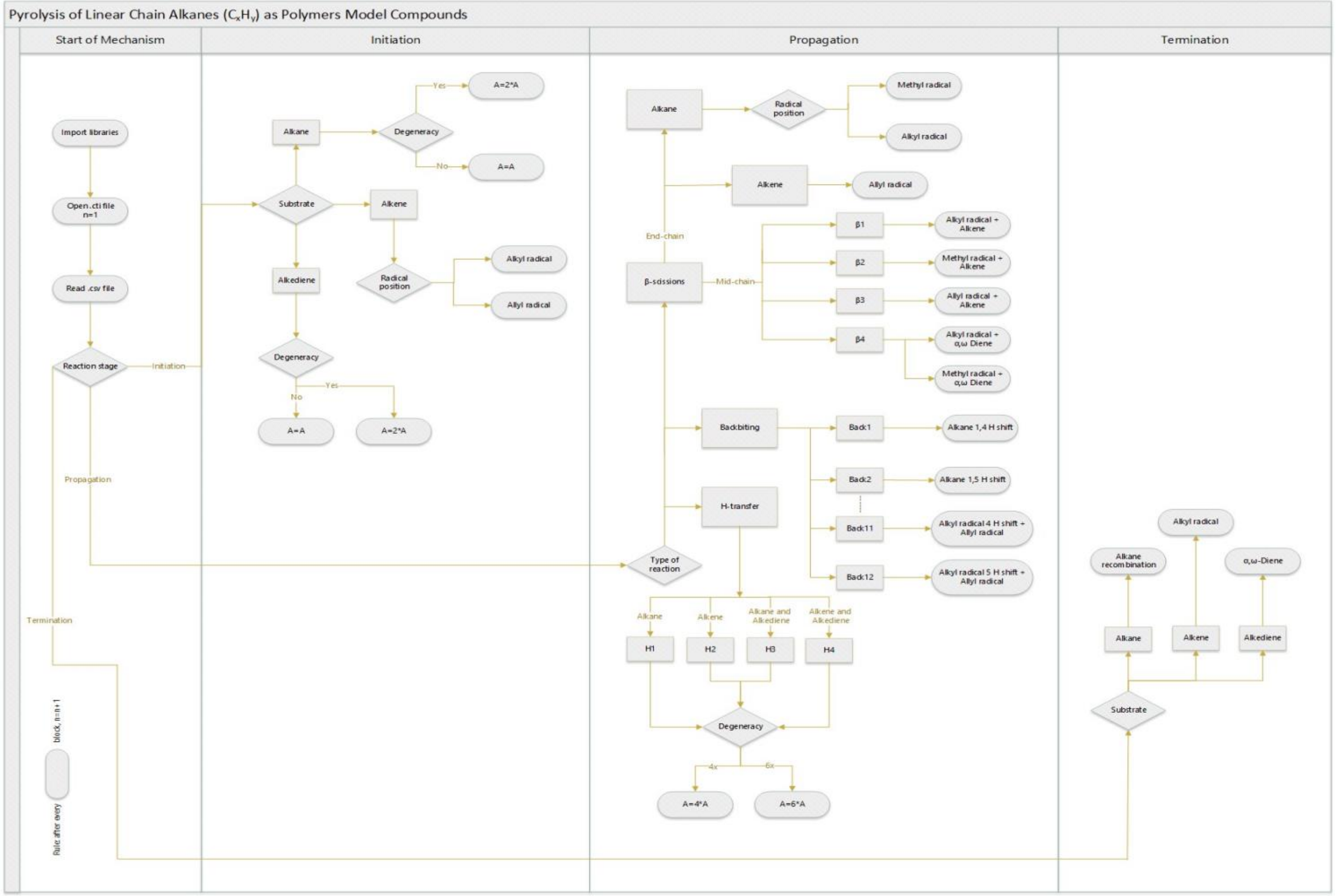

***Figure** A 1. Flowchart on the Kinetic Model developed for Pyrolysis of Linear Chain Alkanes Polymer Compounds by Beirnaert K.* [9].

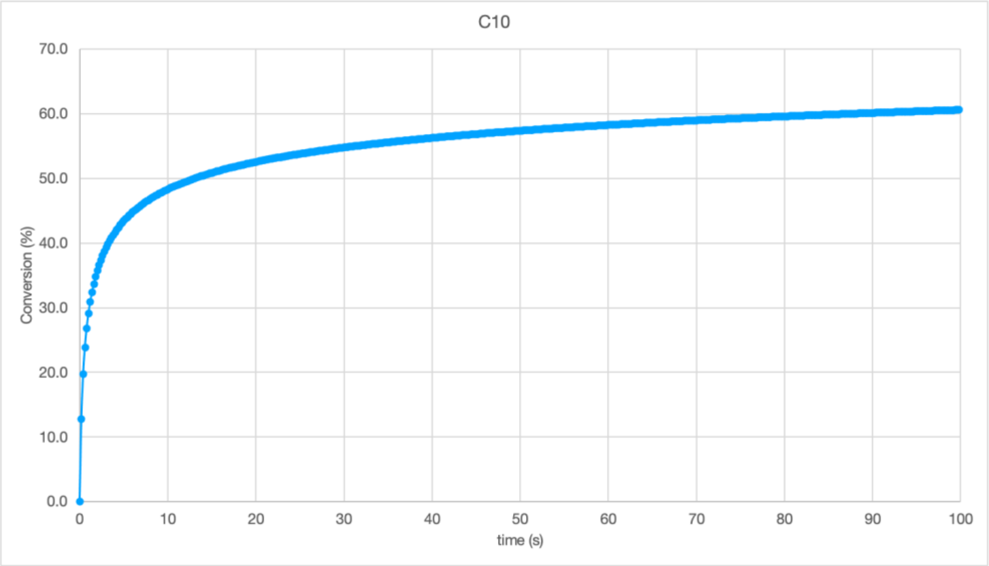

Figure A 2 *Conversion of decane for 100s of reaction time simulated.*

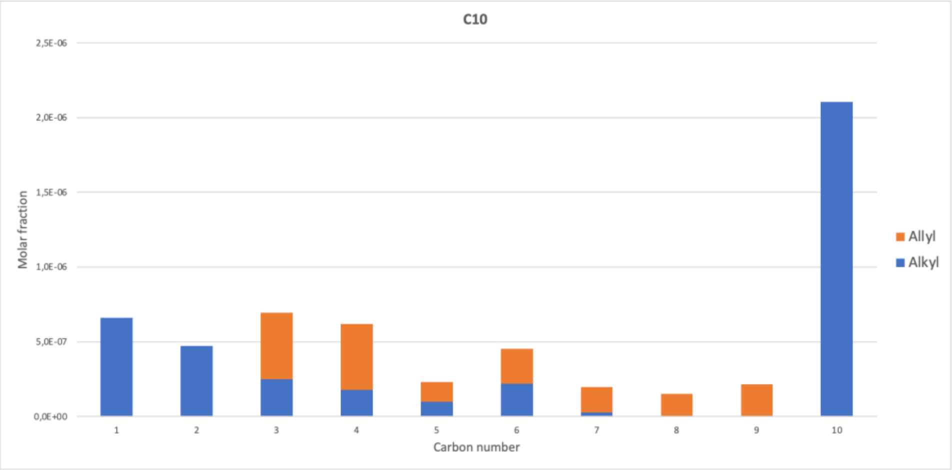

Figure A 3. *Radical distribution (alkyl and allyl) for the pyrolysis of decane, at 15s.*

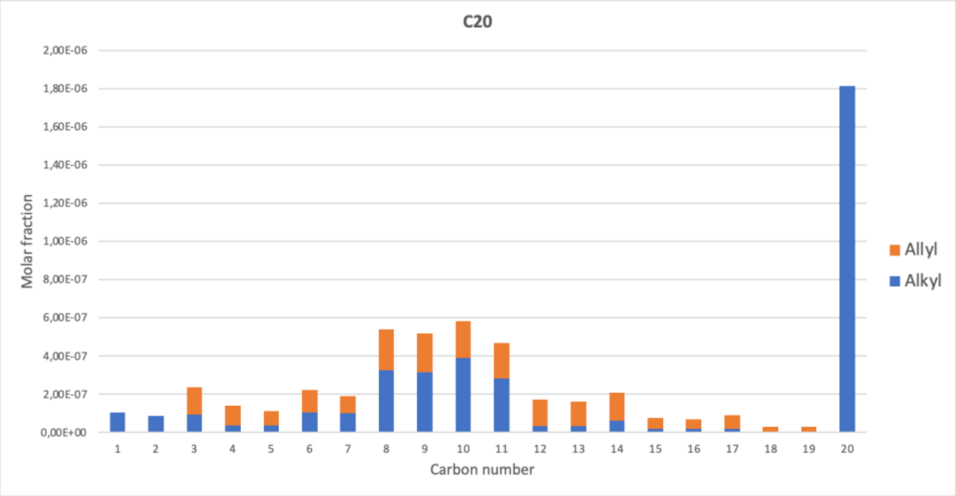

Figure A 4. *Radical distribution (alkyl and allyl) for the pyrolysis of icosane, at 15s.*

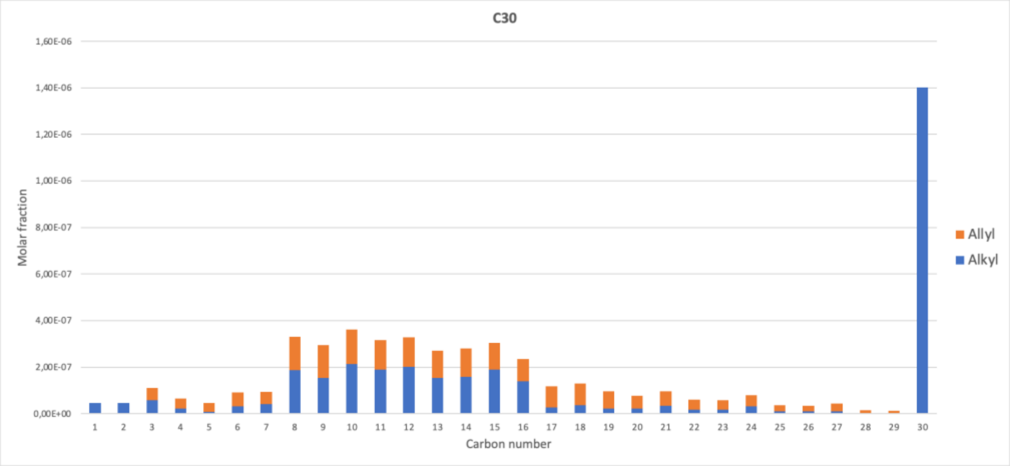

Figure A 5. *Radical distribution (alkyl and allyl) for the pyrolysis of triacontane, at 15s.*

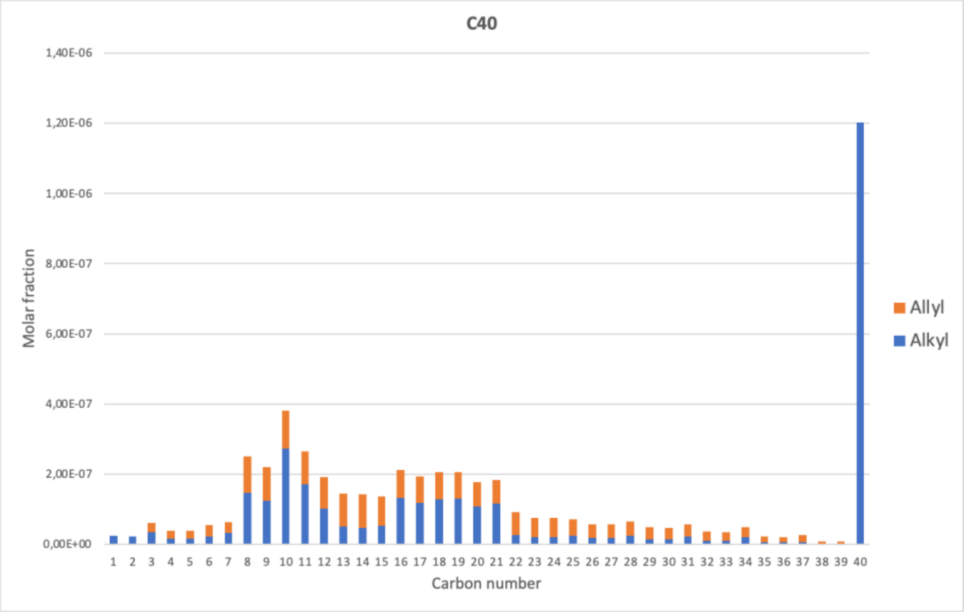

Figure A 6. *Radical distribution (alkyl and allyl) for the pyrolysis of tetracontane, at 15s.*

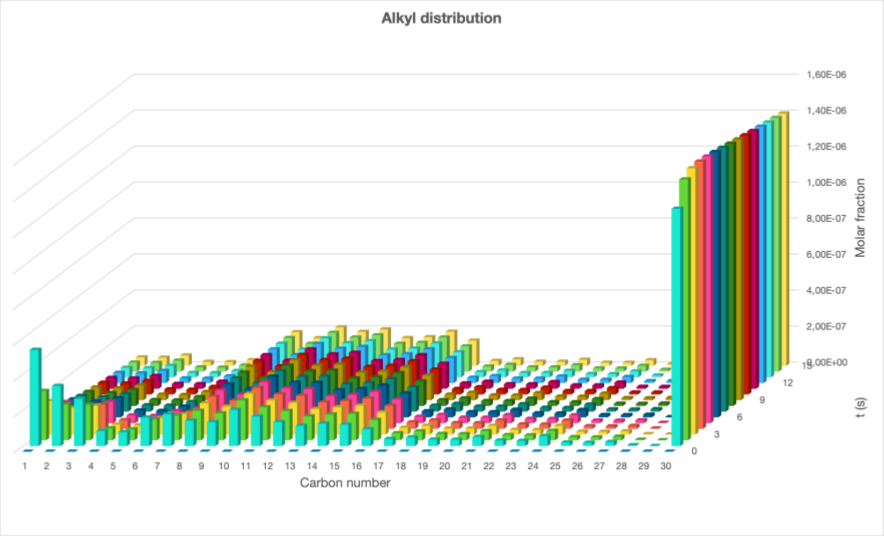

Figure A 7. Alkyl radicals' distribution for the pyrolysis of triacontane.

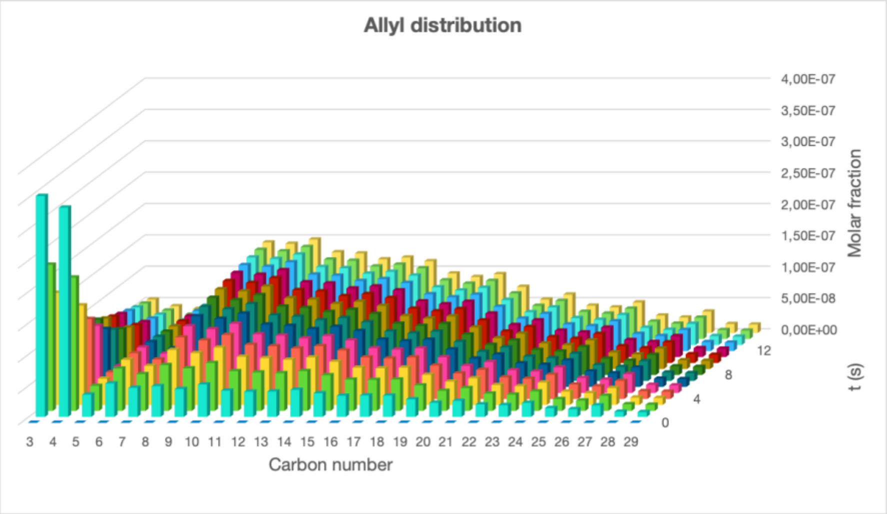

Figure A 8. Allyl radicals' distribution for the pyrolysis of triacontane.

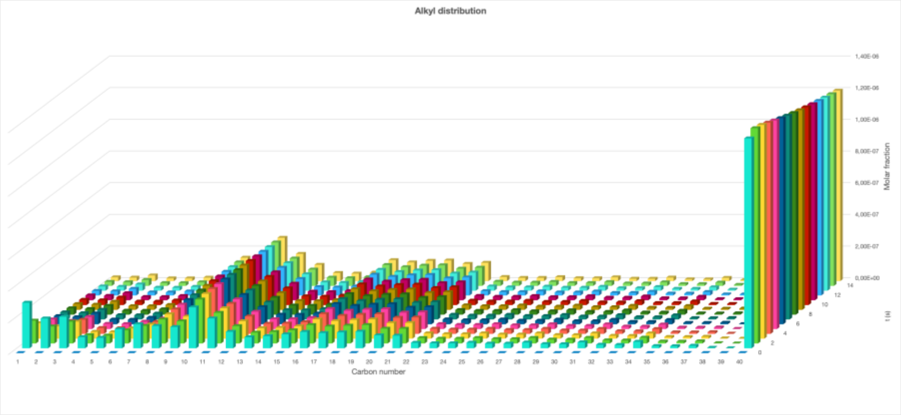

Figure A 9. Alkyl radicals' distribution for the pyrolysis of tetracontane.

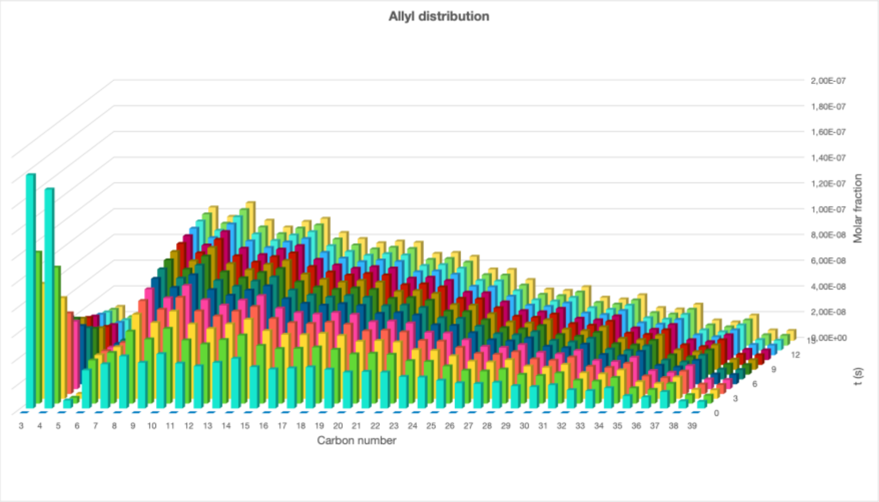

Figure A 10. *Allyl radicals' distribution for the pyrolysis of tetracontane.*

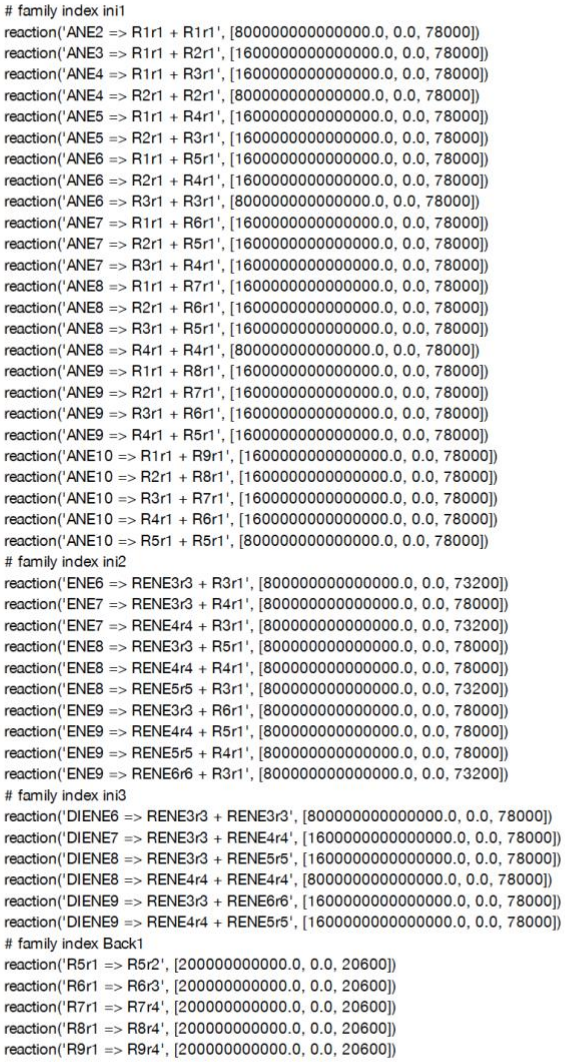

```
# family index ini1
reaction('ANE2 => R1r1 + R1r1', [800000000000000.0, 0.0, 78000])
reaction('ANE3 => R1r1 + R2r1', [1600000000000000.0, 0.0, 78000])
reaction('ANE4 => R1r1 + R3r1', [1600000000000000.0, 0.0, 78000])
reaction('ANE4 => R2r1 + R2r1', [800000000000000.0, 0.0, 78000])
reaction('ANE5 => R1r1 + R4r1', [1600000000000000.0, 0.0, 78000])
reaction('ANE5 => R2r1 + R3r1', [1600000000000000.0, 0.0, 78000])
reaction('ANE6 => R1r1 + R5r1', [1600000000000000.0, 0.0, 78000])
reaction('ANE6 => R2r1 + R4r1', [1600000000000000.0, 0.0, 78000])
reaction('ANE6 => R3r1 + R3r1', [800000000000000.0, 0.0, 78000])
reaction('ANE7 => R1r1 + R6r1', [1600000000000000.0, 0.0, 78000])
reaction('ANE7 => R2r1 + R5r1', [1600000000000000.0, 0.0, 78000])
reaction('ANE7 => R3r1 + R4r1', [1600000000000000.0, 0.0, 78000])
reaction('ANE8 => R1r1 + R7r1', [1600000000000000.0, 0.0, 78000])
reaction('ANE8 => R2r1 + R6r1', [1600000000000000.0, 0.0, 78000])
reaction('ANE8 => R3r1 + R5r1', [1600000000000000.0, 0.0, 78000])
reaction('ANE8 => R4r1 + R4r1', [800000000000000.0, 0.0, 78000])
reaction('ANE9 => R1r1 + R8r1', [1600000000000000.0, 0.0, 78000])
reaction('ANE9 => R2r1 + R7r1', [1600000000000000.0, 0.0, 78000])
reaction('ANE9 => R3r1 + R6r1', [1600000000000000.0, 0.0, 78000])
reaction('ANE9 => R4r1 + R5r1', [1600000000000000.0, 0.0, 78000])
reaction('ANE10 => R1r1 + R9r1', [1600000000000000.0, 0.0, 78000])
reaction('ANE10 => R2r1 + R8r1', [1600000000000000.0, 0.0, 78000])
reaction('ANE10 => R3r1 + R7r1', [1600000000000000.0, 0.0, 78000])
reaction('ANE10 => R4r1 + R6r1', [1600000000000000.0, 0.0, 78000])
reaction('ANE10 => R5r1 + R5r1', [800000000000000.0, 0.0, 78000])
# family index ini2
reaction('ENE6 => RENE3r3 + R3r1', [800000000000000.0, 0.0, 73200])
reaction('ENE7 => RENE3r3 + R4r1', [800000000000000.0, 0.0, 78000])
reaction('ENE7 => RENE4r4 + R3r1', [800000000000000.0, 0.0, 73200])
reaction('ENE8 => RENE3r3 + R5r1', [800000000000000.0, 0.0, 78000])
reaction('ENE8 => RENE4r4 + R4r1', [800000000000000.0, 0.0, 78000])
reaction('ENE8 => RENE5r5 + R3r1', [800000000000000.0, 0.0, 73200])
reaction('ENE9 => RENE3r3 + R6r1', [800000000000000.0, 0.0, 78000])
reaction('ENE9 => RENE4r4 + R5r1', [800000000000000.0, 0.0, 78000])
reaction('ENE9 => RENE5r5 + R4r1', [800000000000000.0, 0.0, 78000])
reaction('ENE9 => RENE6r6 + R3r1', [800000000000000.0, 0.0, 73200])
# family index ini3
reaction('DIENE6 => RENE3r3 + RENE3r3', [800000000000000.0, 0.0, 78000])
reaction('DIENE7 => RENE3r3 + RENE4r4', [1600000000000000.0, 0.0, 78000])
reaction('DIENE8 => RENE3r3 + RENE5r5', [1600000000000000.0, 0.0, 78000])
reaction('DIENE8 => RENE4r4 + RENE4r4', [800000000000000.0, 0.0, 78000])
reaction('DIENE9 => RENE3r3 + RENE6r6', [1600000000000000.0, 0.0, 78000])
reaction('DIENE9 => RENE4r4 + RENE5r5', [1600000000000000.0, 0.0, 78000])
# family index Back1
reaction('R5r1 => R5r2', [200000000000.0, 0.0, 20600])
reaction('R6r1 => R6r3', [200000000000.0, 0.0, 20600])
reaction('R7r1 => R7r4', [200000000000.0, 0.0, 20600])
reaction('R8r1 => R8r4', [200000000000.0, 0.0, 20600])
reaction('R9r1 => R9r4', [200000000000.0, 0.0, 20600])
```

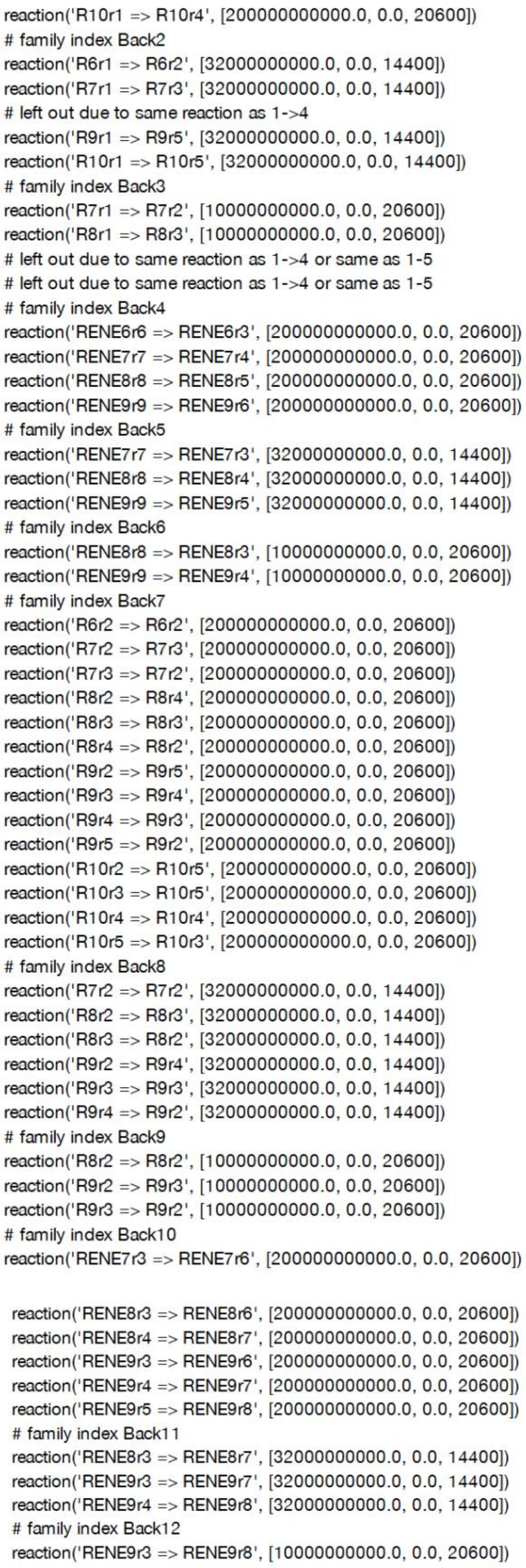

```
reaction('R10r1 => R10r4', [200000000000.0, 0.0, 20600])
# family index Back2
reaction('R6r1 => R6r2', [32000000000.0, 0.0, 14400])
reaction('R7r1 => R7r3', [32000000000.0, 0.0, 14400])
# left out due to same reaction as 1->4
reaction('R9r1 => R9r5', [32000000000.0, 0.0, 14400])
reaction('R10r1 => R10r5', [32000000000.0, 0.0, 14400])
# family index Back3
reaction('R7r1 => R7r2', [10000000000.0, 0.0, 20600])
reaction('R8r1 => R8r3', [10000000000.0, 0.0, 20600])
# left out due to same reaction as 1->4 or same as 1-5
# left out due to same reaction as 1->4 or same as 1-5
# family index Back4
reaction('RENE6r6 => RENE6r3', [200000000000.0, 0.0, 20600])
reaction('RENE7r7 => RENE7r4', [200000000000.0, 0.0, 20600])
reaction('RENE8r8 => RENE8r5', [200000000000.0, 0.0, 20600])
reaction('RENE9r9 => RENE9r6', [200000000000.0, 0.0, 20600])
# family index Back5
reaction('RENE7r7 => RENE7r3', [32000000000.0, 0.0, 14400])
reaction('RENE8r8 => RENE8r4', [32000000000.0, 0.0, 14400])
reaction('RENE9r9 => RENE9r5', [32000000000.0, 0.0, 14400])
# family index Back6
reaction('RENE8r8 => RENE8r3', [10000000000.0, 0.0, 20600])
reaction('RENE9r9 => RENE9r4', [10000000000.0, 0.0, 20600])
# family index Back7
reaction('R6r2 => R6r2', [200000000000.0, 0.0, 20600])
reaction('R7r2 => R7r3', [200000000000.0, 0.0, 20600])
reaction('R7r3 => R7r2', [200000000000.0, 0.0, 20600])
reaction('R8r2 => R8r4', [200000000000.0, 0.0, 20600])
reaction('R8r3 => R8r3', [200000000000.0, 0.0, 20600])
reaction('R8r4 => R8r2', [200000000000.0, 0.0, 20600])
reaction('R9r2 => R9r5', [200000000000.0, 0.0, 20600])
reaction('R9r3 => R9r4', [200000000000.0, 0.0, 20600])
reaction('R9r4 => R9r3', [200000000000.0, 0.0, 20600])
reaction('R9r5 => R9r2', [200000000000.0, 0.0, 20600])
reaction('R10r2 => R10r5', [200000000000.0, 0.0, 20600])
reaction('R10r3 => R10r5', [200000000000.0, 0.0, 20600])
reaction('R10r4 => R10r4', [200000000000.0, 0.0, 20600])
reaction('R10r5 => R10r3', [200000000000.0, 0.0, 20600])
# family index Back8
reaction('R7r2 => R7r2', [32000000000.0, 0.0, 14400])
reaction('R8r2 => R8r3', [32000000000.0, 0.0, 14400])
reaction('R8r3 => R8r2', [32000000000.0, 0.0, 14400])
reaction('R9r2 => R9r4', [32000000000.0, 0.0, 14400])
reaction('R9r3 => R9r3', [32000000000.0, 0.0, 14400])
reaction('R9r4 => R9r2', [32000000000.0, 0.0, 14400])
# family index Back9
reaction('R8r2 => R8r2', [10000000000.0, 0.0, 20600])
reaction('R9r2 => R9r3', [10000000000.0, 0.0, 20600])
reaction('R9r3 => R9r2', [10000000000.0, 0.0, 20600])
# family index Back10
reaction('RENE7r3 => RENE7r6', [200000000000.0, 0.0, 20600])

reaction('RENE8r3 => RENE8r6', [200000000000.0, 0.0, 20600])
reaction('RENE8r4 => RENE8r7', [200000000000.0, 0.0, 20600])
reaction('RENE9r3 => RENE9r6', [200000000000.0, 0.0, 20600])
reaction('RENE9r4 => RENE9r7', [200000000000.0, 0.0, 20600])
reaction('RENE9r5 => RENE9r8', [200000000000.0, 0.0, 20600])
# family index Back11
reaction('RENE8r3 => RENE8r7', [32000000000.0, 0.0, 14400])
reaction('RENE9r3 => RENE9r7', [32000000000.0, 0.0, 14400])
reaction('RENE9r4 => RENE9r8', [32000000000.0, 0.0, 14400])
# family index Back12
reaction('RENE9r3 => RENE9r8', [10000000000.0, 0.0, 20600])
```

Figure A 11. *Simulation of only initiation and isomerization reactions for decane.*